THE JOURNAL OF CHEMICAL PHYSICS

VOLUME 14 NUMBER 4

APRIL, 1946

Published by the
AMERICAN INSTITUTE OF PHYSICS
Lancaster Press, Inc., New York, N. Y.

CHARLES D. CORYELL,
F. O. RICE
L. H. THOMAS
G. W. WHEELAND
E. BRIGHT WILSON, JR.

cated exponents. The solidus (/) should be used wherever possible for fractions.

All illustrations should accompany manuscript and should always be referred to in the text. Line drawings should be made with India ink on plain white paper or on tracing cloth. Coordinate paper is not desirable, but if used must be blue-lined with all coordinates to be reproduced drawn with India ink. Lettering should be of sufficient size to be legible after reduction.

Proof and all correspondence concerning papers in the process of publication should be addressed to the Publications Manager, American Institute of Physics, 57 East 55 Street, New York 22, New York.

Subscription Rates

The United States and Possessions, Spanish and Mexico $10.00
Elsewhere 11.00

Back Numbers

Complete set: Vol. 1, 1933—Vol. [illegible] $130.00
Single issue: $11.00.
Single copies: $1.00 each.

Subscriptions and orders for single copies should be addressed to Prince and Lemon Streets, Lancaster, Pennsylvania, or to the American Institute of Physics, 57 East 55 Street, New York 22, New York.

Changes of address should be sent to the Business Manager, American Institute of Physics.

[illegible] is published [illegible] Prince and Lemon Streets, Lancaster, Pennsylvania.

[illegible], at the Post Office at Lancaster, Pa., under the Act of August 24, 1912. Acceptance for the Act of February 28, 1925, embodied in paragraph [illegible], Sec. P. L. & R., authorized

THE JOURNAL
OF
CHEMICAL PHYSICS

VOLUME 14, NUMBER 4 APRIL, 1946

An Improved Hot Wire Cell for Accurate Measurements of Thermal Conductivities of Gases over a Wide Temperature Range

Results with Air between 87° and 375°K

WILLIAM J. TAYLOR[1] AND HERRICK L. JOHNSTON
Department of Chemistry, The Ohio State University, Columbus, Ohio

(Received December 26, 1945)

An improved hot wire cell of the potential lead type is described, and theoretical treatments given for radiation, end conduction, potential lead conduction, and the "temperature jump" effect. The latter is found to be satisfactorily eliminated by linear extrapolation of reciprocal plots of "apparent conductivities" as a function of pressure. Convection effects are absent at pressures below about 20 cm of mercury. The emissivity from bright platinum was measured. The results confirm the measurements by Milverton. The thermal conductivity of air was measured at seventeen temperatures between 87° and 375°K. Our results, which are believed accurate to within ±0.5 percent, are generally lower than other results which have been reported in recent years, for air. Tabulation of our results is given, together with a critical analysis of possible sources of error. The advantage of our method over either the "thick wire" or "compensating lead" type of cells is pointed out.

A RESEARCH program on the accurate measurement of the absolute thermal conductivities of gases, over a wide temperature range, is being undertaken in this laboratory to supplement investigations on measurements of heat capacity by the velocity of sound method. Investigation of the literature reveals that the only reliable thermal conductivity data on gases, at temperatures other than 0°C, heretofore reported, are those of Archer[2] and of Sherrat and Griffiths[3] on carbon dioxide; of Gregory and Dock[4] on hydrogen; and the older data of Eucken[5] for several gases. The latter measurements were relative to air, and were made at widely spaced intervals.

Data on the thermal conductivities of gases is also of interest in connection with further development of the theory of transport properties of gases. The classical theory is well developed for spherically symmetric molecules possessing translational energy only,[6] but very little progress has been made on the more difficult problem of molecules with internal degrees of freedom. The Chapman-Enskog relationship

$$K = \epsilon \eta C_v \qquad (1)$$

between thermal conductivity (K), viscosity (η), and heat capacity (C_v) is of particular interest.

[1] Fellow of the Charles A. Coffin Foundation 1939–40, E. I. du Pont Fellow 1940–41.
[2] C. T. Archer, Phil. Mag. **19**, 901 (1935).
[3] G. G. Sherrat and E. Griffiths, Phil. Mag. **27**, 68 (1939).
[4] H. Gregory and E. H. Dock, Phil. Mag. **25**, 129 (1938).
[5] (*a*) A. Eucken, Phys. Zeits. **12**, 1101 (1911); (*b*) **14**, 324
[6] S. Chapman and T. G. Cowling, *Mathematical Theory of Non-Uniform Gases* (Cambridge University Press, New York, 1939).

Other work from this laboratory[7] has supplied data on viscosity and on heat capacity, covering a wide temperature range. It was felt desirable to supplement these results with extensive data on thermal conductivity.

Nearly all precise thermal conductivity measurements on gases have been made with some modification of the hot wire cell. The general method of operation of these cells is well known. In all of them a wire, fixed along the axis of a cylindrical tube, is heated by an electric current. The rise in temperature of the wire, as determined from its resistance increases, together with the power dissipated and the dimensions of the wire and tube, permit calculation of the thermal conductivity of the gas in the tube. The principal correction is for heat conducted longitudinally by the wire, since the thermal conductivity of the metal is much greater than that of the gas. Various modifications of the hot wire cell represent attempts to deal with this difficulty. The principal types that have been used may be referred to as: (1) compensating cells; (2) the "thick-wire" cell; and (3) the potential lead type of cell. Compensating cells[8] involve the use of two cells that differ only in length, so that differential measurements refer, effectively, to the central portion of the longer cell. In the "thick-wire" cell, developed by Kannuluik and Martin,[9] no attempt is made to minimize end conduction by the use of fine wires. Instead, the ends of the cell are so constructed as to lead to relatively simple boundary conditions, so that the problem of the complete heat flow (along the wire and through the gas) may be solved.

In the potential lead type of cell, which has been used by Weber,[10] very fine potential leads are attached to the cell wire so as to give the potential drop through a central segment. End conduction is thus reduced to a small correction.

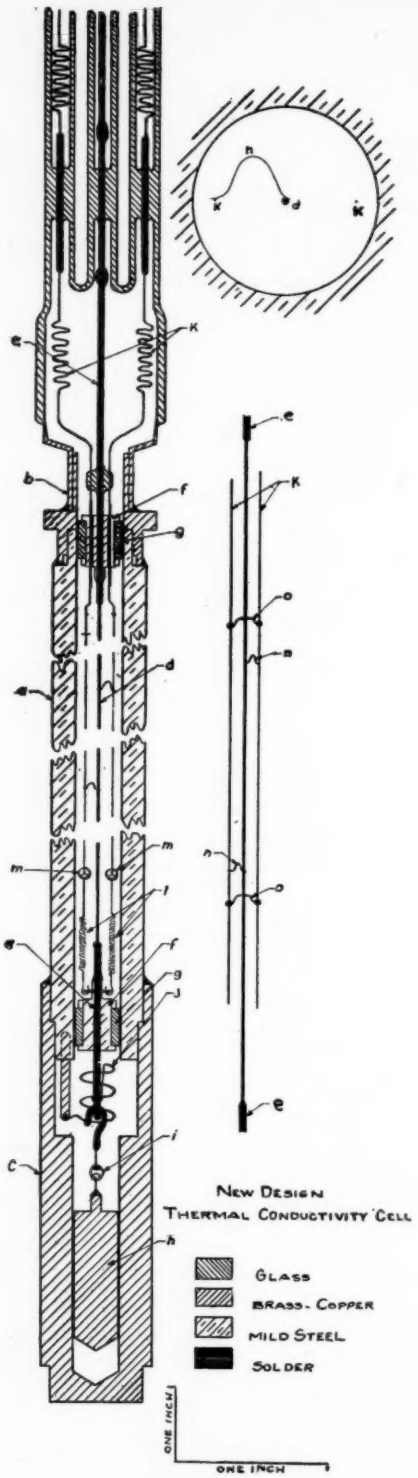

FIG. 1. Thermal conductivity cell.

[7] *Viscosities:* (*a*) H. L. Johnston and K. E. McCloskey, J. Phys. Chem. **44**, 1038 (1940); (*b*) H. L. Johnston and E. R. Grilly, *ibid.* **46**, 948 (1942).
Heat capacities: (*c*) H. L. Johnston and A. T. Chapman, J. Am. Chem. Soc. **55**, 153 (1933); (*d*) H. L. Johnston and M. K. Walker, *ibid.* **55**, 172 (1933); (*e*) H. L. Johnston and D. H. Dawson, *ibid.* **55**, 2744 (1933); (*f*) H. L. Johnston and C. O. Davis, *ibid.* **56**, 271 (1934); (*g*) C. O. Davis and H. L. Johnston, *ibid.* **56**, 1045 (1934); (*h*) H. L. Johnston and E. A. Long, J. Chem. Phys. **2**, 389 (1934); (*i*) H. L. Johnston and M. K. Walker, J. Am. Chem. Soc. **57**, 682 (1935).

[8] A recent investigation with compensating cells is that by B. G. Dickens, Proc. Roy. Soc. **A143**, 517 (1934).

[9] W. G. Kannuluik and L. H. Martin, Proc. Roy. Soc. **A141**, 144 (1933); **A144**, 496 (1934).

[10] S. Weber, Ann. d. Physik **54**, 325 (1917).

The characteristics of these three types of cell may be summarized by the statement that the end conduction is canceled out in the compensating type of cell; is large but subject to a relatively exact correction in the "thick-wire" type of cell; and is essentially absent in the potential lead type of cell.

The potential lead type of cell was chosen for the present series of investigations because of the simplicity of the calculations in the treatment of the data and because the near absence of end-conduction removes the possibility of serious systematic error. Important improvements were made in the design of the cell.

The present paper is limited to a description of the apparatus and method, and to results obtained with air. A subsequent paper by one of us will present data obtained with several other gases.

Air used in this investigation was taken from outside the laboratory and freed from carbon dioxide and water vapor by slowly bubbling it through a train consisting of: (*a*) concentrated sodium hydroxide; (*b*) concentrated sulfuric acid; (*c*) stick potassium hydroxide; and (*d*) phosphorus pentoxide. Finally, it was passed through a liquid nitrogen trap (at less than atmospheric pressure so that no air condensed).

DESCRIPTION OF APPARATUS

The apparatus consists of: (1) the cell; (2) the thermostated bath; and (3) the electrical circuits. Their description follows.

(1) The Cell

An accurately bored steel tube, with a diameter sufficiently small to insure the absence of convection, was used for the cell. Positive centering of the 0.01-inch platinum cell wire was obtained by the use of cylindrical pistons sliding in the tube. Constant tension on the cell wire was maintained by means of a weight, so chosen that there was negligible vibration of the wire. Platinum potential leads, 0.0005 inch in diameter, were used. A more detailed description follows.

The construction of the cell is illustrated in Fig. 1, where it should be noted that the vertical scale of the main drawing is compressed in the ratio 1:2 with respect to the horizontal scale. The full length inset of the wire system is on the same scale as the cell, while the inset showing the cross-sectional view of the tube interior and wires is on an enlarged scale.

The central portion of the cell consists of a mild steel tube, (*a*), 11 inches in length, $\frac{5}{8}$ inch in outside diameter, and approximately 0.800 cm in internal diameter, which was accurately bored by the Winchester Repeating Arms Company, New Haven, Connecticut. The exterior of the tube was chromium plated, to prevent corrosion. At the upper end this tube is soft soldered to a copper-Pyrex glass seal, (*b*), about 2.5 cm in diameter, and at the lower end to a long brass cap, (*c*), forming an extension of the tube.

The cell wire was selected for freedom from irregularities from Bishop C. P. 0.01-inch platinum wire. A 22-cm length, (*d*), was fused to 1-mm platinum leads (*e*, *e*), which, in turn, were silver soldered through holes drilled centrally in small steel cylinders, (*f*, *f*), 0.43 cm in diameter by 1.5 cm in length. The cell wire was brought to the axis of these cylinders by slightly bending the heavy platinum wires until observation with a micrometer comparator showed proper centering. Glass tubes (*g*, *g*), 1.5 cm long, fit closely over the steel cylinders (*f*, *f*), and fit closely within the steel tube. These tubes were specially moulded by the Fischer-Schurman Company, and were selected for concentricity. The glass served to insulate the cell wire, electrically, from the tube. In order to permit the free passage of gas, a 60° section was cut from each of the glass insulators. This use of glass insulated "pistons" insures accurate centering of the cell wire within the tube and at the same time permits vertical motion made necessary to compensate for thermal expansion or contraction of either the upper lead wire or of the cell wire. The possible departure of the cell wire from center is estimated as not more than 0.014 cm, which is about the radius of the wire.

A constant tension is maintained on the cell wire by means of an 18-gram weight, (*h*), suspended from the lower "piston" but insulated from it by a glass bead, (*i*). It is important to maintain constant tension on the cell wire since it is used as a sensitive resistance thermometer. It was determined that, with this amount of loading, vibration of the cell wire was negligible

under normal operating conditions (maximum amplitude 0.001 cm).

The current lead to the upper end of the cell wire enters by way of a tungsten through Pyrex seal. The external portion of this lead is insulated from the bath by a glass tube fused to the seal. The lower end of the cell wire is connected to the steel tube by means of a short spiral, (j), of 0.01-inch copper wire of small rigidity. The lower external current connection is made directly to the metal cell.

The system of potential leads (k, k) enters the cell by tungsten-through-Pyrex seals at the upper end of the copper-Pyrex seal. Like the upper current leads, the external portions of the potential leads are insulated from the bath by glass tubes. The external leads and the portions of these leads that extend between the tungsten to Pyrex seals and the upper piston are of 0.01-inch platinum. The 0.01-inch platinum leads pass downward through 0.02-inch holes in the upper piston, from which they are insulated by means of glass capillaries. Between the two pistons the leads continue as 0.003-inch platinum wires parallel to and 0.3-cm distant from the cell wire. These 0.003-inch wires are held under a 2-gram tension by means of springs (l, l) consisting of 0.15-cm helices of 0.003-inch piano wire, hooked to the lower piston but insulated from the platinum leads by glass beads (m, m).

From the 0.003-inch platinum lead wires connections are made to the central portion of the cell wire—6.3 cm in length—by 0.5-cm lengths of 0.0005-inch diameter platinum Wollaston wire (n, n), the junctions being gold soldered. The junctions with the cell wire each required only 0.015 mg of gold (a 1×5-mm strip of gold leaf) but inspection with a 20× microscope showed that the Wollaston wires emerged cleanly from the gold and normal to the cell wire.

In order to prevent injury to the Wollaston wires by an accidental movement of the parallel "side wires" it was found necessary to add the two semi-circular braces (o, o), of 0.003-inch platinum wire shown in the inset of Fig. 1. These braces are 1 cm distant from the Wollaston wires and are at no point nearer than about 0.25 cm to the cell wire. They are insulated from the "side wires" by 0.5-mm glass beads.

Tests with the completed cell showed that no anomalous effects were caused by the use of the fine Wollaston wires, even though the voltages were measured with a precision of 0.1 microvolt (or 1 part per million). It was determined, by reversing the current in the cell, that no perceptible thermoelectric force was produced in the potential leads by heating of the cell wire.

TABLE I. Dimensions (at 300°K) that enter directly into the calculations of thermal conductivity.

Internal radius of tube (r_2)	=0.40017 cm	(±0.02%)
Radius of cell wire (r_1)	=0.01277 cm	(±0.18%)
Effective length of cell wire (L)	=6.327 cm	(±0.03%)

Dimensions of the cell which enter directly into the accurate calculation of the conductivity of the gas are the internal radius of the cell tube, the radius of the cell wire, and the effective length of the cell wire (that is, the length between the potential leads). The radius of the tube was calculated from its length and volume; the length was measured on a Société Genevoise micrometer comparator and the volume was determined by weighing the mercury required to fill the tube (using plane end pieces). The radius of the platinum cell wire was determined by weighing the segment used in the cell. The length of the segment was measured with a Gaertner cathetometer, after annealing the wire for eight days at 600°C under a tension of 20 grams. The value selected for the density of platinum, which was required in the calculation, was 21.40±0.06 grams cm^{-3} at 20°C.[11]

The effective length of the cell wire was measured with a Gaertner micrometer comparator after the potential leads were attached. The final values obtained for the principal dimensions of the cell at 300°K, and the estimated uncertainties, are given in Table I.

Dimensions that are required only for calculating corrections to the conductivity were

[11] Kahlbaum and Sturm, Zeits. f. anorg. Chemie **46**, 217 (1905), report a density of 21.44 grams cm^{-3} for pure annealed platinum wire; Stas, Oeuvres Complètes, Bruxelles-Leipzig **2**, 742 (1894) found platinum to approach an upper limiting density of 21.46 grams cm^{-3} on working and annealing. The widely quoted value of 21.37 g cm^{-3} is due to a misinterpretation of the work of Richards and Stull, Carnegie Inst. Pub. **76**, 55 (1907), who reported a density of 21.31 grams cm^{-3} but also tabulated the specific gravity referred to 20°C, namely 21.37. Since Richards and Stull worked with a platinum cylinder it might be expected that their result would be lower than the maximum densities quoted above.

determined with less accuracy. They are listed in Table II, together with the estimated uncertainties.

The lengths of the end segments of the cell wire differ by only 0.04 cm and it is permissible to consider them equal, and equal to $(l_0-l)/2$.

(2) Thermostat

In the completed experimental arrangement, the cell is mounted in a thermostat, containing a suitable bath liquid, which may be adjusted to maintain any temperature in the range 120° to 400°K. When the thermostat is carefully adjusted the oscillations of the temperature about its mean value may be reduced to ±0.003°. The mean temperature may vary on the order of 0.01° per hour, but these slow variations introduce no error into the measurements. The thermostat is similar to the cryostat described by Scott and Brickwedde,[12] but the smaller Dewar tube available made necessary a different placement of the cooling and heating surfaces. An improvement is the use of a continuously variable heater control circuit which decreases the tendency of the temperature to oscillate about its mean value.

A Dewar tube 4 inches in diameter and 36 inches deep holds the bath liquid. It stands beneath a circular hole cut in a heavy (400-pound) stone table top, to which the support for the thermal conductivity cell is bolted; the cell makes no direct contact with the other objects in the thermostat. Sections of red-fiber were introduced into all metal supports descending into the bath to minimize heat leak, and the cell is further insulated from its support by red-fiber washers.

The heavy (20-pound) brass stirring well, 2 inches in internal diameter, is placed at one side of the Dewar. A ⅜-inch stainless steel shaft, turning in brass bearings mounted on the outside of the stirring well, drives a 2½-inch propeller at the bottom of the Dewar tube. The shaft is coupled by means of a red-fiber rod to the drive shaft above, which is equipped with oversized ball bearings. With the cooling tube (to be described) in place, the bath liquid is circulated (up through the stirring well) two to four times per minute at 400 r.p.m.

The cooling tube, an unsilvered Pyrex Dewar tube 1½ inches in external diameter and 30 inches deep, with a separation of 1 mm between the walls, is mounted so that the lower 24 inches descends into the stirring well. When cooling is required, liquid oxygen (or nitrogen) is maintained at a constant level in the cooling tube by a float and relay arrangement which controls the flow of liquid oxygen from a reservoir. Control of the cooling rate is effected by varying the gas pressure between the double walls of the cooling tube. A pressure of 0.5-mm Hg of hydrogen gives sufficient cooling at 125°K while it is possible to thermostat a few degrees below room temperature with liquid oxygen in the Dewar by reducing the pressure to 0.002-mm Hg. With 1-cm Hg of hydrogen in the tube, the bath is cooled at an initial rate of 50 degrees per hour; the rate drops to 20 degrees per hour at 160°K and to 5 degrees per hour at 120°K.

The heater consists of 30 ohms of bare Nichrome wire wound bifilarly directly on the part of the cooling tube in the bath. The bath liquid thus circulates through the annular space between the cooling tube and the stirring well, in intimate and simultaneous contact with the cooling and heating surfaces. It is convenient to adjust the pressure in the cooling tube to give somewhat greater than optimum rate of cooling at the desired temperature, and then to reduce the cooling rate to the small optimum value by supplying a constant heating current to the heater. Similarly, in thermostating above room temperature, the constant heating current is adjusted to give a small rate of cooling at the desired temperature.

The actual thermostating, in both cases, is then accomplished by automatic regulation of a few watts of variable heating. A six-junction copper-constantan thermocouple, with the junctions exposed directly to the bath, is balanced against a Leeds and Northrup Type K poten-

TABLE II. Dimensions (at 300°K) that enter only into correction terms.

Total length of cell wire (l_0)	= 22.09 cm	(±0.2%)
External radius of tube (r_3)	= 0.795 cm	(±1%)
Radius of potential leads (Wollaston) (r_L)	= 6.25×10^{-4} cm	(±10%)
Length of potential leads (l_L)	= 0.5 cm	(±10%)

[12] R. B. Scott and F. G. Brickwedde, J. Research Nat. Bur. Stand. 6, 401 (1931).

tiometer. A beam of light is reflected by a Leeds and Northrup Type R galvanometer onto a gas-filled photoelectric cell, which in turn controls the variable component of the heating through a phase shift Thyratron circuit, as described by Strong.[13]

Several bath liquids were employed. Above room temperature a low viscosity mineral oil was used; water was not satisfactory as it was absorbed by the red-fiber. Difluorodichloromethane was used from a degree or two above its melting point, 120°K, to about 160°K. This bath gave excellent thermostating because of its low viscosity. A mixture of 32.7 percent ethyl bromide, 26.5 percent methylene chloride, 15.6 percent trichloroethylene, 13.6 percent chloroform, and 11.6 percent transdichlorethylene (by volume), as described by Scott and Brickwedde,[12] was satisfactory in the range 150° to 250°K. In the range 205° to 300°K, a mixture of equal parts by weight of chloroform and carbon tetrachloride was employed.

Temperatures near 80° and 90°K were obtained by filling the thermostat with liquid nitrogen or liquid oxygen, respectively. It was necessary to stir these baths vigorously to maintain a steady temperature.

(3) Electrical Circuits

The electrical circuit used to measure both the resistance of the "effective length" of the cell wire, and its energy dissipation, is quite simple. Its resistance—which ranged from about 0.029 ohm at 80°K to about 0.177 ohm at 380°K—was determined by dividing the potential difference between the potential leads by the current through the wire. The latter was determined by measuring the potential difference across a standardized manganin resistance of 0.128477 ± 0.000025 ohm, at 25°C, which was inserted in the external circuit of the current leads. Potential differences were measured with a White double potentiometer of 100,000 microvolt range, with a precision of 0.1 microvolt. The current through the cell, and standard resistance, was supplied by two 2-volt heavy duty lead storage cells, of 450-ampere hour capacity, in parallel, and amounted to about 0.1 ampere during (resistance thermometer) calibration of the cell wire and to about 0.5 ampere during thermal conductivity measurements. The current was varied in steps, as desired, by a set of manganin resistors, with mercury contacts, which were in series with the cell wire and were adjustable in steps of 0.01 ohm.

Since it is important that the standardized resistance in series with the cell wire be practically independent of the cell current special attention was given to its design and its construction. It consists of 15 parallel strands of bare manganin wire (0.25 ohm per cm) soldered between copper bars (5×10^{-6} ohm per cm). The entire unit is immersed in yellow ceresin wax. It was calibrated by comparison with National Bureau of Standards certified resistances of nominal 10 ohms, 100 ohms, and 10,000 ohms, respectively. A ratio method was employed, and potential differences were measured on the White potentiometer. The final value of this calibration is given above, its uncertainty being fixed by the small uncertainties assigned to the National Bureau of Standards certification of the standard resistances. The resistance of the standardized resistance proved constant, to within 0.01 percent for currents ranging from 0.06 to 0.6 ampere.

Intercomparisons of the decade coils of the White potentiometer were made in the manner recommended by the manufacturer (Leeds and Northrup) and the resistance ratios were found to lie within permissible tolerances. In the course of the measurements, small contact and thermal electromotive forces in the potentiometer circuit and in external circuits were determined and the proper corrections applied.

TEMPERATURE MEASUREMENTS

(1) Temperature Scale

The temperature scale for this research was established by means of a standard thermocouple, thermocouple *C*, which was mounted in the thermostat. The junction was about 1 cm from the central portion of the steel cell tube. Thermocouple *C* was calibrated against University of California thermocouple No. 101, which

[13] J. Strong, *Procedures in Experimental Physics* (Prentice-Hall, Inc., New York, 1938), p. 447. Note that the connection shown by Strong between the cathode of the photoelectric cell and the plate of the Thyratron should be eliminated.

had been calibrated by Greensfelder and Milner[14] in terms of the hydrogen scale of Giauque, Buffington, and Schulze.[14] The original calibration of couple *C* extended over the range 110° to 300°K. The correction curve was extrapolated to 80°K. The calibration was extended to higher temperatures by comparison, at 323°, 343°, and 373°K, with a mercury-in-glass thermometer certified by the National Bureau of Standards. The three new calibration points lie on a smooth extrapolation of the original table. It is believed that the temperature scale is reliable to about ±0.05 degree over the entire range. The electromotive force of the thermocouple is read on a Leeds and Northrup, White double potentiometer, with a range of 10,000 microvolts in steps of 1 microvolt, and a galvanometer sensitivity of 6 cm on the scale per microvolt. The sensitivity of the thermocouple varies from 20 to 50 microvolts per degree. The precision of measurement of the temperature was 0.003 degree, in a series of measurements at a given temperature.

(2) Calibration of Cell Wire

The calibration of the resistance of the cell wire was carried out concurrently with the thermal conductivity measurements on air. The wire had previously been annealed at 600°C by passing a current through the evacuated cell. The calibration involved a measurement of the resistance of the wire when heated by a current of about 0.1 amp. This value was a compromise between the requirement for minimum heating of the cell wire and the necessity for sensitivity in the measurement of the temperature of the wire. The resultant heating of the cell wire was about 0.50 degree (approximately independent of temperature), and the precision of measurement was 0.003 degree.

The initial correction for the heating of the cell wire was effected by a linear extrapolation of the wire resistance against the square of the current, to zero current. This was possible through the use of the conductivity measurement, made concurrently with about 0.5 ampere. A preliminary correction curve for the wire was then computed, and preliminary thermal conductivities of air calculated. The latter then permitted an accurate calculation of the heating of the wire in the 0.1 ampere runs, and thus the calculation of the final correction curve. The final curve differed from the preliminary curve by 0.07 degree at the lowest temperature and by 0.01 degree at the highest, in just the way it was anticipated the dependence of the resistance and the gas conductivity on the absolute temperature would affect the linearity of the aforementioned extrapolation.

The corrected resistance readings were compared with the temperature, read on the standard thermocouple by means of a deviation plot, on which deviations of the observed resistances from an equation in T were plotted against temperature. The average deviation of the 20 calibration points from a smooth curve on the deviation plot was ±0.015 degree. However, the average deviation of 17 of the 20 points was only ±0.008 degree.

CALCULATION OF THE CONDUCTIVITY

(1) General

The heat produced in the effective length of the cell wire is dissipated principally by conduction through the gas to the cell wall. Corrections are required for longitudinal conduction in the cell wire, for conduction of heat from the cell wire by the potential leads, and for radiation from the cell wire. Correction must also be made for the temperature drop through the cell wall, and for temperature discontinuities between the gas and the surfaces of the cell wire and cell wall —the well-known "temperature-jump" effect.[15]

The temperature-jump correction requires that measurements be carried out at two or more gas pressures.

The heat flow in the gas in the central region of the cell may be regarded as radial—that is, the effect of longitudinal heat flow in the gas is negligible.[16] The differential equation governing the heat flow is, therefore

$$-\partial T/\partial r = (Q - \sum q_i)/2\pi LKr, \qquad (2)$$

where T is the temperature at the radial distance

[14] (*a*) B. S. Greensfelder and R. T. Milner, J. Am. Chem. Soc. **50**, 2205 (1928); (*b*) W. F. Giauque, R. M. Buffington, and W. Schulze, *ibid.* **49**, 2343 (1927).

[15] E. H. Kennard, *Kinetic Theory of Gases* (McGraw-Hill Book Company, Inc., New York, 1938), Chap. VIII.

[16] W. G. Kannuluik and L. H. Martin, Proc. Roy. Soc. (London), have given the necessary equations for calculating the latter effect (see reference 9).

r; Q is the total heat produced per unit time in the effective length, L, of the wire; q_i is the heat flowing per unit time from the effective length of the cell wire by any mechanism other than conduction through the gas; and K is the thermal conductivity of the gas at the temperature T.

(2) Temperature-Jump Correction

In order to account for an apparent small dependence of the conductivity, as measured in a hot wire cell, on the pressure of the gas, it is found necessary to allow for the temperature-jump effect at the surface of the wire and, to a lesser extent, at the cell wall. The existence of such a temperature discontinuity when heat flows across a gas-solid interface is well established, and the temperature jump, δT, is known to be proportional to the temperature gradient in the gas and inversely proportional to the pressure of the gas.[15]

$$\delta T = g\partial T/\partial r = (g'/p)\partial T/\partial r. \tag{3}$$

When account is taken of the temperature jump, Eq. (2) may be integrated to yield the relation

$$1/K_a = (1/K) + (A/p), \tag{4}$$

where K is the true average conductivity of the gas over the range T_1 to T_2, and K_a, the apparent conductivity at the pressure p, is calculated from the relation

$$K_a = K_u - \sum_i K_i. \tag{5}$$

K_u is the uncorrected conductivity of the gas calculated from the experimental data and the equation

$$K_u = Q \ln (r_2/r_1)/2\pi L(T_1 - T_2). \tag{6}$$

K_i is an effective conductivity for the ith subsidiary mechanism of heat conduction, as defined by

$$K_i = q_i \ln (r_2/r_1)/2\pi L(T_1 - T_2). \tag{7}$$

The constant A in the small correction term in Eq. (4) is given by the expression

$$A = [1/\ln (r_2/r_1)][(g_1'/K_1 r_1) + (g_2'/K_2 r_2)], \tag{8}$$

where K_1 and K_2 are the conductivities of the gas at T_1 and T_2, respectively.

It follows from Eq. (4) that a plot of $(1/K_a)$ against $(1/p)$, for constant T_1 and T_2, yields a straight line, and that extrapolation of the line to its intercept at $(1/p)=0$ yields $(1/K)$, where K is the true conductivity. It is clear from Eq. (3) that the temperature jump effect vanishes at $(1/p)=0$, but actual measurements at very high pressures are not practicable because of the great increase of convection at high pressures. The use of Eq. (4) is thus a method of correcting for the temperature-jump effect and at the same time avoiding convection in the gas. Careful experimental tests of Eq. (4), as applied to a hot wire cell, have been made by B. G. Dickens.[8] The results of the present investigation also confirm the correctness of the linear relation predicted by Eq. (4), as will be shown later.

(3) Correction for End Conduction

The correction for end conduction, or for the heat flowing from the effective length of the cell wire into the end-segments of the cell wire, may be calculated with considerable accuracy. The differential equation for the longitudinal temperature distribution in the cell wire may be written

$$\frac{d^2\Theta}{dx^2} - B_1^2\Theta + B_2 = 0, \tag{9}$$

$$B_1 = \left[\frac{2K}{\lambda r_1^2 \ln (r_2/r_1)} - (B_2 R_0'/R_0)\right]^{\frac{1}{2}}, \tag{10}$$

$$B_2 = (R_0 I^2/\pi r_1^2 L\lambda J), \tag{11}$$

where $\Theta = (T_1 - T_2)$, at constant T_2, and x is the longitudinal distance along the wire. The radii of the cell wire and of the cell are r_1 and r_2, respectively, and L is the length of the effective portion of the cell wire. K is the average thermal conductivity of the gas, and λ is the thermal conductivity of the (platinum) cell wire. R_0 is the resistance of the effective length of the cell wire at $\Theta=0$, $(T_1=T_2)$, and R_0' is the temperature coefficient, (dR_0/dT_2). I is the current flowing through the cell wire, and J is the mechanical equivalent of heat.

The boundary conditions on Eq. (9) are that $\Theta=0$ at the ends of the wire, $x=0$ and $x=L_0$, where L_0 is the total length of the cell wire. The nature of the solution depends upon whether the constant B_1 is real or imaginary; B_1 is real for the present cell, under the conditions of opera-

tion. Instead of calculating directly the heat flowing from the effective length of the cell wire, Θ may be integrated over the range $x=(L_0-L)/2$ to $x=(L_0+L)/2$ to give the average temperature, Θ av., of the effective length, which is related to the observed resistance R. The result is:

$$\Theta \text{ av.} = [(R-R_0)/R_0'] = (B_2/B_1^2)\left[1-(2/B_1L)\frac{\sinh (B_1L/2)}{\cosh (B_1L_0/2)}\right]. \quad (12)$$

As L_0 increases without limit, the correction for end conduction vanishes, and Θ av. approaches the constant value (B_2/B_1^2). The effective conductivity for end conduction, K_e, is therefore:

$$K_e=[(2/B_1L)\sinh (B_1L/2)/\cosh (B_1L_0/2)]K_u, \quad (13)$$

where K_u is given by Eq. (6).

For the present cell, and for $I=0.5$ ampere, K_e decreases from 0.0086×10^{-5} to 0.0006×10^{-5} cal. deg.$^{-1}$ cm^{-1} sec.$^{-1}$ as K_u increases from 2×10^{-5} to 5×10^{-5} cal. deg.$^{-1}$ cm^{-1} sec.$^{-1}$. The maximum value of the correction in the present investigation was 0.5 percent.

(4) Lead Wire Correction

The correction for the heat flowing from the cell wire to the platinum potential leads is not susceptible to as accurate a calculation as the other corrections. The following treatment is a modification of that of S. Weber.[10] The temperature distribution in the potential lead, as a function of the distance from the cell wire, x, should satisfy Eq. (9) approximately, with $B_2=0$ and

$$B_1=[2K/\lambda(r_1')^2\ln (r_2'/r_1')]^{\frac{1}{2}}, \quad (14)$$

where r_1' is the radius of the potential lead, and r_2' is an effective radius, of the order of magnitude of the radius of the tube, r_2. The boundary conditions are $\Theta=(T_1-T_2)$ at $x=0$ and $\Theta=0$ at $x=L'$, where L' is the length of the potential leads. The heat flowing into the potential leads may be calculated from the value of $(d\Theta/dx)$ at $x=0$ (only half of this heat contributes to the correction). The result may be expressed as the effective conductivity of the potential leads, K_p, by means of Eq. (7),

$$K_p=\lambda(r_1')^2B_1\ln (r_2/r_1)/2L\tanh (B_1L'). \quad (15)$$

It is clear that K_p is not sensitive to the value of (r_2'/r_1'). It seems safe to assume that

$$10^2<(r_2'/r_1')<10^4$$

since these limits correspond to

$$0.06 \text{ cm}<r_2'<6 \text{ cm}$$

and r_2' should be of the order of magnitude of $r_2=0.4$ cm. For (r_2'/r_1') in this range, and for the values of the gas conductivity that occur

$$0.99<\tanh (B_1L')<1,$$

so that the correction is essentially independent of L'. On setting $\tanh (B_1L')$ equal to unity, and introducing the above mentioned limits for (r_2'/r_1') and the numerical values of the other constants, Eq. (15) reduces to

$$K_p\times10^5=(0.012\pm0.002)(K\times10^5)^{\frac{1}{2}}. \quad (16)$$

The largest value of the correction in the measurements on air was 0.80 percent, and the average value was 0.50 percent.

(5) Radiation Correction

A correction is required for the transfer of heat by radiation from the cell wire. Milverton[17] has measured the radiation loss from a polished platinum wire in a hot-wire cell, over the range 0° to 100°C. His results are in essential agreement with the theoretical expression for radiation between two coaxial cylindrical surfaces.[18] A measurement of the radiation loss from the present cell was carried out at 317°K. Conduction of heat by the residual gas in the evacuated cell was negligible. Under the conditions of the measurement, Eqs. (10)–(12) applied, with an obvious change in the meaning of K, since radiation replaced thermal conduction. The result of the measurement, expressed as the emissivity of the platinum wire, was 5.3 percent higher than the value found by Milverton at the same temperature.

For the calculation of the radiation correction in the thermal conductivity measurements, the value of the emissivity of platinum measured at 317°K in the present cell was adopted, together

[17] S. W. Milverton, Phil. Mag. **17**, 414 (1934).
[18] M. Jakobs and G. A. Hawkins, *Elements of Heat Transfer* (John Wiley and Sons, Inc., New York, 1942), pp. 125–126.

TABLE III. Thermal conductivity of air at 273.263°K.

Time (A.M.)		2:08	2:50	3:26	4:06	4:39	7:46
Pressure, p	(cm Hg)	19.55	8.94	4.37	1.70	0.615	8.30
Reciprocal of pressure, $(1/p)$		0.051	0.112	0.229	0.588	1.63	0.120
E.m.f. of thermocouple C	(microvolts)	254.2	254.3	254.2	254.3	254.4	254.1
Wall temperature, T_2	(°K)	266.457	266.454	266.457	266.454	266.452	266.460
E.m.f. across 0.128477 ohm resistor	(microvolts)	69437.3	69433.6	69429.2	69422.9	69410.3	69435.8
Cell current, I	(ampere)	0.54046	0.54044	0.54040	0.54035	0.54025	0.54045
E.m.f. across cell	(microvolts)	70047.5	70049.4	70056.5	70084.4	70175.7	70053.8
Cell resistance, R	(ohm)	0.129606	0.129616	0.129638	0.129701	0.129894	0.129620
Wire temperature, T_1	(°K)	280.068	280.089	280.134	280.265	280.663	280.097
Average temperature, $T_{av}=\frac{1}{2}(T_1+T_2)$	(°K)	273.263	273.272	273.296	273.360	273.558	273.279
Temperature interval, $\Theta=(T_1-T_2)$	(°K)	13.611	13.635	13.677	13.811	14.211	13.637
Uncorrected conductivity, $K_u=0.020720(RI^2/\Theta)$	(cal./cm sec. deg.)	5.763	5.753	5.735	5.681	5.528	5.752×10^{-5}
Sum of effective conductivities of end conduction, potential leads and radiation	(cal./cm sec. deg)	0.105	0.105	0.105	0.105	0.105	0.105×10^{-5}
Apparent conductivity, K_a (at T_{av} and p)	(cal./cm sec. deg.)	5.658	5.648	5.630	5.576	5.423	5.647×10^{-5}
Apparent conductivity, K_a (at 273.263°K and p)	(cal./cm sec. deg.)	5.658	5.648	5.629	5.574	5.418	5.647×10^{-5}
$(1/K_a)$, at p cm Hg)		1.7674	1.7705	1.7765	1.7940	1.8457	1.7709×10^{4}
$[1.7650+0.0496(1/p)]\times10^4$		1.7675	1.7706	1.7764	1.7942	1.8458	1.7710×10^{4}

True conductivity, at 273.263°K, $K=(1/1.7650\times10^4)=5.666\times10^{-5}$ cal. cm^{-1} sec.$^{-1}$ deg.$^{-1}$.

with the temperature coefficient found by Milverton. The effective conductivity for radiation, K_r, was then calculated from Eq. (7). In the thermal conductivity measurements on air, the correction amounted to 0.20 percent at 100°K, 0.74 percent at 200°K, 1.65 percent at 300°K, and 2.59 percent at 375°K.

(6) Wall Correction

A small correction for the temperature drop through the wall of the steel cell tube is readily calculated from the internal and external radii of the tube, and the thermal conductivity of the steel, 0.11 cal. cm^{-1} sec.$^{-1}$ deg.$^{-1}$. The greatest value of the correction in the measurements on air was 0.01 percent.

SAMPLE CALCULATION

The complete calculation of the thermal conductivity of air at 273.263°K is given in Table III for purposes of illustration. In this particular experiment the conductivity of air was measured at six pressures, over a period of about six hours. The uncorrected conductivity, K_u, at each pressure, is first calculated from Eq. (6). The effective conductivities for end conduction, K_e, the potential leads, K_p, and radiation, K_r, were 0.0004, 0.0286, and 0.0764×10^{-5} cal. cm^{-1} sec.$^{-1}$ deg.$^{-1}$, respectively. Subtraction of the sum of these corrections from K_u, as in Eq. (5), yields the apparent conductivity, K_a, at the pressure p and the average temperature for the experiment. The values of K_a are then corrected to a constant temperature, which is taken here as the average temperature of the measurement at the highest pressure, 273.263°K. These minute corrections may be made with an approximate temperature coefficient. According to Eq. (4) a linear relation should exist between $(1/K_a)$ and $(1/p)$. As shown in the table, the six points show a maximum deviation from a linear relation in $(1/p)$ of about 0.02 percent. Extrapolation of this linear relation to $(1/p)=0$ yields the true thermal conductivity of air at 273.263°K, 5.666×10^{-5} cal. cm^{-1} sec.$^{-1}$ deg.$^{-1}$.

EXPERIMENTAL RESULTS

Results obtained with air, in the temperature range 87° to 376°K, are given in Table IV. All data were obtained in August 1941 and the dates, listed in the first column, indicate the order in which measurements were made. Temperatures, in the second column, are the mean of the wire and the cell wall, which usually differed by about 13° in temperature. Pressures, in the third column, are those at which apparent

conductivities were measured. The true conductivities, in the fourth column, were obtained by plotting $(1/K_a)$ against $(1/p)$ and extrapolating to $(1/p)$ equal zero as described in the Sample Calculation.

The average percentage deviations from a straight line, in the $(1/p)$ plots, are shown in the fifth column and the percentage deviations from a smooth curve of K *versus* temperature, in the sixth. These indicate the precision of the data.

Values of the slopes in the $(1/K_a)$ *versus* $(1/p)$ plots are given in the seventh column. These will be referred to in a subsequent paper dealing with accommodation coefficients. For immediate purposes, they serve as a sensitive check on the reliability of the K's determined by extrapolation. Thus, the abnormally high slope in the 149.12° runs—which is clear out of line with the values at adjacent temperatures—makes the accuracy of that K somewhat suspect. Indeed, this is confirmed by the relatively large deviation of this K from the smooth curve of K *versus* temperature, as shown in Fig. 2.

The runs at 268.72° and at 279.45°K were taken with a single pressure only—namely 8.30 cm of Hg—and were made for the purpose of investigating the possible effect of the magnitude of the temperature interval. Their K's were obtained by using the observed $d(1/K)/d(1/p)$ at 273.26° for extrapolation to $(1/p)$ equals zero. Neither these two runs nor the one at 149.12° were given any weight in obtaining the smoothed curve of K *versus* T.

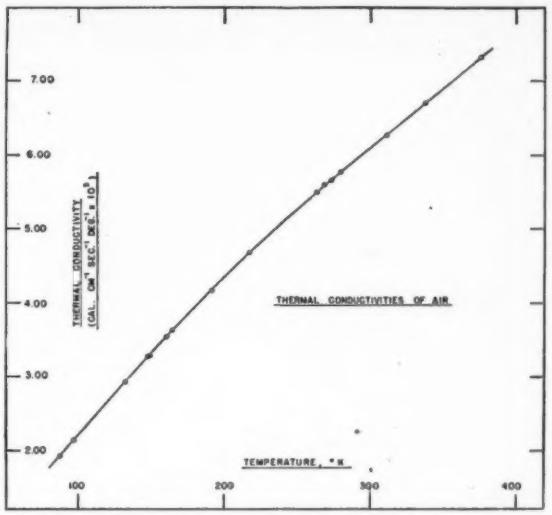

FIG. 2. Thermal conductivities of air.

Smoothed values of the thermal conductivities, at even temperatures, are given in Table V.

The table includes temperature coefficients, together with the smoothed conductivities, for use in making interpolations.

ACCURACY OF THE RESULTS

The average deviation of our 14 experimental values (the 149.12, 268.72, and 279.45° runs excepted for the reasons previously given) from the smooth curve on which Table V is based is

TABLE IV. Thermal conductivities of air.

Date (1941)	T, °K	Pressures (cm Hg, 0°C)	$K\times10^5$	% dev. $(1/K_a)$	% dev. K	$\frac{d(1/K)}{d(1/P)}$
Aug. 31	87.50	1.58, 9.53	1.922		−0.05	378
Aug. 30	97.04	2.04, 4.96, 9.595	2.141	0.03	+0.19	145
Aug. 28	132.33	2.135, 5.18, 9.69	2.924	0.04	−0.17	254
Aug. 28	147.61	2.01, 9.305	3.268		+0.09	299
Aug. 23	149.12	2.43, 9.66	3.283		−0.45*	1444
Aug. 24	160.41	1.955, 9.92	3.542		−0.03	505
Aug. 29	164.13	2.25, 10.06	3.628		+0.17	383
Aug. 25	191.30	2.075, 4.95, 10.12	4.171	0.00	−0.31	313
Aug. 26	217.42	1.74, 4.76, 10.36	4.684	0.02	−0.11	405
Aug. 26	240.78	2.24, 9.79	5.114		+0.04	434
Aug. 26	262.99	1.975, 5.28, 10.50	5.503	0.02	+0.20	448
Aug. 7	268.72	8.30	5.607		+0.34*	
Aug. 7	273.263	19.55, 8.94, 4.37, 1.70, 0.615, 8.30	5.666	0.02	+0.04	496
Aug. 7	279.45	8.31	5.774		+0.17*	
Aug. 13	310.75	1.87, 11.39	6.268		−0.05	547
Aug. 14	337.56	1.745, 10.32	6.705		+0.00	576
Aug. 14	375.76	1.16, 2.66, 5.68, 12.30	7.319	0.01	−0.01	574
			Average deviation		±0.104	

* These points were given no weight in obtaining the smoothed values of K, and have been omitted from the average deviation.

TABLE V. Smoothed values of the thermal conductivities of air as a function of the temperature.

T, °K	$K \times 10^5$	(dK/dT)
80	1.755	0.0224
90	1.979	224
100	2.203	224
110	2.427	224
120	2.651	224
130	2.875	223
140	3.097	221
150	3.317	2185
160	3.534	215
170	3.747	2105
180	3.955	2055
190	4.158	2005
200	4.356	1955
210	4.549	1905
220	4.737	1855
230	4.920	1805
240	5.098	176
250	5.272	172
260	5.442	1685
270	5.609	1655
280	5.773	163
290	5.935	162
300	6.097	162
310	6.259	162
320	6.421	162
330	6.583	1615
340	6.744	161
350	6.905	161
360	7.066	161
370	7.227	161
380	7.388	161
273.1	5.660	1647

± 0.104 percent. This corresponds to approximately $\pm 0.014°$ in the temperature interval and is about the precision with which we were able to maintain, and to measure, the temperature of the thermostated bath. Our precision is therefore limited, principally, by the evaluation of bath temperature.

To evaluate the accuracy of the smoothed values given in Table V consideration must be given to the influence of possible systematic errors. These are as follows:

(1) Shape Factor

A small systematic error, which may amount to 0.12 percent as a maximum, may enter through slight uncertainties in the dimension of the cell or slight inaccuracy in the centering of the wire. This limit is arrived at by considerations of the figures presented in Table I, in conjunction with application of the formula given by Kannuluik and Martin[9] for the effect of the possible 0.014-cm inaccuracy in the centering of the wire (cf. infra).

(2) Energy Input

A maximum systematic error of ± 0.06 percent may enter through slight errors in (*a*) standard cell voltage, (*b*) standard resistance, and (*c*) potentiometer calibration—all of which contribute to the measured energy input.

(3) Temperature Head Between Cell Wire and Cell Wall

Systematic errors associated with evaluation of the radial temperature difference between the cell wire and the cell wall may contribute ± 0.20 percent at most to errors in thermal conductivities. This figure is regarded as a liberal estimate and takes into account: (*a*) inaccuracies in the potentiometer coils (0.01 percent) which may contribute both to thermocouple and wire resistance measurements; (*b*) drift in the standard cell used with the potentiometer (<0.005 percent); (*c*) drift in the standard 0.128477-ohm resistance during the month in which measurements were made; (*d*) error in calibration of the cell wire (<0.01°); (*e*) drift in calibration of the cell wire (<0.01°); (*f*) error in the temperature coefficient of e.m.f. of the thermocouple (<0.05 percent); (*g*) the very small temperature difference between the inner and outer surfaces of the cell wall (<0.01 percent); and (*h*) the possible existence of a small temperature difference between the outer surface of the cell wall and the thermocouple. The relatively large external surface of the metal cell and the rapid stirring of the bath liquid make it unlikely that any significant temperature difference of the type (*h*) existed.

TABLE VI. Limits in systematic errors introduced through determination of average gas temperature and through radiation and conduction corrections, as functions of the temperature (°K).

Source of error	Total magnitude of correction (percent of conductivity)	Limiting systematic errors (percent of conductivity) 80°	180°	280°	380°
Gas temperature		±0.08	±0.03	±0.02	±0.01
Radiation correction	0.1 to 2.5	0.02	0.05	0.07	0.18
End conduction correction	0.5	0.08	0.01	0.00	0.00
Potential leads cond. corr.	0.15 to 0.8	0.23	0.15	0.13	0.11

TABLE VII. Systematic error limits (total).

T, °K	Total systematic error (percent) Random	Additive
80	±0.35	±0.79
180	±0.29	±0.62
280	±0.28	±0.60
380	±0.32	±0.68

Drift in the standard 0.128477-ohm resistance amounted to only 8 parts in 13,000 over a period of eight months and could not have much exceeded 1 part in 13,000 during the month that measurements were under way.

The runs at 268.72°, 273.26°, and 279.45°K (previously mentioned) were made for the express purpose of finding if there might be any systematic trend in the results as a function of the magnitude of the temperature difference between cell wire and cell wall. To accomplish this, all three runs were made at a pressure of 8.30 cm of Hg and with a bath temperature of 266.45°K. All other conditions except the wire temperature were kept comparable. Temperature heads for the three runs were, respectively, 4.535°, 13.638°, and 25.985°. Corrected by the same $d(1/K)/d(1/p)$ to zero $(1/p)$ the K's of these three runs deviated from the smooth K *versus* T curve by the respective amounts +0.34 percent, +0.04 percent, and +0.17 percent. No systematic trend is evident and the 0.34 percent deviation corresponds to an error of only 0.015° in the temperature interval, which is within the recognized range of experimental error. We conclude that no systematic error has been introduced by our adoption of an approximate 13° temperature head for the majority of the runs.

(4) Average Gas Temperature

While temperature *differences* are measured much more accurately, we cannot claim much better than ±0.05°, in an absolute sense, for our temperature scale. With account taken of some further error in calibration of the cell wire, we regard ±0.06° as a liberal estimate of the uncertainty in the average temperature of the gas in the cell. This is equivalent to a systematic error of ±0.08 percent in the thermal conductivity of air at 80°K and to ±0.013 percent at 380°K. Equivalent errors at intermediate temperatures are shown in Table VI.

(5) Systematic Errors in Corrections for Radiation, End Conduction, and Conduction of Heat by the Potential Leads

The corrections referred to here have been discussed in a previous section, and magnitudes of the corrections indicated. Like the error in average gas temperature, systematic errors in making these corrections are dependent on the temperature at which runs are made. Table VI summarizes the magnitude of these corrections at several temperatures and of the errors in the thermal conductivity which may enter through their presence. In arriving at these estimates consideration has been given to the error limits in both the correction equations and in the data they employ.

(6) Temperature-Jump Correction

The short extrapolation in the $(1/K_a)$ *versus* $(1/p)$ plot, which corrects for the temperature discontinuities between gas and wire and between

TABLE VIII. Comparison of our own results on the thermal conductivity of air with those of other observers.

T, °K	This research $K\times10^5$	Published values $K\times10^5$	Method*	Worker	Year
81.6	1.791	1.80	*HW(C)*	Eucken[a]	1913
194.6	4.250	4.26	*HW(C)*	Eucken[a]	1913
273.1	5.660	5.62	*HW(PL)*	Schleiermacher[b]	1888
273.1	5.660	5.72	*HW(PL)*	Schwarze[c]	1901
273.1	5.660	5.69	*HW(PL)*	Schwarze[c]	1902
273.1	5.660	(5.66)	*HW(C)*	Eucken[a]	1913
273.1	5.660	5.68	*HW(PL)*	Weber[d]	1917
273.1	5.660	5.67		Putzki[e]	1918
273.1	5.660	5.92	*HW(PL)*	Schneider[f]	1926
273.1	5.660	5.74	*HW(C)*	Weber[g]	1927
273.1	5.660	5.85	*HW(C)*	Gregory and Archer[h]	1933
273.1	5.660	5.81	*HW(C)*	Milverton[i]	1934
273.1	5.660	5.84	*HW(C)*	Dickens[j]	1934
273.1	5.660	5.76	*HW(TW)*	Kannuluik and Martin[k]	1934
273.1	5.660	5.72	*P P*	Hercus and Sutherland[l]	1934
273.1	5.660	5.78	*HW(C)*	Northdurft[m]	1937
313.1	6.308	6.84	*HW(PL)*	Schneider[f]	1926
323.1	6.470	6.68	*HW(AH)*	Sherratt and Griffiths[n]	1939
353.1	6.953	7.18	*HW(C)*	Milverton[i]	1934
373.1	7.275	7.18	*HW(C)*	Eucken[a]	1913
373.1	7.275	7.59	*HW(AH)*	Sherratt and Griffiths[n]	1939

* *Key to symbols:*
HW(C), compensating type of hot wire cell.
HW(PL), potential lead type of hot wire cell.
HW(TW), thick wire type of not wire cell.
HW(AH), hot wire cell with auxiliary heaters.
PP, parallel plate method.

[a] See reference 5.
[b] Schleiermacher, Wied. Ann., **34**, 623 (1888).
[c] Schwarze, Phys. Zeits., **3**, 264 (1901, 1902); Diss. Halle, 1902; Ann. d. Physik **11**, 303 (1903).
[d] See reference 10.
[e] Putzki, Diss. Halle, 1918; cf. Trautz and Zündel, Zeits. f. tech. Physik **12**, 273 (1931), Table I.
[f] E. Schneider, Ann. d. Physik **79**, 177 (1926).
[g] S. Weber, Ann. d. Physik **54**, 437 (1917); **82**, 479 (1927).
[h] H. S. Gregory and C. T. Archer, Phil. Mag. **15**, 301 (1933).
[i] See reference 17.
[j] See reference 8.
[k] See reference 16.
[l] E. C. Hercus and Sutherland, Proc. Roy. Soc. **A145**, 599 (1934).
[m] W. Northdurft, Ann. d. Physik **28**, 137 (1937).
[n] See reference 3.

gas and cell wall, is made with great accuracy. In the 273.26° series of runs the linearity of the reciprocal plot was well established in runs at six pressures that varied between 0.615 and 19.55 cm of Hg (cf. Table III), and the precision was high (±0.02 percent) on individual runs. The average difference between the apparent conductivity measured at the highest pressure and the true conductivity obtained by extrapolation was 0.18 percent, and the maximum difference was 0.37 percent (except for the 149.12° run for which the slope was anomalously high and the difference 0.49 percent). We estimate that the error introduced by the extrapolations —where runs were made at two or more different pressures—cannot exceed about 0.03 percent.

(7) Convection

The linearity in the reciprocal plots referred to in the previous paragraph indicates freedom from effects of convection. This was further confirmed in a separate series of runs made with oxygen in the cell, at 322.06°K. Seven runs were made in this series. Five runs in the pressure range 0.75 to 11.29 cm of Hg gave an average deviation from a straight line of only 0.01 percent, while runs at 28.5 and 75 cm, respectively, deviated from the linear plot by amounts of 0.08 percent and 0.14 percent, respectively. The deviations at these higher pressures were the result of convection. Convection was suspected in these two runs, even before the results were calculated and plotted because a small but continuous fluctuation of the cell resistance was observed that disappeared upon reducing the pressure. In the measurements on air at 273.26°K no convection was observed at 19.55-cm pressure.

We are confident that there is no significant influence of convection in the conductivities obtained for air.

(8) Over-all Systematic Error

The combined effect of the several sources of systematic error referred to in the paragraphs above has been calculated, as a function of temperature, on the basis of two limiting assumptions: (*a*) that the several errors are random in sign and (*b*) that they are all additive. Results are shown in Table VII.

The true situation must be somewhere between these extremes (for the *maximum* error) and can probably be regarded as 0.5±0.1 percent. We thus believe that our smoothed values of the conductivities in Table V are correct to within about one-half of one percent in an absolute sense. *Probable errors* are, of course, even less than this.

COMPARISON WITH THE RESULTS OF OTHER INVESTIGATORS

Comparison of our own results (smoothed values of Table V) with those of other workers is shown in Table VIII.

As is apparent from the table, very few measurements have been made, by other workers, at temperatures other than 0°C. Below the ice point the only published data are the two values reported by Eucken, which are relative to air at 0°C. These agree well with our own measurements.

Our own value at 273.1, which we believe to be reliable to within 0.5 percent, lies 2.5 percent below the average of values obtained with compensating cells; about 1.5 percent below Kannuluik and Martin's result with the thick wire cell; 1 percent below Hercus and Sutherland's determination by the parallel plate method; and from 0.2 percent to 1 percent below most other values by the potential lead type cell.

The errors in our own measurements have been carefully considered (cf. infra) and it is difficult to see how our results can be low beyond the ±0.5 percent claimed for accuracy unless we have overcorrected for end conduction, radiation or conduction by potential leads. However, the *total* correction for end conduction, at 273.1°, is only 0.01 percent. The radiation correction is 1.34 percent but can be applied accurately. It

TABLE IX. Temperature coefficient of the thermal conductivity of air at 273.1°K.

Investigator	$(dK/dT) \times 10^3$
This research	2.91
Schneider	3.9
Gregory and Archer	2.97
Dickens	2.9
Milverton	2.81
Schwarze	2.53
Weber	3.65
Schleiermacher	2.81
Eucken	2.71

was determined experimentally by us and is in agreement with the careful work of Milverton.[17] Furthermore, it corresponds to a reflectivity of 96 percent, which is in reasonable agreement with optical measurements for the wave-lengths of maximum intensity at 273.1°K (~10 microns). While the potential lead correction is less certain its full magnitude at 273.1° is only 0.51 percent.

From the standpoint of absolute accuracy the advantage of our method is that the energy and temperature measurements are made directly on the effective length of the cell wire, with a correction of only 0.5 percent necessary for the cell leads. The use of compensating cells assumes cancellation of end effects in the two cells amounting to 5 or 10 percent of the heat produced in the effective length of the wire. In the thick wire cell as much as 50 percent of the heat flows from the ends of the cell, and is evaluated by means of an auxiliary determination of the thermal conductivity of the wire. It would seem that the possibility of serious systematic error is least with the potential lead method.

The temperature coefficient of the thermal conductivity of air at 273.1°K has been much in dispute.[17] The value obtained in this research is 0.00291. A tabulation of values obtained, by various workers, is shown in Table IX.

ACCOMMODATION COEFFICIENTS

Accommodation coefficients may be computed from the slope of the $(1/K_a)$ *versus* $(1/p)$ plots. A theoretical treatment of this will be reserved for a subsequent paper from this laboratory. The paper will include tabulations of accommodation coefficients on bright platinum for air, from the data of this research, and for nine other gases, from data obtained by Johnston and Grilly.

THE JOURNAL OF CHEMICAL PHYSICS VOLUME 14, NUMBER 4 APRIL, 1946

The Thermal Conductivites of Eight Common Gases between 80° and 380°K

HERRICK L. JOHNSTON AND EDWARD R. GRILLY
Department of Chemistry, The Ohio State University, Columbus, Ohio

(Received December 26, 1945)

Thermal conductivities of O_2, N_2, CO, NO, H_2, He, N_2O, CO_2, and CH_4 have been measured between 80°K and 380°K, with the potential lead type of hot wire cell developed by Taylor and Johnston. Results—which have a precision generally better than 0.1 of one percent and are believed to be accurate to ±0.5 of one percent—are tabulated for the eight gases. Comparisons with the results of other investigators are also shown in tabular form.

WE have measured thermal conductivities of oxygen, nitric oxide, hydrogen, carbon monoxide, carbon dioxide, nitrous oxide, methane, and helium over the temperature range 80°K (or temperatures at which the vapor pressures amounted to about 10 cm of Hg) to 380°K. Measurements were made at intervals of about 15°.

APPARATUS AND METHOD

Apparatus and method have been described in an earlier paper by Taylor and Johnston.[1] The following slight modifications were made for this work:

(1) Thermocouple *C*, used by Taylor and Johnston, was replaced by two new copper-constantan thermocouples, designated couples *V* and *W*. These were calibrated at 90°K (b.p. O_2), 195°K (s.p. CO_2), 234°K (f.p. Hg), 273°K (m.p. H_2O), 305°K (t.p. Na_2SO_4), and 373°K (b.p. H_2O) by the method suggested in the Symposium on Temperature.[2] The two thermocouples were used simultaneously to measure the bath temperature. They always agreed with each other to within 0.1 microvolt, which is within 0.005°, throughout the course of the measurements.

[1] W. J. Taylor and H. L. Johnston, J. Chem. Phys. **14**, 219 (1946).

[2] *Temperature, Its Measurement and Control in Science and Industry*, American Institute of Physics (Reinhold Publishing Corporation, New York, 1941).

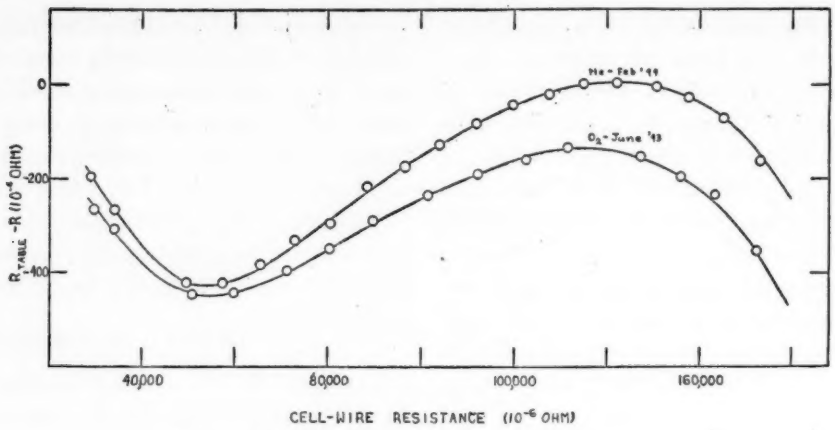

FIG. 1. Shift of cell wire calibration with time.

(2) The multiple junction thermocouple used in thermostating the cryostat bath was replaced by a resistance thermometer, which gave steadier thermostating.

(3) The float system for controlling the level of liquid air in the cryostat was replaced by an air thermometer, which actuates a relay by making and breaking contacts with the mercury in a U tube with which it is joined.

(4) Two sets of high capacity batteries were substituted for the one set used by Taylor and Johnston to supply energy to the cell wire. One set was used for the higher heating current (0.5 ampere) and was kept stabilized at this discharge rate during the full day when measurements were in progress, while the other set was used and stabilized for the lower current (0.1 ampere) used in calibrating the wire.

(5) Kerosene was substituted, as thermostat bath liquid, for the mineral oil employed by Taylor and Johnston. Because of its lower viscosity, kerosene provides more uniform thermostating.

To eliminate "temperature jump" apparent conductivities were always measured at three different pressures. These were usually taken close to one, five, and ten cm of Hg, respectively.

Calibrations of the cell wire were made simultaneous with the thermal conductivity measurements, in the manner described by Taylor and Johnston. During the period of our work the resistance of the cell wire decreased slowly but steadily, indicative of a continuing relief of strain. Figure 1 shows this effect over the eight months period that encompassed our measurements. The radius of the circles is equivalent to approximately 0.02°. New calibration curves were constructed as often as necessary, from the calibration data taken simultaneous with the conductivity measurements.

TABLE I. Thermal conductivity of oxygen.

Date	T, °K	$K \times 10^5$	% dev. from curve
6/19/43	86.53	1.851	0.00
6/19/43	94.55	2.035	0.00
11/4/42	98.02	2.113	−0.02
6/20/43	127.22	2.774	−0.08
10/28/42	130.99	2.861	0.00
6/20/43	144.56	3.166	0.00
10/28/42	151.24	3.316	+0.06
6/20/43	167.28	3.676	+0.22
6/20/43	185.17	4.051	−0.22
6/17/43	205.38	4.488	0.00
6/17/43	229.36	4.981	+0.01
6/17/43	250.87	5.408	−0.01
6/17/43	272.07	5.819	0.00
6/17/43	290.90	6.175	−0.01
6/22/43	323.86	6.828	+0.02
6/22/43	341.99	7.201	−0.10
6/22/43	357.63	7.547	+0.05
6/22/43	376.30	7.956	+0.05
Average deviation from smooth curve			±0.047%

PREPARATION OF GASES

Pure gases were prepared by the methods outlined below. Where reference is made to fractional distillation the procedure followed was the efficient "bubbler" method described by Johnston and Giauque.[3] Only the middle third of the liquid was retained in each of the several cycles.

[3] H. L. Johnston and W. F. Giauque, J. Am. Chem. Soc. 51, 3194 (1929).

TABLE II. Thermal conductivity of nitric oxide.

Date	T, °K	$K \times 10^5$	% dev. from curve
7/1/43	129.86	2.786	+0.04
7/1/43	147.82	3.165	−0.06
7/1/43	174.57	3.719	+0.01
7/1/43	191.51	4.077	+0.13
6/26/43	208.40	4.420	+0.02
6/26/43	227.76	4.793	−0.04
6/26/43	245.51	5.139	−0.04
3/8/44	266.20	5.544	+0.04
3/8/44	283.03	5.860	−0.08
3/8/44	298.80	6.168	+0.02
3/8/44	313.38	6.444	+0.01
3/8/44	330.56	6.752	−0.21
3/8/44	346.25	7.056	−0.07
3/8/44	361.97	7.361	+0.08
3/8/44	376.77	7.630	0.00
Average deviation from smooth curve			±0.057%

TABLE III. Thermal conductivity of hydrogen.

Date	T, °K	$K \times 10^5$	% dev. from curve
11/5/43	84.70	13.90	−0.57
11/5/43	93.99	15.41	+0.33
12/23/43	125.60	19.91	−0.35
12/23/43	142.23	22.46	+0.22
12/23/43	158.70	24.89	+0.36
11/2/43	175.95	27.19	−0.22
11/2/43	192.28	29.38	−0.67
3/31/44	200.40	30.68	−0.03
11/2/43	207.66	31.62	−0.15
3/31/44	218.18	33.09	−0.02
3/31/44	236.56	35.56	+0.02
3/31/44	254.38	37.68	+0.20
3/31/44	274.02	39.75	+0.01
11/7/43	277.69	40.05	−0.17
11/7/43	293.28	41.64	−0.03
11/9/43	324.28	44.53	+0.11
11/9/43	341.27	45.97	−0.15
11/9/43	357.31	47.51	−0.04
11/9/43	374.25	49.10	+0.04
Average deviation from smooth curve			±0.194%

Oxygen: Pure oxygen was obtained by passing commercial oxygen (99.5 percent) over potassium hydroxide, hot copper oxide, potassium hydroxide, and phosphorous pentoxide in turn. This was followed by fractional distillation.

Nitric Oxide: Nitric oxide was prepared and purified by the method of Johnston and Giauque.[3]

Hydrogen: Hydrogen was prepared by the electrolysis of potassium hydroxide solution. The product was passed over platinized asbestos followed by phosphorus pentoxide and was passed through a liquid air trap as the final step. A spectroscopic analysis by P. G. Wilkinson[4] indicated that the mole percent of oxygen impurity was less than 0.01 percent.

[4] P. G. Wilkinson, Ph.D. Dissertation, The Ohio State University, 1941.

TABLE IV. Thermal conductivity of carbon dioxide.

Date	T, °K	$K \times 10^5$	% dev. from curve
11/15/43	186.38	2.073	+0.02
11/15/43	200.86	2.285	−0.02
11/15/43	216.49	2.527	−0.03
11/16/43	230.68	2.752	+0.01
11/16/43	245.57	3.002	−0.02
11/16/43	259.60	3.245	0.00
11/16/43	274.22	3.505	0.00
11/16/43	287.75	3.754	−0.02
11/16/43	302.38	4.031	+0.05
11/16/43	311.24	4.199	0.00
11/13/43	333.87	4.649	0.00
11/13/43	347.32	4.932	−0.04
11/13/43	363.36	5.273	0.00
11/13/43	379.49	5.614	+0.09
Average deviation from smooth curve			±0.020%

TABLE V. Thermal conductivity of nitrous oxide.

Date	T, °K	$K \times 10^5$	% dev. from curve
12/18/43	190.25	2.175	0.00
12/18/43	206.88	2.438	−0.04
12/18/43	225.80	2.760	+0.04
12/18/43	232.06	2.870	0.00
12/18/43	249.05	3.172	−0.04
12/18/43	262.40	3.421	+0.10
12/19/43	275.60	3.669	+0.03
12/19/43	290.59	3.958	0.00
12/19/43	303.43	4.217	0.00
2/21/44	317.55	4.511	+0.03
2/21/44	332.42	4.829	+0.10
2/21/44	348.08	5.150	−0.20
2/21/44	364.11	5.505	−0.12
2/21/44	378.45	5.836	+0.05
Average deviation from smooth curve			±0.053%

Carbon Dioxide: Carbon dioxide was prepared by thermally decomposing sodium bicarbonate as described by Wilkinson,[4] who showed the oxygen content of gas so prepared to be less than 0.001 percent.

Carbon Monoxide: Carbon monoxide was prepared by dropping formic acid into concentrated sulfuric acid. The product was passed through a 50 percent potassium hydroxide solution, dried over phosphorus pentoxide, and fractionally distilled. Wilkinson[4] obtained gas with less than 0.001-mole percent impurity, by this method.

Nitrous Oxide: Cylinder nitrous oxide ("Puritan" hospital quality) was passed over phosphorous pentoxide, and fractionally distilled. According to Quinn and Wernimont[5] and Blue

[5] E. L. Quinn and G. Wernimont, J. Am. Chem. Soc. **51**, 2004 (1929); **52**, 2725 (1930).

TABLE VI. Thermal conductivity of carbon monoxide.

Date	T, °K	$K\times10^5$	% dev. from curve
12/20/43	87.41	1.802	−0.02
12/20/43	97.87	2.039	+0.02
12/21/43	130.06	2.717	−0.50
12/21/43	145.31	3.054	−0.33
12/21/43	155.07	3.261	+0.07
11/19/43	176.06	3.682	−0.16
11/19/43	192.28	4.013	0.00
11/19/43	207.36	4.308	−0.03
11/19/43	222.62	4.604	+0.03
11/19/43	237.21	4.876	+0.01
11/19/43	253.12	5.162	−0.03
11/19/43	267.08	5.412	−0.03
11/20/43	282.15	5.683	0.00
11/20/43	296.90	5.950	+0.12
11/20/43	312.00	6.210	0.00
11/22/43	328.89	6.502	−0.09
11/22/43	344.66	6.788	0.00
2/23/44	357.58	7.021	0.00
2/23/44	376.96	7.372	0.00
Average deviation from smooth curve			±0.076%

TABLE VII. Thermal conductivity of methane.

Date	T, °K	$K\times10^5$	% dev. from curve
1/13/44	96.76	2.451	0.00
1/10/44	125.35	3.195	−0.33
1/10/44	140.49	3.608	0.00
1/10/44	155.29	4.005	+0.05
1/10/44	169.93	4.406	+0.25
1/12/44	185.41	4.805	−0.16
1/12/44	201.24	5.245	−0.11
1/12/44	216.69	5.684	0.00
1/12/44	231.71	6.117	+0.08
1/12/44	246.86	6.554	+0.04
1/12/44	262.85	7.025	0.00
1/12/44	278.72	7.510	0.00
1/12/44	294.49	8.026	+0.25
1/14/44	324.00	8.986	−0.25
1/14/44	338.60	9.539	+0.02
1/14/44	353.96	10.146	+0.10
1/14/44	368.33	10.729	0.00
1/14/44	383.57	11.376	+0.01
Average deviation from smooth curve			±0.092%

and Giauque[6] the impurities in this grade of commercial nitrous oxide are nitrogen, oxygen, and water. These should all be easily removed by fractional distillation.

Methane: Methane was obtained from natural gas[7] by passing the latter through a trap at 193°K, followed by two consecutive tubes of charcoal[8] at 193°K. After this the product was fractionally distilled. Storch and Golden[9] used this method on natural gas of similar composition. In their experience they found the following concentration of impurities after the passage

TABLE VIII. Thermal conductivity of helium.

Date	T, °K	$K\times10^5$	% dev. from curve
2/1/44	82.79	15.72	0.00
2/1/44	92.71	16.96	+0.15
2/3/44	122.67	19.91	−0.02
2/3/44	137.90	21.41	−0.42
2/3/44	154.30	23.13	−0.16
2/3/44	169.89	24.72	+0.05
2/3/44	184.32	26.09	0.00
2/4/44	200.24	27.50	−0.32
2/4/44	216.89	29.12	+0.04
2/4/44	231.74	30.42	−0.04
2/4/44	248.42	31.87	+0.02
2/4/44	264.36	33.19	−0.03
2/4/44	280.53	34.50	0.00
2/4/44	296.18	35.74	+0.08
2/18/44	328.79	38.05	−0.04
2/18/44	344.43	39.12	+0.06
1/31/44	359.59	39.99	−0.07
1/31/44	375.68	40.94	0.00
Average deviation from smooth curve			±0.083%

TABLE IX. Smoothed thermal conductivities ($K\times10^5$).

T, °K	O_2	CO	He	H_2	CH_4	NO	CO_2	N_2O
80	1.701	1.652	15.34	13.31				
90	1.930	1.870	16.43	14.78	2.272			
100	2.159	2.086	17.51	16.25	2.536			
110	2.387	2.302	18.58	17.71	2.800			
120	2.614	2.516	19.64	19.17	3.065	2.580		
130	2.840	2.730	20.68	20.63	3.331	2.792		
140	3.064	2.942	21.71	22.09	3.595	3.003		
150	3.287	3.153	22.73	23.54	3.860	3.214		
160	3.508	3.361	23.73	24.98	4.128	3.423		
170	3.728	3.565	24.72	26.42	4.396	3.631		
180	3.946	3.768	25.68	27.84	4.667	3.838	1.984	2.021
190	4.162	3.968	26.63	29.25	4.940	4.042	2.126	2.173
200	4.375	4.166	27.56	30.64	5.216	4.245	2.272	2.330
210	4.584	4.361	28.49	32.00	5.496	4.445	2.424	2.493
220	4.790	4.553	29.39	33.33	5.778	4.643	2.580	2.661
230	4.993	4.741	30.28	34.64	6.063	4.840	2.741	2.823
240	5.194	4.926	31.15	35.89	6.351	5.035	2.907	3.011
250	5.392	5.107	32.00	37.09	6.643	5.229	3.077	3.192
260	5.586	5.286	32.83	38.23	6.940	5.423	3.251	3.377
270	5.780	5.465	33.65	39.32	7.242	5.615	3.429	3.564
280	5.970	5.644	34.45	40.35	7.549	5.807	3.611	3.755
290	6.159	5.821	35.23	41.33	7.862	5.999	3.796	3.949
300	6.350	5.998	36.00	42.27	8.186	6.189	3.984	4.149
310	6.547	6.175	36.74	43.19	8.518	6.379	4.175	4.352
320	6.748	6.351	37.46	44.11	8.862	6.568	4.371	4.562
330	6.954	6.528	38.15	45.02	9.219	6.756	4.571	4.775
340	7.164	6.705	38.81	45.94	9.590	6.944	4.777	4.991
350	7.378	6.884	39.44	46.85	9.978	7.131	4.988	5.206
360	7.594	7.065	40.05	47.77	10.372	7.318	5.202	5.425
370	7.812	7.246	40.62	48.69	10.797	7.504	5.416	5.644
380	8.033	7.427	41.17	49.60	11.220	7.690	5.630	5.861
273.1	5.839	5.521	33.90	39.65	7.336	5.674	3.485	3.623
293.1	6.218	5.876	35.48	41.64	7.962	6.057	3.854	4.011
298.1	6.314	5.964	35.86	42.10	8.123	6.153	3.948	4.110

[6] R. W. Blue and W. F. Giauque, J. Am. Chem. Soc. **57**, 992 (1935).

[7] The following analysis was furnished us by Mr. A. M. Hutchison of the Ohio Fuel Gas Company, as typical of the natural gas in the Columbus mains: carbon dioxide, 0.5 percent; oxygen, 0.0 percent; hydrogen, 1.3 percent; carbon monoxide, 0.6 percent; nitrogen, 5.0 percent; illuminants, 0.0 percent; methane, 80.6 percent; higher hydrocarbons, 12 percent.

[8] The charcoal was baked under vacuum at 450°C for forty hours and was maintained at 193°K while the gas was passed through.

[9] H. H. Storch and P. L. Golden, J. Am. Chem. Soc. **54**, 4662 (1932).

TABLE X. Comparisons of our own results on thermal conductivities at 273.1°K with those reported by other observers.

Gas	$K \times 10^5$	% dev. from J and G	Method*	Author	Year
O_2	5.839		*P L*	This research	1944
	5.89	+0.9	*C*	Northdurft[a]	1937
	5.90	+1.1	*C*	Dickins[b]	1934
	5.83	−0.2	*T W*	Kannuluik and Martin[c]	1934
	5.89	+0.9	*C*	Gregory and Marshall[d]	1928
	5.768	−1.2	*P L*	Weber[e]	1917
	(5.839)	0.0	*C*	Eucken[f]	1911
	Av.	+0.0			
NO	5.674		*P L*	This research	1944
	5.680	+0.1	*C*	Eucken[g]	1913
CO	5.521		*P L*	This research	1944
	5.58	+1.0	*C*	Dickins[b]	1934
	5.37	−3.0	*T W*	Kannuluik and Martin[c]	1934
	5.633	+2.0	*C*	Gregory and Archer[h]	1928
	5.557	+0.6	*C*	Eucken[g]	1913
	Av.	+0.1			
CH_4	7.336		*P L*	This research	1944
	7.21	−1.7	*C*	Dickins and Mann[i]	1931
	7.200	−1.8	*P L*	Weber[e]	1917
	7.319	−0.2	*C*	Eucken[g]	1913
	Av.	−1.2			
He	33.90		*P L*	This research	1944
	35.10	+3.6	*C*	Dickins[b]	1934
	34.30	+1.2	*T W*	Kannuluik and Martin[c]	1934
	34.38	+1.4	*P L*	Weber[e]	1917
	34.21	+0.9	*C*	Eucken[f]	1911
	Av.	+1.5			
H_2	39.65		*P L*	This research	1944
	41.82	+5.4	*C*	Archer[j]	1938
	42.45	+7.4	*C*	Northdurft[a]	1937
	42.69	+7.5	*C*	Gregory[k]	1935
	41.70	+5.1	*C*	Dickins[b]	1934
	41.3	+4.0	*T W*	Kannuluik and Martin[c]	1934
	40.62	+2.5	*C*	Hercus and Laby[l]	1922
	42.38	+6.8	*P L****	Weber[m]	1927
	40.43	+1.9	*C***	Gregory and Archer[h]	1926
	41.75	+5.3	*P L*	Schneider[n]	1926
	41.65	+5.0	*P L****	Weber[e]	1917
	40.8	+2.7	*C*	Eucken[g]	1913
	40.6	+2.5	*C*	Eucken[f]	1911
	Av.	+4.4			
CO_2	3.485		*P L*	This research	1944
	3.47	−0.4	*C*	Archer[o]	1935
	3.51	+0.7	*C*	Dickins[b]	1934
	3.43	−1.5	*T W*	Kannuluik and Martin[c]	1934
	3.604	+3.4	*C***	Gregory and Marshall[d]	1927
	3.431	−1.5	*P L*	Weber[m]	1927
	3.393	−2.7	*P L*	Weber[e]	1917
	3.442	−1.2	*C*	Eucken[g]	1913
	3.421	−1.8	*C*	Eucken[f]	1911
	Av.	−0.6			
N_2O	3.623		*P L*	This research	1944
	3.64	+0.4	*C*	Dickins[b]	1934
	3.61	−0.3	*T W*	Kannuluik and Martin[c]	1934
	3.740	+3.2	*C***	Gregory and Archer[h]	1928
	3.530	−2.6	*P L*	Weber[e]	1917
	3.601	−0.6	*C*	Eucken[g]	1913
	Av.	0.0			

[a] W. Northdurft, Ann. d. Physik **28**, 137 (1937).
[b] B. G. Dickins, Proc. Roy. Soc. (London) **A143**, 517 (1934).
[c] W. G. Kannuluik and L. H. Martin, Proc. Roy. Soc. (London) **A144**, 496 (1934).
[d] H. Gregory (Spencer-Gregory) and S. Marshall, Proc. Roy. Soc. (London) **A114**, 354 (1927); **A118**, 594 (1928).
[e] S. Weber, Ann. d. Physik **54**, 437 (1917).
[f] A. Eucken, Physik. Zeits. **12**, 1101 (1911).
[g] A. Eucken, Physik. Zeits. **14**, 324 (1913).
[h] H. Gregory (Spencer-Gregory) and C. T. Archer, Proc. Roy. Soc. (London) **A110**, 91 (1926).
[i] B. G. Dickins and W. B. Mann, Proc. Roy. Soc. (London) **A134**, 77 (1931).
[j] C. T. Archer, Proc. Roy. Soc. (London) **A165**, 474 (1938).
[k] H. S. Gregory (Spencer-Gregory), Proc. Roy. Soc. (London) **A149** 35 (1935).
[l] E. O. Hercus and T. H. Laby, Phil. Mag. **3**, 1061 (1927).
[m] S. Weber, Ann. d. Physik **82**, 479 (1927).
[n] E. Schneider, Ann. d. Physik **80**, 215 (1926).
[o] C. T. Archer, Phil. Mag. **19**, 901 (1935).
* Key to symbols: *P L* Potential lead type of hot wire cell,
C Compensating type of hot wire cell,
T W Thick wire cell.
** Temperature jump correction omitted or uncertain.
*** The hydrogen prepared by Weber was purified with charcoal at 80°K, which might have increased the parahydrogen content and thus the thermal conductivity.

through charcoal: oxygen, 0.2 percent; nitrogen, 2.0 percent; higher hydrocarbons, less than 0.05 percent. We believe that the conditions that pertained during our purification of methane were such as to yield at least as high purity at corresponding stages of the process. Our final product showed a triple point temperature of 90.63 ±0.04°K which compares with the value 90.67 ±0.03°K reported by Clusius and Weigant,[10] for pure methane. It yielded a vapor pressure of 82.4 mm of Hg at 90.06°K. There is no data in the literature which can serve as a comparison for the vapor pressure. However the triple point comparison sets an upper limit of 0.15 percent for the mole fraction of impurity in our methane. The probable purity is considerably higher than this.

Helium: The helium was bought from the Linde Air Products Company as "spectroscopically pure." A spectroscopic analysis made on a portion of this gas, in connection with a previous investigation,[11] gave evidence of barely perceptible traces of argon and of neon. A repeat analysis, just before our thermal conductivity measurements were begun, yielded a similar result.

EXPERIMENTAL RESULTS

Experimental values of the thermal conductivities obtained for the several gases are presented in Tables I to VIII. The first column in each of these tables gives the dates on which the data were taken. The second column gives the average gas temperatures (cf. reference 1). The third column gives the thermal conductivities. These are obtained by extrapolating the re-

[10] K. Clusius and K. Weigand, Zeits. f. physik. Chemie **B46**, 1 (1940).

[11] H. L. Johnston and E. R. Grilly, J. Phys. Chem. **46**, 948 (1942).

TABLE XI. Comparisons of our own results on thermal conductivities with those reported by other investigators, at temperatures other than 273.1°K.

Gas	T, °K	$K\times10^5$ This res.	$K\times10^5$ Other res.	% dev. from J and G	Author	Year
CO_2	285.1	3.703	3.69	−0.3	Archer[a]	1935
	309.7	4.169	3.99	−4.3		
	347.7	4.940	4.65	−5.8		
	373.6	5.493	5.12	−7.0		
	194.6	2.193	2.24	+2.5	Eucken[b]	1911
	373.0	5.480	5.08	−8.0		
	339.3	4.763	4.95	+4.0	Sherrat and Griffiths[c]	1939
	341.7	4.812	4.76	+1.1		
	342.1	4.821	4.80	−0.4		
	380.0	5.630	(5.62)	−0.2		
H_2	94.6	15.46	15.3	−1.0	Spencer-Gregory and Dock[d]	1938
	96.6	15.75	15.5	−1.5		
	96.3*	15.71	15.6	−0.7		
	99.1	16.11	15.9	−1.3		
	99.3	16.15	16.0	−0.7		
	202.5	30.98	31.1	+0.3		
	209.4	31.92	31.7	−0.7		
	222.7	33.68	33.9	+0.7		
	224.5	33.92	34.5	+1.8		
	226.0	34.12	35.0	+2.6		
	280.4	40.39	42.2	+4.5		
	81.6	13.54	13.56	+0.2	Eucken[e]	1913
	81.5	13.53	13.63	+0.7	Eucken[b]	1911
	83.4	13.81	14.16	+2.5		
	90.4	14.84	15.16	+2.2		
	194.6	29.89	31.40	+5.0		
	373.0	48.96	51.16	+4.4		
O_2	81.6	1.738	1.763	+1.5	Eucken[b]	1911
	90.4	1.939	1.991	+2.6		
	194.6	4.260	4.397	+2.7		
	373.0	7.878	7.608	−3.4		
CO	82.1	1.698	1.690	−0.5	Eucken[e]	1913
	91.6	1.905	1.890	−0.8		
	198.4	4.134	4.118	−0.4		
He	81.4	15.49	15.20	−2.0	Eucken[e]	1913
	80.3	15.39	14.92	−3.0	Eucken[b]	1911
	194.6	27.06	26.96	−0.4		
	373.0	40.78	40.82	+0.1		
NO	201.7	4.279	4.262	−0.4	Eucken[e]	1913
N_2O	201.3	2.351	2.776**	+18.1	Eucken[e]	1913
CH_4	91.5	2.312	2.303	−0.4	Eucken[e]	1913
	197.5	5.147	5.061	−1.7		

[a] See Table X, refernce o.
[b] See Table X, reference f.
[c] G. G. Sherrat and E. Griffiths, Phil. Mag. **27**, 68 (1939).
[d] H. Spencer-Gregory and E. H. Dock, Phil. Mag. **25**, 129 (1938).
[e] See Table X, reference g.
* Probably intended for 97.3°.
** This abnormally large value must be due to the presence of air.

ciprocals of the apparent conductivities (cf. reference 1) against the reciprocals of pressure—for pressures of approximately one, five, and ten cm as referred to above—to $(1/p)$ equals zero. The fourth column lists the percentage deviations from smooth curves of the K's *versus* temperature. Thermal conductivities are expressed in the usual units, namely calories per second per centimeter per degree.

Smoothed values of the thermal conductivities, at even temperatures, are given in Table IX.

A good estimate of the precision of the measured conductivities is obtained by reference to the average percentage deviations from the respective smooth curves, in the plots of K *versus* temperature. Except for hydrogen, for which the average deviation amounts to almost 0.2 percent, these range from 0.02 percent (carbon dioxide) to 0.09 percent (methane). The absolute accuracy of the smoothed values should be about the same as obtained for air, by Taylor and Johnston[1] —namely ±0.5 percent. The careful error analysis made in that paper should be applicable here, with little modification.

COMPARISONS WITH THE RESULTS REPORTED BY OTHER INVESTIGATORS

Few measurements of thermal conductivity have been reported at temperatures other than the ice point. Comparisons with results reported by other investigators at 273.1°K are listed in Table X, for the percentage deviations from our own values, and with a reference to the method employed.

Comparisons at temperatures other than 273.1° are given in Table XI. Our own values in this table are from our smooth curves.

All of the values in Tables X and XI are obtained by methods which yield absolute values for the conductivity, except those of Eucken, who expressed his data relative to air at 273.1°K. For our purposes, his values have been shifted to correspond to $K_{273.1}=5.839\times10^{-5}$ for oxygen.

ACCOMMODATION COEFFICIENTS

Accommodation coefficients may be computed from the reciprocal plots of apparent conductivity *versus* pressure. In a subsequent paper we will give accommodation coefficients on bright platinum for the several gases included in this research.

THE JOURNAL OF CHEMICAL PHYSICS VOLUME 14, NUMBER 4 APRIL, 1946

Energy Levels and Thermodynamic Functions for Molecules with Internal Rotation

II. Unsymmetrical Tops Attached to a Rigid Frame

KENNETH S. PITZER
Department of Chemistry, University of California, Berkeley, California
(Received December 27, 1945)

Formulas are derived which make the tables and equations of the first paper of this series applicable to this more general class of molecules. Additional approximations are involved and these are examined carefully.

INTRODUCTION

IN the first paper of this series,[1] hereafter designated I, a treatment was given for all molecules which could be regarded as rigid frames with attached symmetrical tops. The present paper will consider molecules composed of a rigid frame with attached, unsymmetrical tops. A third paper will discuss compound rotations—rotating groups attached in turn to other rotating groups.

With the more complex situation it does not seem feasible to attain the same accuracy and rigor as in I. However, it seems probable that the methods proposed will give thermodynamic results with errors not appreciably greater than the best current experiments. Also the energy separations of the lowest and first excited levels should be given without excessive error.

Unsymmetrical, attached rotating tops fall into three classes. First, balanced groups, where the center of gravity of the top is on its axis of rotation. The balance may be accidental or due to a twofold symmetry axis (if a three- or higher-fold axis is present the top is symmetrical). A phenyl group is an example. Second, groups with a small "off balance" factor such as OH, NH_2, CH_2D, $CCL^{35}{}_2Cl^{37}$. For each of these classes it seems unlikely that the over-all moments of inertia will change greatly with internal rotation. Since the properties of interest are not sensitive too small changes in moments of inertia, it is permissible to ignore them and treat the molecule in terms of the various quantities appropriate to the equilibrium configuration.

The third class comprises groups with large off-balance factors such as CH_2Cl, $CHBr_2$, CHO, etc. Here the changes in moment of inertia are too large to dismiss. However it must be realized that vibrational motions are also affected. Consequently, any attempt to correct for these effects on rotation alone will have little practical value. Indeed it can be shown that the changes in the mass or inertia factor for the various normal modes of vibration just cancel the changes in moment of inertia provided all motions are treated classically. Since vibration frequencies are usually known only for the equilibrium configuration, it seems best again to take all quantities appropriate to the equilibrium configuration and to ignore changes with angle in the first approximation. However this leaves the question of how nearly classical are the vibrations that effectively compensate the changes in moment of inertia. Study of individual cases indicates that the answer will almost always be favorable, however each case should be studied from this point of view.

In molecules of these types the potential energy function is likely to be much more complex than with symmetrical groups. The direct numerical integration of the classical partition function is a practical procedure and will be of a good approximation for cases with large moments of inertia. The quantum mechanical energy levels are formally given by Eq. (18)-I and the associated discussion for a reasonably general case. However, the labor involved in this method may be large. Once the energy levels are obtained the partition function sums are readily computed.

[1] K. S. Pitzer and W. D. Gwinn, J. Chem. Phys. **10**, 428 (1942).

DEFINITIONS

For the entire molecule, of mass M, including all rotating groups in their equilibrium positions, find the principal axes of rotation through the center of gravity and the principal moments of inertia,[2] I_1, I_2, and I_3.

For each top, m, take the rotation axis as z and make x pass through the center of gravity of the top. If the top is balanced, define x arbitrarily and in any case make y perpendicular to both x and z. Although it makes no real difference, it is simpler not to include atoms on the axis of rotation as part of the top. Thus the rotating group is just the off axis H atom for an OH radical. If m_i is the mass of the ith atom, then

$A_m=\sum_i m_i(x_i^2+y_i^2)$ the top moment of inertia about z.
$B_m=\sum_i m_i x_i z_i$ the xz product of inertia.
$C_m=\sum_i m_i y_i z_i$ the yz product of inertia.
$U_m=\sum_i m_i x_i$ the off-balance factor.

In each case the sum is over only those atoms in mth top. The array of quantities:

$$\begin{vmatrix} \alpha_m{}^{1x} & \alpha_m{}^{2x} & \alpha_m{}^{3x} \\ \alpha_m{}^{1y} & \alpha_m{}^{2y} & \alpha_m{}^{3y} \\ \alpha_m{}^{1z} & \alpha_m{}^{2z} & \alpha_m{}^{3z} \end{vmatrix}$$

are the direction cosines between the axes of the mth top (x, y, z) and the axes of the whole molecule $(1, 2, 3)$. (All sets of axes must be uniformly either right-handed or left-handed. To check this verify that the determinant of α's is $+1$.) The vector from the center of gravity of the whole molecule to the origin of coordinates of the top is $\mathbf{r}_m$ with components $r_m{}^1$, $r_m{}^2$, $r_m{}^3$ on the principal axes.

$$\Lambda_{mm'}=\sum_i\left\{\frac{\alpha_m{}^{iy}\alpha_{m'}{}^{iy}U_mU_{m'}}{M}+\frac{\beta_m{}^i\beta_{m'}{}^i}{I_i}\right\},$$

where

$$\beta_m{}^i=\alpha_m{}^{iz}A_m-\alpha_m{}^{ix}B_m-\alpha_m{}^{iy}C_m+U_m(\alpha_m{}^{i-1,\,y}r_m{}^{i+1}-\alpha_m{}^{i+1,\,y}r_m{}^{i-1}).$$

The superscripts $i-1$ and $i+1$ refer to cyclic shifts of axes so that if $i=1$, $i-1=3$ and if $i=3$, $i+1=1$.

The reduced moment of inertia for internal rotation if there is only a single rotation (or the first approximation if there are several) is:

$$I_m=A_m-\Lambda_{mm}=A_m-\sum_i\left\{\frac{(\alpha_m{}^{iy}U_m)^2}{M}+\frac{(\beta_m{}^i)^2}{I_i}\right\}. \quad (1)$$

A second approximation is given by Eq. (1b)-I but using the new definitions of $\Lambda_{mm'}$ given above.

For the case of balanced tops, all of these additional terms are zero, so that the old formulas apply.

SUMMARY OF RESULTS

All essential results are now given by the equations and tables of paper I using the new definitions of I and Λ.

If the potential energy can be represented by:

$$V=\sum_m \tfrac{1}{2}V_m{}^0(1-\cos n_m\phi_m), \quad (2)$$

then the tables in paper I apply. However, if the symmetry number, n_m, corresponds to an approximate symmetry of the potential curve rather than an exact symmetry of the rotating group, then $(R\ln n_m)$ must be added to the functions S and $(H_0{}^0-F_T{}^0)/T$.

Examples:

Sym. ethane d_2 (CH_2D-CH_2D). One CH_2D is the frame; the other is the rotating group with a small off-balance factor and an approximate symmetry number of 3 for the potential energy. Use $n_m=3$ for the tables but add $R\ln 3$ to entropy and free energy function.

Ethylbenzene. With the CH_2 as the rigid frame, the methyl group is symmetrical; the phenyl is balanced; the internal symmetry numbers are 3, and 2, respectively. Presumably there is no large cross term in the potential energy.

m-Chloro ethylbenzene. Now the phenyl group has an off-balance factor and its symmetry number of 2 is only an approximation for the potential energy. The tables of paper I may be used with $n=2$ (for the phenyl rotation) but add $R\ln 2$ to the entropy and free energy function.

If the potential energy cannot be expressed by Eq. (2), then the tables in I cannot be applied

[2] The calculations can be made without finding principal axes by using the products of inertia. However, the equations are much more complex so it is doubtful if that method would ever be much easier. One principal axis is obvious in most all molecules, either a rotational symmetry axis or perpendicular to a plane of symmetry.

but the methods described in the last section of I must be used.

PROOFS

Two mathematical arguments remain to be given. First, that with the new definitions, the kinetic energy is given by Eq. (7)-I for motion at the equilibrium configuration.

Let there be a frame of axes of fixed direction with origin at the center of gravity when all particles are in original positions. Then (0) is a set of axes with the same origin but rotating with angular velocity ω_0. Then for each rotating group there is a set of axes (m) whose origin is fixed in (0) and which rotates with angular velocity ω_m with respect to (0). Actually the direction of ω_m, though arbitrary is also fixed in (0). Each particle, of mass m_i, is located in one of these frames by a vector ϱ_{0i} or ϱ_{mi}. The vector $\mathbf{r}_m$ is from the origin of (0) to the origin of (m).

The velocity of a particle i in the main frame is

$$\mathbf{v}_i=\omega_0\times\varrho_i, \tag{3}$$

while that of a particle mj in the group m is

$$\mathbf{v}_{mj}=\omega_0\times(\mathbf{r}_m+\varrho_{mj})+\omega_m\times\varrho_{mj}. \tag{4}$$

The kinetic energy is then

$$2T'=\sum_i m_i\mathbf{v}_i\cdot\mathbf{v}_i+\sum_m\sum_j m_{mj}\mathbf{v}_{mj}\cdot\mathbf{v}_{mj}, \tag{5}$$

where the sums cover all appropriate particles such that each particle is included once.

Now in general the center of gravity may move with a velocity

$$\mathbf{v}=(\textstyle\sum_i m_i\mathbf{v}_i\times\sum_m\sum_j m_{mj}\mathbf{v}_{mj})/M. \tag{6}$$

However, this can only arise from the group rotations because the main frame rotation is about its center of mass. Hence

$$\mathbf{v}=(\textstyle\sum_m\omega_m\times\sum_j m_{mj}\varrho_{mj})/M. \tag{7}$$

The kinetic energy of this center of gravity motion is

$$2T''=M\mathbf{v}\cdot\mathbf{v}, \tag{8}$$

and must be subtracted from T' to give the true kinetic energy of rotation T.

$$\begin{aligned}2T=&\{\textstyle\sum_i m_i(\omega_0\times\varrho_i)^2\\&+\sum_m\sum_j m_{mj}[\omega_0\times(\mathbf{r}_m+\varrho_{mj})]^2\}\\&+\sum_m\sum_j m_{mj}\{2[\omega_0\times(\mathbf{r}_m+\varrho_{mj})]\\&\cdot[\omega_m\times\varrho_{mj}]+[\omega_m\times\varrho_{mj}]^2\}\\&-\frac{1}{M}\{\textstyle\sum_m\omega_m\times\sum_j m_{mj}\varrho_{mj}\}^2.\end{aligned} \tag{9}$$

Let us now expand the vectors and assume the principal axes are used for the system (0). We replace ω_m by the scalar $\dot\varphi_m$ used in I, and add primes to the components of ω_0.

$$\begin{aligned}2T=&\sum_{i=1}^{3}I_i(\omega_i')^2+2\sum_{i=1}^{3}\sum_{m=1}^{N}\omega_i'U_m\dot\varphi_m(\alpha_m^{i-1,y}r_m^{i+1}-\alpha_m^{i+1,y}r_m^{i-1})\\&+2\sum_{i=1}^{3}\sum_{m=1}^{N}\omega_i'\dot\varphi_m(\alpha_m^{i,z}A_m-\alpha_m^{i,x}B_m-\alpha_m^{i,y}C_m)\\&+\sum_{m=1}^{N}A_m\dot\varphi_m^2-\frac{1}{M}\left\{\sum_{m=1}^{N}\sum_{m'=1}^{N}\dot\varphi_mU_m\dot\varphi_{m'}U_{m'}\sum_{i=1}^{3}\alpha_m^{i,y}\alpha_{m'}^{i,y}\right\}.\end{aligned} \tag{10}$$

Introduce the substitution,

$$\omega_i'=\omega_i-\textstyle\sum_m\beta\dot\varphi_m^i/I_i, \tag{11}$$

then

$$\begin{aligned}2T=&\sum_{i=1}^{3}I_i\omega_i^2+\sum_{m=1}^{N}A_m\dot\varphi_m^2-\sum_{m=1}^{N}\sum_{m'=1}^{N}\dot\varphi_m\dot\varphi_{m'}\\&\times\sum_i\left(\frac{\alpha_m^{i,y}\alpha_{m'}^{i,y}U_mU_{m'}}{M}+\frac{\beta_m^i\beta_{m'}^i}{I_i}\right),\end{aligned} \tag{12}$$

which is Eq. (7)-I when the new value of $\Lambda_{mm'}$ is used.

The second mathematical argument concerns the compensation of changes in moment of inertia with changes of vibration frequency. Let us first take as an example a chain of four successive atoms at tetrahedral bond angles. The internal rotation is about the central bond and the rotating top is grossly unsymmetrical. Kassel[3] has given the needed equations for this case. The appropriate classical partition function

[3] L. Kassel, J. Chem. Phys. **3**, 326 (1935); **4**, 276 (1936). In the latter article the terms for the hydrogen atoms are removed from the equations for *n*-butane.

for vibration and rotation is:

$$Q=\frac{8\pi^2}{\sigma}\left(\frac{2\pi kT}{h^2}\right)^2\left(\frac{kT}{h}\right)^a\int_0^{2\pi}\frac{[S]^{\frac{1}{2}}}{\prod_{i=1}^{a}\nu_i}e^{-V(\varphi)/kt}d\varphi. \quad (13)$$

Where a is the number of modes of vibration, ν_i the frequency of the ith mode, S is the effective product of moments of inertia for external and internal rotation, and φ is the angle of internal rotation.

From Kassel's work we find

$$\prod_{i=1}^{a}\nu_i=\left(\frac{1}{2\pi}\right)^5\left(\frac{k^3b^2}{m^5}\right)^{\frac{1}{2}}\frac{4}{9}Y, \quad (14)$$

where

$$Y^2=(9+24\gamma^2-8\gamma^4)(33-8\gamma^2-16\gamma^4) \quad (15)$$

and

$$\gamma=\cos(\phi/2)$$

(Kassel's ϕ or α is half of ϕ as used here).

$$[S]^{\frac{1}{2}}=8(mr_0^2/9)^2Y. \quad (16)$$

Thus the factor Y which expresses the change in the product of vibration frequencies with internal rotation exactly compensates the same factor in the product of moments of inertia. Consequently, the vibration frequencies and moments of inertia could have been computed for any particular configuration and would have given the correct result.

It would be quite impractical to work out a general case by this method; the generality of the result may be seen by using the method introduced by the writer for long chain molecules.[4] Here one avoids normal coordinates completely.

Let us assume there are p atoms in the rigid frame of which the 1st and 2nd atoms are on the axis of internal rotation. Then the atoms of the rotating top, $p+1$ to n, are attached to the 1st atom or to others in the rotating top. The partition function is given by an equation analagous to Eq. (12) of reference (4).

$$Q=A\int\cdots\int e^{-V/RT}dx_1\cdots dz_n, \quad (17)$$

$$A=\left(\frac{2\pi kT}{h^2}\right)^{3n/2}\prod_{i=1}^{n}m_i^{\frac{1}{2}}, \quad (18)$$

where m_i is the mass of the ith atom, V is the potential energy, and x_1-z_n are coordinates describing the positions of the various atoms. The integrations are, strictly, over the volume of the container.

Selecting arbitrarily atom 1, it may be placed anywhere in the container of volume v without change in potential energy. Hence the integration gives just the factor v. Converting to polar coordinates for the second atom (relative to atom 1), integration over the angles (with no change in potential energy) gives 4π so that now

$$Q=B\int\cdots\int e^{-V/RT}dx_3\cdots dz_n, \quad (19)$$

$$B=A4\pi v\int_0^R\exp[-V(r_1)/RT]r_1^2dr_1. \quad (20)$$

The upper limit of integration in (20), R, is any number several times larger than the equilibrium value of r_1. The whole value of the integral comes from the region near r_1 so the exact value of R is not important, indeed for a harmonic force law it may be infinity. For other force laws, however, the integral might not converge at infinity.

Selecting as 3 an atom bonded to atom 2 and at an angle less than 180° from the 1–2 bond, one again used polar coordinates. Now the potential energy depends on r and θ but not φ.

$$Q=C\int\cdots\int e^{-V/RT}dx_4\cdots dz_n, \quad (21$$

$$C=B2\pi\int_0^{\pi}\int_0^R\exp[-V(r_3,\theta_3)/RT]\times r_3^2\sin\theta_3dr_3d\theta_3. \quad (22)$$

From now on each atom in the frame can be treated in terms of coordinates defined with reference to lower numbered atoms with the potential energy depending on r, θ, and φ.

$$Q=D\int\cdots\int e^{-V/RT}dx_p\cdots dz_n, \quad (23)$$

$$D=C\prod_{i=4}^{p}\left(\int_0^{2\pi}\int_0^{\pi}\int_0^R\exp[-V(r_i\theta_i\varphi_i)/kT]\times r_i^2\sin\theta_idr_id\theta_id\varphi_i\right). \quad (24)$$

The first atom in the rotating top defines the position of the top. Hence the potential energy

[4] K. S. Pitzer, J. Chem. Phys. 8, 711 (1940).

of internal rotation is $V(\varphi_{p+1})$ while r and θ have typical bond stretching and bending energies. The remaining atoms in the top give terms similar to the later atoms of the frame.

$$Q = DEF \int_0^{2\pi} \exp\left[-V(\varphi_{p+1})/kT\right] d\varphi_{p+1}, \quad (25)$$

$$E = \int_0^{\pi} \int_0^{R} \exp\left[-V(r_{p+1}\theta_{p+1})/kT\right] \times r_{p+1}^2 \sin\theta_{p+1} dr_{p+1} d\theta_{p+1}, \quad (26)$$

$$F = \prod_{i=p+2}^{n} \left(\int_0^{2\pi} \int_0^{\pi} \int_0^{R} \exp\left[-V(r_i\theta_i\varphi_i)/kT\right] \times r_i^2 \sin\theta_i dr_i d\theta_i d\varphi_i \right). \quad (27)$$

Thus we see from Eq. (25) that the factor for internal rotation is independent of the other coordinates and has essentially the same form as with symmetrical groups. This proves that the result obtained with the four atom chain is general and that for a classical treatment it is permissible to calculate vibration frequencies and moments of inertia for just a single position with respect to internal rotation. Of course, if desired this method may be employed to actually calculate the classical partition function.[4]

This argument was based, for simplicity, on a reasonably simple valence force potential energy function in order to obtain the explicit form of Eq. (25). However, the critical point is the integration of the kinetic energy terms to give Eqs. (17) and (18) in which, so far as inertia or kinetic energy terms are concerned, all increments of internal rotation angle are weighted equally. Thus, the basic conclusion, that the changes in inertial quantities cancel one another, is quite independent of the force field assumed here. However, if there are cross terms in the potential energy between internal rotation and vibrational motions, then the use of vibration frequencies for the equilibrium configuration will represent an approximation. This could be removed by combining Eq. (25) with others as necessary and integrating the multiple integral with the cross terms in the potential energy present.

It is true that for most molecules of interest only some of the vibrations can be treated classically. Very roughly, vibrations may be classified as (1) hydrogen vibrations, (2) bond stretching motions of heavy atoms, and (3) bending motions of heavy atoms. The frequencies in the first two groups are largely independent of the arrangement of more distant parts of the molecule. Consequently, the third group must be principally responsible for the changes which compensate the moments of inertia. However, the vibration frequencies of this third group are usually below 400 cm^{-1} and consequently nearly classical motions at or above room temperature.

Taking again the four atom chain as studied by Kassel,[3] we find that the product of stretching frequencies varies with internal rotation only by 5 percent while the product of bending frequencies changes by 45 percent. While we have no general proof of this point, it seems probable that this example is typical. If so, the method proposed above will be a good approximation.

The writer wishes to thank Professor W. D. Gwinn for checking these derivations.

THE JOURNAL OF CHEMICAL PHYSICS VOLUME 14, NUMBER 4 APRIL, 1946

On the Diffusion of Vapors through Polymers

PAUL DOTY
Department of Chemistry, Polytechnic Institute of Brooklyn, Brooklyn 2, New York
(Received February 5, 1946)

The rate of permeation of a gas through a polymer as a function of temperature may be represented as $P = P_0 e^{-E/RT}$. All available data on the permeability of gases through polymers show that for a given gas there is a linear relation between log P_0 and E (the energy of activation for permeation). An explanation is offered for this apparent relationship. The effect of plasticization on permeation of water vapor is studied experimentally and it is shown that the lowering of the heat of solution is the predominant effect. From the data the entropy of solution may be calculated and interpreted as showing that water molecules dissolved in the unplasticized polymer exhibit much less freedom than when they are dissolved in plasticized polymer. Other calculations show (in agreement with Barrer) that a large number of degrees of freedom are simultaneously operative in the process of the diffusion of a gas molecule through a polymer.

INTRODUCTION

THE studies of Barrer[1] together with his compilation and analysis of existing data[2] have contributed most significantly to our fundamental understanding of the transmission of gases and vapors through polymeric substances. These investigations demonstrated that transmission results from activated diffusion and that the molecular diameter of the diffusing gas is of only secondary importance. The process of permeation is visualized as follows when a film of polymeric substance separates two quantities of gas or vapor at different pressures. The gas molecules dissolve in the polymer and move about by jumping into holes which form and disappear in their immediate neighborhood. These holes are the result of fluctuations in the thermal motion of segments of the polymer molecules. The concentration gradient in the film causes a drift of the diffusing gas toward the lower concentration region.

The rate of transfer of vapor across a film of unit thickness per unit area per unit pressure difference is known as the permeability constant and characterizes the effectiveness of the film as a barrier. It has been shown that the permeability constant, P, may be resolved into the product of the diffusion constant, D, and the solubility coefficient, S. The dimensions of D are area per unit time; S has dimensions of volume of gas (at stated conditions) per volume of polymer. With a proper choice of units we may write: $P = DS$. This relation has been verified for permanent gases[1,2] and water vapor[3] in a number of polymeric substances.

It is important to note that it has likewise been verified that P, D, and S vary exponentially with reciprocal absolute temperature for permanent gases. Thus:

$$P = P_0 \exp(-E/RT), \tag{1}$$

$$D = D_0 \exp(-E_D/RT), \tag{2}$$

$$S = S_0 \exp(-\Delta H/RT). \tag{3}$$

Since P and D are essentially rate constants, E and E_D may be interpreted as energy of activation for permeation and diffusion, respectively. The solubility coefficient is an equilibrium constant, hence ΔH may be identified as the heat of solution. Moreover, P_0 and D_0 correspond to frequency factors in the Arrhenius equation of chemical kinetics. Barrer[1,2] has interpreted his measurements of these quantities in terms of the transition state theory to show that the activated state for diffusion involves many degrees of freedom indicative of the formation of a "hole" for the diffusion molecule to move into.

In this paper it is desired to present some further interpretations of this problem based upon investigations of water vapor-polymer systems, some of which have been previously

[1] R. M. Barrer, Trans. Faraday Soc. **34**, 849 (1938); **35**, 628 (1939); **35**, 644 (1939); **36**, 1235 (1940).
[2] R. M. Barrer, *Diffusion in and through Solids* (Cambridge University Press, New York, 1941).
[3] P. M. Doty, W. H. Aiken, and H. Mark, Ind. Eng. Chem. (in press).

published.[3] Specifically, we should like to point out an apparent relation between P_0 and E in Eq. (1) and report some measurements on the water vapor-polyvinyl chloride system with and without plasticizer from which some significant conclusions may be drawn. Finally, it may be shown that our data confirm Barrer's views summarized in the preceding paragraph.

THE APPARENT RELATION BETWEEN P_0 AND E

The temperature dependence of the permeability constant has been determined for a number of polymers with water vapor.[3] From these data P_0 and E in Eq. (1) can be evaluated. In Table I these constants are listed for all the materials measured.

In Fig. 1, $\log P_0$ is plotted *versus* E. Two other measurements of polyvinyl chloride-acetate, which are mentioned later, are included in the graph. The diameters of the circles are rough indications of the probable experimental error involved. The closeness of fit of the experimental data to a straight line, the large range of variables covered (ten decades in P_0 and 18,000 calories in E), and the complete randomness with which the materials tested were selected clearly indicate that in a very general sense $\log P_0$ has been demonstrated to be a linear function of the energy of activation. Such a conclusion recalls the controversies that have occurred in chemical kinetics over apparent relations between A and E in the Arrhenius equation ($k = Ae^{-E/RT}$) for reaction rates.[4] A number of these claims were shown to be illusory because the rate constant, k, was nearly constant in the series of reactions considered, thus forcing a change in E to be reflected in $\log A$. This situation hardly exists here because the permeability constant (corresponding to k) for the films measured varied one thousand-fold.

TABLE I. Energies of activation for permeation and log P_0 for water vapor.

Polymer	E(cal./mole)	log P_0
Polystyrene	0	−6.08
Polyvinyl chloride-acetate	2350	−5.10, −4.80
Polyvinyl chloride	4000	−3.51
Polyethylene (calendered)	8000	−1.34
Polyethylene (cast)	10200	+0.13
Rubber hydrochloride	12800	+1.63
Polyvinylidene chloride	17500	+4.20

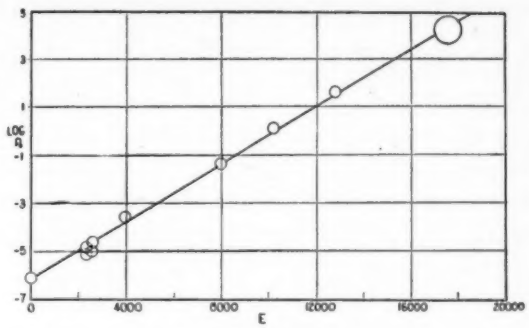

FIG. 1. The correlation of log P_0 and E (cal./mole) for the permeation of water vapor through various polymeric materials.

If we accept the relation as real, it is necessary to attempt an interpretation, consider its range of application, and test it on other data if any exist. In the few cases in chemical kinetics where a *bona fide* relation between log A and E has been found, an explanation involving the frequency of vibration in the activated state has been postulated.[4] Evidence described in the next section indicates that there is no direct relation between heat of solution and E. It seems therefore unwise to seek an analogy with this case in chemical kinetics. However, it is relevant to note that Hammett *et al.*[5] have demonstrated that in a number of cases log A varies only with that portion of the energy of activation which is kinetic energy. In view of the picture of the permeation process described in the Introduction, it would seem that, since no bonds are broken in the diffusion process, the energy of activation is largely kinetic energy, and we may reason as follows. Imagine that in some particular reference system the permeation was characterized by a certain P_0 and E. On passing then to a system with a lower energy of activation E', it seems reasonable, in view of the picture of permeation described above, that the lowering of E has been due to the simultaneous cooperation of a number of factors. That is, in this latter case, more degrees of freedom are activated in hole formation. A hole is considered to form when several segments simultaneously move outward from a given region. The translational motion of each

[4] C. N. Hinshelwood, *The Kinetics of Chemical Change* (Oxford University Press, New York, 1940).

[5] L. P. Hammett, *Physical Organic Chemistry* (McGraw-Hill Book Company, Inc., New York, 1940).

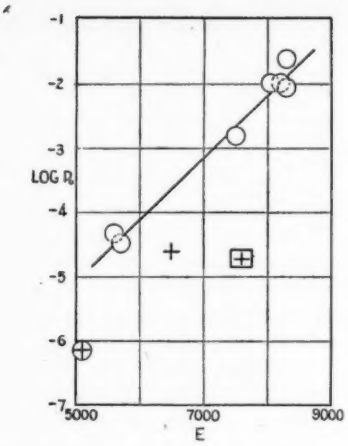

FIG. 2. The correlation of log P_0 and E (cal./mole) for the permeation of hydrogen through various polymeric materials. ⊕ = Bakelite; + = ebonite; ⊞ = Cellophane.

segment would involve at least three degrees of freedom. Each additional degree of freedom operative in the latter case can be thought of as reducing E by a given amount e, and if n degrees of freedom are involved the change is given by $E-E'=\Delta E=ne$. However, the chance that each of these degrees of freedom is favorably activated at the moment of activation is considerably less than unity. Thus for n of them to be favorable at once the probability of reaction will be reduced in the ratio $P'/P=a^n$, where a is less than unity and is the average probability of one degree of freedom being favorably activated at the time of the activation. If we take logarithms and eliminate n there is obtained

$$\log P-\log P'=(\Delta E/e)\log 1/a$$
$$\Delta \log P=\Delta E[(1/e)\log 1/a]=k\Delta E. \quad (4)$$

Thus it is found that log P will be a linear function of E. The validity of the relation just derived requires that log $(1/a)$ is directly proportional to e. That is, the more the energy of activation is lowered by the proper activation of a certain degree of freedom, the less likely (logarithmically) is this activation to occur. This concept is statistical in nature: it cannot be expected to hold for every degree of freedom concerned with permeation in all polymers. However, it is expected that the average behavior of the various degrees of freedom would conform; consequently, the essential point in this logarithmic relation is the assumption that the primary act of permeation* depends upon a number of rarely fulfilled conditions corresponding to a large number of degrees of freedom. The conformance of experimental data to the derived logarithmic relation lends credence to the assumption on which the derivation was based.

It is necessary to note the probable limitations of this general behavior. All of the materials investigated were pure, unplasticized, linear polymers. On the basis of the present information nothing can be stated regarding plasticized polymers, cross-linked polymers, or polymers with which the diffusing gas has a specific interaction, such as the water-cellulose system.

The only other data available for testing this apparent relation between P_0 and E are those of Barrer[1] and deBoer and Fast[6] on the permeation of hydrogen and of Barrer on helium and nitrogen through several organic membranes. In Table II values of log P_0 calculated from these data are listed together with the energy of activation for all films studied. These values are plotted in Figs. 2–4. Unfortunately these data do not

TABLE II. Energies of activation for permeation and log P_0 for some permanent gases.

Material	E(cal./mole)	log P_0
—Hydrogen—		
Bakelite	5100	−6.14
Celluloid	5600	−4.35
Nitrocellulose	5700	−4.49
Ebonite	6500	−4.64
Cellulose triacetate	7500	−2.85
Cellophane	7600	−5.23
Polyethylene	8050	−2.00
Butadiene-acrylonitrile copolymer	8200	−1.99
Polychloroprene	8300	−2.08
Neoprene (vulcanized)	8300	−1.65
—Helium—		
Ebonite	5900	−4.52
Rubber (vulcanized)	6300	−3.59
Polyethylene	7700	−2.44
Neoprene (vulcanized)	8800	−1.55
Cellophane	10100	−3.13
—Nitrogen—		
Butadiene-styrene copolymer	7900	−2.67
Butadiene-methyl methacrylate copolymer	9500	−1.68
Butadiene-acrylonitrile copolymer	9800	−1.89
Neoprene	10500	−1.27
Bakelite	10500	−3.01

* This argument could be presented equally well in terms of diffusion. See Discussion.

[6] J. H. deBoer and J. Fast, Rec. Trav. chim. Pays-Bas. 57, 317 (1938).

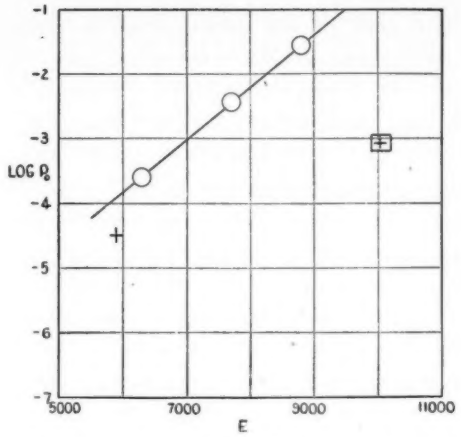

FIG. 3. The correlation of log P_0 and E (cal./mole) for the permeation of helium through various polymeric materials. + = ebonite; ⊞ = Cellophane.

extend over a large range of the variables and hence they cannot be considered decisive. However, it is encouraging to note that a linear relation is exhibited by all systems measured except those of Cellophane, ebonite, and Bakelite. Since none of these materials are pure linear polymers, the relation is confirmed with the restrictions originally pointed out. Vulcanized rubbers also fall in the linear relationship. It thus appears as though moderate cross-linking does not cause deviations from linear behavior, but excessive cross-linking such as is found in Bakelite and ebonite does cause deviations. Consequently, we may conclude that all available data on the temperature dependence of permeability of gases in pure polymeric substances conform to the equation $P = P_0 e^{-E/RT}$ and exhibit a linear relationship between log P_0 and E, except for very highly cross-linked materials.

THE EFFECT OF PLASTICIZATION ON PERMEATION

In order to determine in detail the effect of plasticization and composition on the permeability constant, the diffusion constant, and the solubility coefficient, some experiments have been performed on pure polyvinyl chloride, a polyvinyl chloride-acetate copolymer (Vinylite VYNW), and the latter polymer with the two different plasticizers added. The permeability constants and diffusion constants were measured in the manner described in a previous publication.[7] The data for polyvinyl chloride are taken from a previous publication.[3]

Polyvinyl chloride was chosen as the pure polymer with which comparisons could be made. The chloride-acetate copolymer differs from the polyvinyl chloride in that five percent of the chlorine is replaced by acetate groups. For plasticization, two plasticizers were chosen which represent rather extreme degrees of interaction with water. Tricresyl phosphate is typical of plasticizers which are immiscible with water, whereas the other plasticizer chosen was a mixed glycol ester of 6, 8, and 10 carbon fatty acids (SC plasticizer), which is fairly miscible with water but is also quite miscible with the polymer.

The results of our measurements with these four films at various temperatures are summarized in Table III. In Figs. 5–8 the logarithms of P, D, and S are plotted against reciprocal absolute temperature. From the slopes of these graphs the energies of activation for permeation and diffusion and the heat of solution have been calculated and are recorded in Table IV.

There are several interesting conclusions to be obtained from the data as summarized in Table IV. First of all, the resolution of P into the product of D and S appears to be verified under the rather diverse conditions existing in the films measured. Moreover, the variation of these quantities with temperatures is in all cases of the

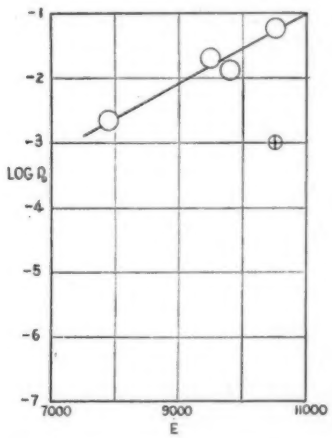

FIG. 4. The correlation of log P_0 and E (cal./mole) for the permeation of helium through various polymeric materials. ⊕ = Bakelite.

[7] P. M. Doty, W. H. Aiken, and H. Mark, Ind. Eng. Chem. 16, 686 (1944).

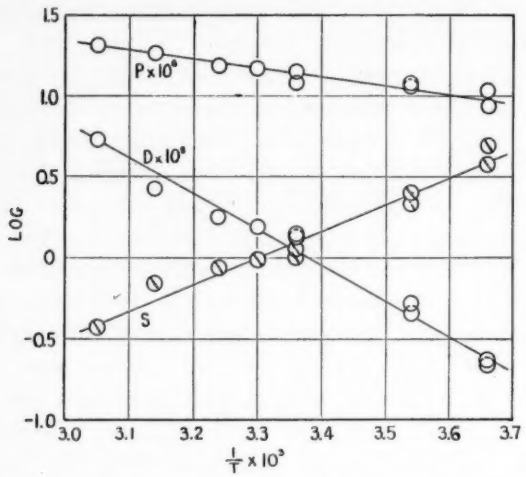

FIG. 5. A plot of logarithm of P, D, and S *versus* reciprocal absolute temperature for the permeation of water vapor through polyvinyl chloride.

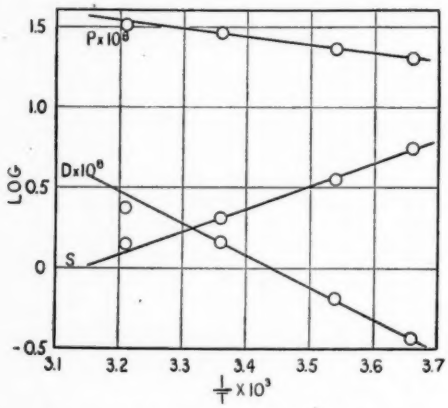

FIG. 6. A plot of logarithm of P, D, and S *versus* reciprocal absolute temperature for the permeation of water vapor through polyvinyl chloride-acetate.

form previously found for the transmission of permanent gases through polymer membranes. In other words, the inclusion of a rather large amount of solvent into the polymeric system does not alter the fundamental nature of the permeation.

Examination of Table IV indicates that E has the same value for the two pure polymers, but the value is considerably increased by the addition of either of the plasticizers. Moreover, this increase due to plasticization results almost entirely from the change in the heat of solution that has taken place. That is, the energy of activation for diffusion is relatively constant in all four films, but the heat of solution is quite sensitive to composition both of the polymer itself and that of the added solvent. Similarly, P_0 is greatly increased by the addition of plasticizer, but D_0 is not significantly changed.

The heat of solution of water vapor in polyvinyl chloride is very large. This probably results from the strong interaction of the C—Cl dipoles with the OH groups. When some of the chlorine is replaced by acetate in the copolymer, the heat of mixing is somewhat lowered; the addition of 25 percent trioctyl phosphate or SC plasticizer reduces the heat of mixing very considerably. Either the plasticizer molecules solvate the C—Cl dipoles to a great extent, thus preventing their

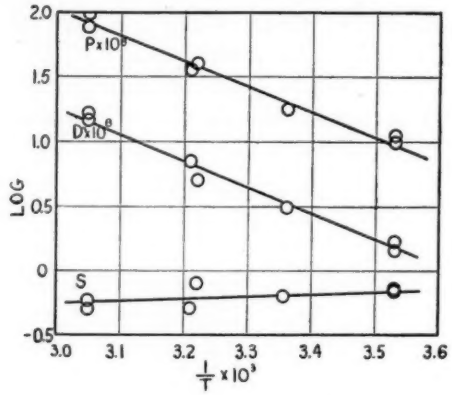

FIG. 7. A plot of logarithm of P, D, and S *versus* reciprocal absolute temperature for the permeation of water vapor through chloride-acetate plus 25 percent tricresyl phosphate.

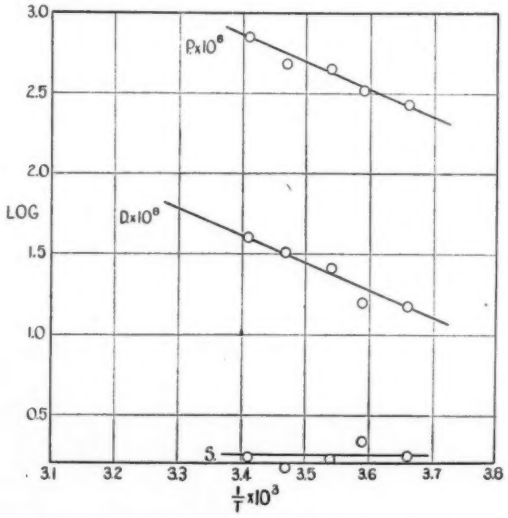

FIG. 8. A plot of logarithm of P, D, and S *versus* reciprocal absolute temperature for the permeation of water vapor through chloride-acetate plus 25 percent mixed glycol esters of 6, 8, and 10 carbon fatty acids (SC plasticizer).

TABLE III. P, D, and S (calc.) at different temperatures for the permeation of water vapor through polyvinyl chloride.

Temperature	$P \times 10^9$	$D \times 10^5$	S
	Polyvinyl chloride		
0°	8.58	.232	3.7
0	10.95	.218	5.02
10	11.5	.525	2.19
10	12.2	.476	2.56
25	14.1	1.63	.863
25	11.9	1.35	.882
30	14.9	1.55	.96
35	15.5	1.76	.88
45	18.7	2.61	.716
55	20.3	5.41	.375
	Polyvinyl chloride-acetate-copolymer		
0°	16.0	.309	5.18
10	22.9	.65	3.52
25	29.2	1.45	2.01
38	32.4	2.31	1.40
	Polyvinyl chloride acetate and 25 percent tricresyl phosphate		
10°	11.1	1.58	.70
10	9.9	1.4	.706
25	19.7	3.1	.635
38	42.0	5.14	.82
38	35.2	6.98	.504
55	103.0	16.6	.621
55	76.0	15.0	.506
	Polyvinyl chloride acetate and 25 percent mixed glycol ester		
0°	26.6	15.1	1.76
5	32.7	15.3	2.20
10	44.2	26.2	1.69
15	47.1	31.9	1.48
20	70.0	39.7	1.76

interaction with water, or the plasticizer may be so hydrophobic as to almost neutralize the hydrophilic nature of the polymer. The former assumption seems more probable since both hydrophobic and hydrophilic plasticizers increase ΔH by about the same amount.

The above data may also be used to calculate the entropy change which occurs when a mole of water vapor dissolves in the polymeric material. Thus one can estimate the amount of freedom which the dissolved water molecules possess. The free energy change for the transfer of one mole of water from the vapor (at 1-cm Hg pressure) to the polymer, is $\Delta F = -RT \ln S$. ΔH for the same process is listed in Table IV. ΔS, the change in entropy, is then found from the relation, $\Delta F = \Delta H - T\Delta S$. The entropy changes at 20° and 50° are recorded in Table V.

It can be seen from Table V that there is a considerable entropy decrease involved in the process of solution of water in polyvinyl chloride. Its magnitude indicates that the water molecules have lost almost as much entropy as that involved when the vapor condenses to ice. They must, therefore, be rather tightly held in the film, possessing little freedom except when moving from one point of attraction to another. In the copolymer almost the same conditions prevail. However, when plasticizer is introduced, the entropy change is lowered to that corresponding to the ordinary solution of a gas in a liquid. Thus water molecules in the plasticized film are about as free to move as they would be in an ordinary liquid solvent. It appears then that the effect of the plasticizer has been twofold. First, it has greatly lowered the heat of solution of water in the film and this in turn has increased $\log P_0$ and E. Second, the freedom of movement of the water molecules is enormously increased when plasticizer is present.

DISCUSSION

If the values of $\log P_0$ and E for the plasticized samples of polyvinyl chloride-acetate (Table IV) were plotted on the graph in Fig. 1, it is seen that these two points would fall above the straight line joining the points for pure polymeric substances. In considering Barrer's data for permanent gases it was noted that the points for Bakelite and ebonite were considerably lower than the straight line determined by the other materials. The data for Cellophane must be excluded from consideration because it is a composite film. Since it is a coated regenerated cellulose material the actual thickness which is used in evaluating the permeability constant is meaningless.

TABLE IV. Energies of activation and heats of solution.

Film material	E	$\log P_0$	E_D	$\log D_0$	ΔH
Polyvinyl chloride	2600	−4.96	10,000	−1.17	−7400
Polyvinyl chloride-acetate	2600	−4.62	9,100	−0.60	−6500
Polyvinyl chloride-acetate +25% tricresyl phosphate	8700	−0.30	9,300	−0.72	− 600
Polyvinyl chloride-acetate +25% SC plasticizer	7800	+0.30	7,800	−0.61	0

An obvious suggestion may be advanced to explain the deviations just summarized, if we interpret the behavior as the increase or decrease of the energy of activation at constant value of

log P_0, that is, at a constant value of the entropy of activation, $\Delta S\ddagger$. Viewed in this manner the addition of small molecules (liquid) merely lowers the energy of activation for permeation by acting essentially as a lubricant for the matrix of polymer chains through which the gas molecules diffuse. Conversely, excessive cross-linking produces such rigidity even on a sub-microscopic scale that the attainment of the activated state requires a greater energy.

The explanation offered here for the observed relations between log P_0 and E are admittedly not compelling and have clearly been motivated by the data and not by *a priori* reasoning. At least two objections could arise. First, a linear relation between log P_0 and E may seem unreal since it has been demonstrated that P_0 is a composite quantity equal to the product of D_0 and S_0 and that E is equal to E_D plus ΔH. If D_0, S_0, E_D, and ΔH were all independent quantities, it would be practically impossible to believe that a simple linear relation had been found between log D_0S_0 and $(E_D+\Delta H)$. This situation could be resolved if it could be shown that S_0 and ΔH change very little from system to system in comparison to D_0 and E_D and hence it is only the relation between log D_0 and E_D that is actually being considered. Since data on these quantities are not available for the measurements with water vapor, we can only examine the data on the permanent gases. Here the ΔH for the various systems vary up to 500 cal./mole and log S_0 up to 0.4 from the average. Since the points in Figs. 2–4 seem to follow a linear relation with just about these tolerances, we can conclude that in view of the available experimental data the apparent linear relation between log P_0 and E may be a reflection of a real linear relation between log D_0 and E_D.

Secondly, in the argument used to obtain a relation between log P_0 and E it may appear that the energy of activation of a particular degree of freedom will surely differ as the polymer is changed, and hence the argument would be useful only in explaining a trend—not a relationship. As previously pointed out this objection becomes less and less valid the larger the number of degrees of freedom involved, for the deviation of the quantity from the average is less significant the larger the number of degrees of freedom.

TABLE V. Entropies of solution of water in various polymers.

Polymer	20°	50°
Polyvinyl chloride	−24.4	−24.2
Polyvinyl chloride-acetate	−20.8	−20.1
Polyvinyl chloride-acetate+25% tricresyl phosphate	−3.6	−3.6
Polyvinyl chloride-acetate+25% SC plasticizer	−2.7	−2.7

It is just this condition of a large number of degrees of freedom operating in the activated state that Barrer[1,2] has postulated on the basis of both kinetic and statistical considerations. Using the following equation due to Wheeler,[8] the number of degrees of freedom used in acquiring energy of activation for diffusion may be calculated on the basis of a reasonable model assuming the vibration frequency of the diffusing particle to be approximated by 2.5×10^2.

$$d^2=D_0e^{(n-1)}\frac{6(n-1)!}{2}\left(\frac{RT}{E_D+(n-1)RT}\right)^{(n-1)}. \quad (5)$$

d is the mean free path and n is the number of degrees of freedom involved. Using data contained in Table IV this equation can be solved for d by assigning various values to n. Thus for $n=6$, $d=4.5$A, and for $n=11$, $d=1.6$A, it is to be expected that the mean free path of a water molecule would certainly be somewhat less than the distance between the carbon-chlorine dipoles along the polyvinyl chloride chain. Thus a value of 1.6A is a good estimate and it thus appears that Wheeler's treatment of diffusion may be interpreted as postulating a large number of degrees of freedom for activation.

Wynne-Jones and Eyring[9] have derived an expression for the rate constant which may be transformed into the following expression for D_0 with only moderate approximations.

$$D_0=\exp(\Delta S\ddagger/R)(kT/h)(d^2/2.72). \quad (6)$$

If we assume that the mean free path of the water molecule in polyvinyl chloride systems is 1.6A, Eq. (6) can be solved to obtain $\Delta S\ddagger=13.9$ e.u. Slightly larger values were obtained by

[8] T. S. Wheeler, Trans. Nat. Inst. Sci. India 1, 333 (1938).
[9] W. F. Wynne-Jones and H. Eyring, J. Chem. Phys. 3, 492 (1935).

Barrer using 5.0A for the mean free path in the case of the permanent gases. Even if these estimated values of d are doubled, $\Delta S\ddagger$ is only reduced by about 3 e.u. This large value of $\Delta S\ddagger$, if it were all due to the diffusing molecule, would correspond to more than its entropy of solution. Since this is not possible, the medium must share in the entropy change. Thus the data on the diffusion of water vapor corroborate the conclusions reached by Barrer for permanent gases: that activation energy is shared in part or wholly in various degrees of freedom of the polymeric system.

ACKNOWLEDGMENT

The experimental data reported here were obtained in the course of work sponsored by the National Research Council and the Research and Development Branch of the Office of the Quartermaster General. It is a pleasure to acknowledge the assistance of Miss Helen Luben in the experimental work.

THE JOURNAL OF CHEMICAL PHYSICS VOLUME 14, NUMBER 4 APRIL, 1946

The Electrical Potential at the Interface between Vitreous Silica and Solutions of Barium Chloride

LLOYD A. WOOD AND LAWRENCE B. ROBINSON
Department of Chemistry, Harvard University, Cambridge, Massachusetts

(Received February 18, 1946)

The zeta-potential of vitreous silica in contact with several solutions of barium chloride has been determined by the measurement of streaming potentials. Solutions of seven concentrations between 10^{-6} M and 10^{-2} M, inclusive, were studied, and the zeta-potential was found to decrease in a regular manner with increasing concentration. It is evident that there is no maximum in the curve of the zeta-potential *vs.* concentration, as most experimenters have reported.

IT is the purpose here to report measurements of the zeta-potential of vitreous silica in contact with solutions of barium chloride. The zeta-potential is not directly measurable, but is obtained conveniently from measurement of streaming potentials arising from the flow of the solutions through vitreous silica capillaries. The physical significance of the streaming potential measurements and their relation through Helmholtz's equation to the zeta-potential have been critically examined elsewhere.[1] The apparatus and technique for obtaining the necessary reliable streaming potential data for the computation of zeta-potentials have been described previously,[2] together with measurements of the zeta-potential of silica in contact with dilute potassium chloride solutions. Added interest is lent to this investigation by the fact that the data obtained make possible a test of Langmuir's interpretation[3] of the Jones-Ray effect[4] observed with barium chloride.

EXPERIMENTAL

The apparatus and experimental technique employed in this investigation have been described previously[2] and no important changes have been made. Duplicate sets of streaming potential apparatus with capillaries of different diameters were operated concurrently so that observations with one could be corroborated with the other. Previous work has demonstrated that initial measurements of the zeta-potential are not usually reliable, because the surfaces of the capillaries sometimes require many days to attain equilibrium with the solution. It has not

[1] L. A. Wood, J. Am. Chem. Soc. **68**, 432 (1946).
[2] Grinnell Jones and L. A. Wood, J. Chem. Phys. **13**, 106 (1945).
[3] I. Langmuir, Science **88**, 430 (1938); J. Chem. Phys. **6**, 894 (1938).
[4] Grinnell Jones and W. A. Ray, J. Am. Chem. Soc. **59**, 187 (1937); **63**, 288 (1941); **63**, 3262 (1941); **64**, 2744 (1942).

TABLE I. Examples of data obtained with 1.00×10^{-3} M $BaCl_2$ (thirteenth day).

Flow	P cm	E millivolts	R ohms $\times10^{-6}$	κ ohms^{-1} cm^{-1} $\times10^{6}$	$E\kappa/P$ $\times10^{4}$	ζ millivolts
			Capillary I			
$L\leftarrow L'$	24.90	33.2	87.71	266.4	3.55	−34.2
$L\rightarrow L'$	24.70	34.0	87.87	265.9	3.66	−35.4
			Capillary II			
$L\leftarrow L'$	24.50	33.1	327.9	265.1	3.58	−34.6
$L\rightarrow L'$	24.10	32.8	326.8	266.0	3.62	−35.0

TABLE II. Summary of measurements with 1.00×10^{-3} M $BaCl_2$.

Time days	No.[a]	Capillary I $\kappa\times10^{6}$	Capillary I ζ mv	Capillary I Av. deviation	Capillary II $\kappa\times10^{6}$	Capillary II ζ mv	Capillary II Av. deviation
2	18	266.7	−37.0	1.1%	268.7	−33.0	2.7%
3	18	266.2	−35.7	0.6	268.0	−33.6	1.2
4	18	266.8	−35.7	0.6	268.2	−33.6	1.2
5	18	267.9	−34.9	0.3	268.2	−33.5	0.9
6	18	267.8	−34.7	0.6	268.3	−33.6	1.2
7	30	266.3	−34.3	0.6	267.6	−33.9	0.6
8	24	267.9	−34.1	0.6	268.0	−33.8	0.3
9	18	267.9	−33.9	0.6	267.9	−34.2	1.2
10	12	268.4	−34.7	0.6	268.2	−34.0	2.1
11[b]	6	267.0	−34.7	0.7	266.2	−42.1	0.7
12	6	267.2	−34.4	0.3	266.6	−37.1	0.5
13	12	266.3	−34.6	1.7	265.3	−34.8	0.3

[a] "No." denotes the number of individual measurements constituting the series summarized. Since each measurement was duplicated with Capillary II, the same number of measurements was made with each capillary. Four individual measurements are given in Table I.

[b] A new sample of the solution was placed in each set of apparatus preceding this measurement.

been found possible to control the previous treatment of the surfaces so that the potentials are immediately reproducible, and the practice in this laboratory has been to study the variation of the zeta-potential with time until it was reasonably certain that the equilibrium potential was reached. The two capillaries were adjudged to have reached equilibrium when they reached the same value and remained unchanged for several days, but in general it was necessary to be satisfied with somewhat less than this ideal behavior. With solutions of barium chloride the approach to a constant value was much more rapid than with any of the solutions which have been studied in this laboratory at the date of writing, including potassium chloride, thorium chloride, and lanthanum chloride.

The capillary surfaces were prepared for measurements with solutions of a given concentration by immersing them in hot nitric acid (redistilled) for a day or more. Then steam and hot water from a silica condenser was drawn through them for about an hour, in order to remove the nitric acid, followed by a final rinse while hot with about 20 cc of the solution about to be measured. This cleaning treatment was given the capillaries preceding a change in the concentration of the solution. It was found effective in establishing conditions for eventual agreement of the zeta-potential of the two capillaries within a few millivolts.

TABLE III. Examples of data obtained with 1.00×10^{-4} M $BaCl_2$ (fourteenth day).

Flow	P cm	E millivolts	R ohms $\times10^{-6}$	κ ohms^{-1} cm^{-1} $\times10^{6}$	$E\kappa/P$ $\times10^{4}$	ζ millivolts
			Capillary I			
$L\leftarrow L'$	25.20	626.3	833.3	28.04	6.97	−67.3
$L\rightarrow L'$	24.90	623.2	826.5	28.27	7.08	−68.4
			Capillary II			
$L\rightarrow L'$	24.50	680.7	3225	26.95	7.49	−72.3
$L\leftarrow L'$	24.26	660.7	3145	27.64	7.53	−72.7

In obtaining streaming potential measurements, the experimental procedure was to apply a measured pressure difference, P, between the two reservoirs at either end of the connecting capillary, and while the solution was flowing through the capillary, the following measurements were made in rapid succession: the electrical resistance, R, of the capillary was measured, then three measurements of the streaming potential, E, and of the pressure, P, were made, followed by a second resistance measurement. Then the direction of flow was reversed under approximately the same pressure, and the above procedure was repeated. These measurements were usually repeated two or three times with somewhat different pressures. No dependence of the quantity $E\kappa/P$ on the pressure was ever observed.

In presenting the data obtained, it is impractical to give all of the large number of individual measurements, but in order to furnish examples of the experimental data, a representative example, selected at random, of the data obtained with each capillary will be given for each solution. Then a table summarizing the results of each series will be given. The measurements are

TABLE IV. Summary of measurements with 1.00×10^{-4} M $BaCl_2$.

Time days	No.[a]	Capillary I $\kappa\times10^6$	Capillary I ζ mv	Capillary I Av. deviation	Capillary II $\kappa\times10^6$	Capillary II ζ mv	Capillary II Av. deviation
9[b]	18	27.80	−67.6	0.4%	27.38	−72.3	0.4%
10	12	27.80	−67.2	0.3	27.28	−72.2	0.3
11	18	27.88	−67.1	0.4	27.62	−73.2	0.3
12	24[c]	27.98	−67.7	0.4	27.71	−73.9	1.9
13	18	27.87	−67.4	0.4	27.26	−72.5	1.8
14	18	28.09	−67.7	0.4	27.43	−72.9	0.8
15[d]	12	27.85	−66.8	0.7	27.06	−72.0	2.2

[a] See footnote (a) in Table II.
[b] Preceding these measurements were earlier series. The first sample of the solution was found to give higher values for κ so it was thought probable that it had inadvertently become slightly contaminated. Therefore a new sample of the solution was placed in the apparatus on the eighth day. The zeta-potentials determined with the first sample were somewhat lower than those above.
[c] As a result of experimental difficulties, only 18 measurements were obtained for Capillary II in this series.
[d] Following the preceding series, both capillaries were warmed to see whether any change in the zeta-potential would result. When there was no change, the measurements were discontinued.

TABLE V. Examples of data obtained with 1.00×10^{-5} M $BaCl_2$ (eighth day).

Flow	P cm	E millivolts	R ohms $\times10^{-6}$	κ ohms^{-1} cm^{-1} $\times10^6$	$E\kappa/P$ $\times10^4$	ζ millivolts
			Capillary I			
$L\rightarrow L'$	23.80	7420	6983	3.346	10.43	−100.8
$L\leftarrow L'$	23.50	7330	7113	3.285	10.25	−99.0
			Capillary II			
$L\rightarrow L'$	23.20	6735	24,390	3.564	10.35	−100.0
$L\leftarrow L'$	23.10	6395	24,390	3.564	9.87	−95.3

TABLE VI. Summary of measurements with 1.00×10^{-5} M $BaCl_2$.

Time days	No.[a]	Capillary I $\kappa\times10^6$	Capillary I ζ mv	Capillary I Av. deviation	Capillary II $\kappa\times10^6$	Capillary II ζ mv	Capillary II Av. deviation
2	18	3.523	−94.3	1.1%	3.697	−90.4	2.3%
3	12	3.521	−97.3	2.0	3.668	−90.4	1.4
4	24	3.489	−97.4	1.4	3.706	−90.5	2.5
5	18	3.462	−98.3	3.1	3.688	−92.8	3.7
6	6	3.290	−96.8	2.8	3.477	−88.8	5.1
7[b]	24	3.299	−100.8	0.9	3.574	−97.3	1.7
8	18	3.292	−99.3	0.7	3.556	−96.7	2.1
9	18	3.306	−97.7	0.8	3.478	−93.6	2.2
10	18	3.400	−99.7	1.5	3.681	−97.3	2.3

[a] See Note (a) of Table II.
[b] Preceding the measurements on the seventh day, the solution in both sets of apparatus was mixed by forcing all the solution into reservoir L and bubbling a small amount of nitrogen through it.

discussed in the chronological order in which they were made, except for those with 10^{-6} M and 10^{-2} M, which are discussed at the end. The temperature was 25°C±0.03° in every instance. The values for the fundamental physical constants are taken from the tabulation of Birge,[5] except the data for the dielectric constant and viscosity coefficient, which were assumed to be the same as for pure water, as given by Dorsey.[6] The zeta-potential, ζ, is obtained from the equation of Helmholtz:[1,7]

$$\zeta=(4\pi\eta E\kappa)/(DP),$$

in which η is the viscosity coefficient, κ is the specific conductance of the liquid in the capillary, and D is the dielectric constant, the other quantities being defined above.

Measurements

The behavior of the capillary surface with the 10^{-3} M $BaCl_2$ was unusual in that there was little variation and almost perfect agreement. Two individual measurements with each capillary are given in Table I. The large reservoirs at either end of the capillaries were identified as L and L', and the direction of flow is indicated accordingly. It is believed that the precision of all the measurements is 0.5 percent or better. The two potentials given for each capillary are the first measurements of two successive series of three, as described above, carried out on the thirteenth day of observation. Ten other similar measurements were made on that day with each capillary. All the measurements made with this concentration of $BaCl_2$ are summarized in Table II. It was observed that the zeta-potential of Capillary I was initially −37.0 millivolt and on long standing decreased slightly to about −34 millivolt. The zeta-potential of Capillary II was −33 millivolt initially, and this increased slightly to about −34 millivolt on standing. When a fresh solution was substituted after the measurements on the tenth day, the potential of Capillary I appeared to be undisturbed, while that of the other capillary was considerably increased. Because the potential of Capillary II soon returned to about −34 millivolt, it was presumed that the equilibrium had been upset for some unknown reason but that it was soon

[5] R. T. Birge, Rev. Mod. Phys. **13**, 233 (1941); Am. J. Phys. **13**, 63 (1945).
[6] N. E. Dorsey, *Properties of Ordinary Water Substance* (Reinhold Publishing Corporation, New York, 1940), pp. 187 and 364.
[7] H. Helmholtz, Wied. Ann. **7**, 337 (1879).

TABLE VII. Examples of the data obtained with 5.00×10^{-4} M $BaCl_2$ (fifth day).

Flow	P cm	E millivolts	R ohms $\times10^{-6}$	κ ohms^{-1} cm^{-1} $\times10^{6}$	$E\kappa/P$ $\times10^{4}$	ζ millivolts
			Capillary I			
$L\leftarrow L'$	24.18	105.5	175.0	133.5	5.82	−56.3
$L\rightarrow L'$	23.86	103.9	175.0	133.5	5.81	−56.2
			Capillary II			
$L\leftarrow L'$	24.66	104.4	650.1	133.7	5.66	−54.7
$L\rightarrow L'$	24.46	106.2	650.1	133.7	5.80	−56.1

TABLE VIII. Summary of measurements with 5.00×10^{-4} M $BaCl_2$.

Time days	No.[a]	Capillary I $\kappa\times10^{6}$	ζ mv	Av. deviation	Capillary II $\kappa\times10^{6}$	ζ mv	Av. deviation
2	18	133.2	−55.1	0.4%	131.9	−53.8	1.1%
3	18	133.4	−55.7	0.4	132.4	−52.7	1.3
4	24	133.0	−55.6	0.4	131.5	−55.0[b]	1.3
5	24	133.6	−56.1	0.4	133.2	−55.2	1.3
6	18	133.6	−56.3	0.2	133.0	−55.0	1.6
7	30	133.7	−56.5	0.3	133.6	−55.2	1.6

[a] See Note (a) of Table II.
[b] The increase in the potential of Capillary II on the fourth day may be attributed to the fact that, preceding these measurements, the solution in reservoir L' was forced into reservoir L to remix the solution in order to eliminate the electrode asymmetry and decrease the average deviation. Although this did not result, the disturbance of the double layer caused by flow of the solution through the capillary apparently had the effect of hastening the attainment of equilibrium.

reestablished. The accepted value for the zeta-potential with this solution was −34 millivolt.

With 10^{-4} M $BaCl_2$ the observations were somewhat less satisfactory. In Table III are given individual measurements to serve as examples of the measured quantities, selected as in Table I. It will be noticed that with both capillaries there was a slight asymmetry of the observed zeta-potentials, which was the result of asymmetry of the silver-silver chloride electrodes. Such asymmetries were common occurrences, particularly with the more dilute solutions, and were ascribed to slight differences in concentration which arose in the solutions. These differences may have been caused by some of the silver chloride dissolving from the electrodes or by the glass of the reservoir walls dissolving, or by the ingress of some other impurity. The asymmetries could usually be eliminated, or greatly diminished, by remixing the solution, which was done by forcing all the solution into one reservoir and bubbling a small amount of nitrogen through it for stirring. Then half the solution was forced back through the capillary to the empty reservoir so that the measurements could be continued. However, with 10^{-4} M $BaCl_2$ the asymmetries were not large enough to make this necessary, as is evident from the "average deviations" from the mean of each series as given in Table IV, the summary of the measurements with this concentration. Earlier measurements were made, but it was found that the conductivity figures were high as compared with those observed with the fresh sample of the solution placed in the apparatus on the eighth day of observation. Therefore the measurements prior to the ninth day were discarded. The zeta-potential of Capillary II was always about 5 millivolts higher than that with Capillary I, and there appeared to be no tendency for them to converge. However, the two values were considered to be in close enough agreement so that further work was unwarranted. The accepted value for the zeta-potential was taken as −70 millivolt, the average on the thirteenth and fourteenth days, when it seemed that constant values had been reached.

In Table V are examples of the individual measurements with 10^{-5} M $BaCl_2$. In the in-

TABLE IX. Examples of the data obtained with 2.50×10^{-3} M $BaCl_2$ (second day).

Flow	P cm	E millivolts	R ohms $\times10^{-6}$	κ ohms^{-1} cm^{-1} $\times10^{6}$	$E\kappa/P$ $\times10^{4}$	ζ millivolts
			Capillary I			
$L\rightarrow L'$	27.34	16.8	36.32	643.3	3.95	−38.2
$L\leftarrow L'$	27.00	16.9	36.29	643.8	4.03	−38.9
			Capillary II			
$L\rightarrow L'$	28.00	13.6	134.91	644.3	3.13	−30.2
$L\leftarrow L'$	27.80	13.9	134.95	644.1	3.22	−31.1

TABLE X. Summary of measurements with 2.50×10^{-3} M $BaCl_2$.

Time days	No.[a]	Capillary I $\kappa\times10^{6}$	ζ mv	Av. deviation	Capillary II $\kappa\times10^{6}$	ζ mv	Av. deviation
1	12	645.0	−38.5	0.3%	643.8	−30.6	2.0%
2	6	643.7	−38.6	1.0	644.1	−30.7	1.6
5	6	642.6	−38.6	0.3	642.2	−30.0	0.3
7[b]	6	634.2	−37.9	0.5	635.4	−31.2	0.3
8	12	641.2	−38.1	0.5	640.5	−31.8	2.5

[a] See Note (a) in Table II.
[b] A new sample of the solution was placed in both sets of apparatus preceding these measurements.

TABLE XI. Measurements with 1.00×10^{-2} M $BaCl_2$.[a]

Flow	P cm	E millivolts	R ohms $\times10^{-4}$	κ ohms^{-1} cm^{-1} $\times10^{6}$	$E\kappa/P$ $\times10^{4}$	ζ millivolts
A. Examples of the data obtained (fourteenth day)						
$A\rightarrow B$[a]	37.23	3.4	13.65	2369	0.216	−2.1
$A\leftarrow B$	40.64	3.2	13.73	2356	0.185	−1.8

B. Summary of the data

Time days	No.[b]	κ $\times10^{6}$	E/P av.	ζ millivolts	Average deviation millivolts
1	4	2363	0.114	−2.6	0.62
14	12	2365	0.081	−1.84	0.21
15	12	2369	0.081	−1.86	0.17

[a] The apparatus used for these measurements is that described in reference 8.
[b] The "No." is the number of measurements which were averaged to yield the figures reported. Two such measurements are given in A.

stances given, there is a slight asymmetry in the values from Capillary I, and a much larger asymmetry with Capillary II. These were observed to some extent in all the measurements, summarized in Table VI, and were responsible for the larger average deviations. Mixing the solutions prior to the measurements on the seventh day decreased the asymmetry with both capillaries, but did not entirely eliminate it with either set of apparatus. However, averaging the zeta-potentials causes the cancellation of a constant asymmetry so that the accuracy of the measurements is greater than that indicated by the average deviation. The accepted equilibrium zeta-potential value was −98 millivolt, the average of the measurements on the tenth day.

The next solution measured was the 5×10^{-4} M $BaCl_2$, and examples of individual measurements are given in Table VII. In the examples there appeared to be no asymmetry with Capillary I, but there was a noticeable amount with Capillary II. This is also evident from the figures for the average deviations in Table VIII, wherein all the measurements with this concentration are summarized. Little or no variation with time was observed with Capillary I, but there was a slight increase in the zeta-potential with Capillary II. The accepted value of the zeta-potential was −55 millivolt.

Measurements were then made with 2.5×10^{-3} M $BaCl_2$ (see Table IX), which were somewhat more difficult to obtain because of the low streaming potential and the difficulty of determining the zero point for the resistance measurements with the direct current bridge. The relatively high conductivity of the solution resulted in considerable polarization of the electrodes when the bridge current was applied, causing the zero point to shift. However, the measurements of E and R are considered accurate to better than 1 percent. Essentially constant zeta-potentials were observed with Capillary I, all at about −38 mv, a higher value than was observed previously with a more dilute solution. (See Table X.) With Capillary II, the zeta-potential was about −31 millivolt most of the time, reaching −32 on the last day of observation. Substituting a fresh solution after the measurements of the fifth day brought about no appreciable change in the zeta-potential of either capillary. The accepted value was −35 millivolt, the average of the measurements on the eighth day. Reference is made below to the fact that this is higher than the potential to be expected from the measurements with more dilute solutions. These results were less gratifying than those with the other concentrations, in that the two capillaries acquired potentials relatively far apart, and the accepted value was not as concordant with the other measurements as might be desired.

A few measurements were made with 10^{-2} M $BaCl_2$ in the simpler apparatus constructed for measurements with pure water previously described elsewhere.[8] The greater ease of manipu-

TABLE XII. Measurements with 1.00×10^{-6} M $BaCl_2$.[a]

Flow	P cm	E millivolts	R ohms $\times10^{-6}$	κ ohms^{-1} cm^{-1} $\times10^{6}$	$E\kappa/P$ $\times10^{4}$	ζ millivolts
A. Examples of the data obtained (third day)						
$A\leftarrow B$	18.52	10,007	14,790	2.187	11.81	−114.1
$A\rightarrow B$	15.07	8,013	14,660	2.206	11.73	−113.3

B. Summary of the data

Time days	No.	$\kappa\times10^{6}$	E/P av.	ζ millivolts	Average deviation
1	24	2.298	520.7	−115.7	0.6%
2	24	2.415	504.3	−117.7	0.8
3[b]	36	2.250	527.3	−114.5	2.1
4	24	2.310	513.0	−114.5	0.6
5	22	2.315	523.0	−117.1	0.5
6	12	2.339	504.7	−114.1	0.9

[a] The apparatus used for these measurements is that described in reference 8. Bright platinum electrodes were used instead of silver-silver chloride electrodes to avoid introduction of silver ions and additional chloride ions.
[b] A new sample of the solution was placed in the apparatus preceding these measurements.

[8] L. A. Wood, J. Am. Chem. Soc. 68, 437 (1946).

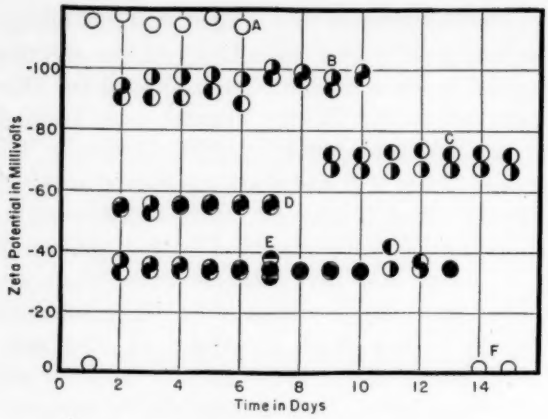

FIG. 1. Variation of the zeta-potential with time.

Data from all-silica apparatus: ○.
Data from Capillary I: ◑; data from Capillary II: ◐.
A: 10^{-6} *M*; *B*: 10^{-5} *M*; *C*: 10^{-4} *M*; *D*: 5×10^{-4} *M*; *E*: 10^{-3} *M*; *F*: 10^{-2} *M*.
Selected data for 2.5×10^{-3} *M*: ◓ for Capillary I; ◒ for Capillary II.

lation of this apparatus, and the fact that the low streaming potential limited the accuracy of its measurement, rendered the use of this apparatus more desirable than the more elaborate apparatus employed in the above measurements. The results of the measurements with this concentration are given in Table XI. The conductance, κ, is calculated from R with the cell constant, (length)/(cross section), of 32,345. The summary of the data indicates that the zeta-potential with this solution is about -2 millivolt. While the percentage deviation is very large, because of the low streaming potential, the actual magnitude of the average deviation is comparable to that of the 10^{-3} *M* solutions.

Measurements were made with 10^{-6} *M* $BaCl_2$, using the same all silica apparatus. With such a dilute solution, it is particularly important to avoid the introduction of impurities either from the glass or the silver-silver chloride electrodes of the more elaborate apparatus suitable for use with less dilute solutions. Therefore the bright platinum electrodes were used, and since the liquid came in contact only with these and with the silica, this danger was avoided. However, the values obtained for the specific conductance were larger than would be expected, as can be seen from the data in Table XII. The water used in preparing the solutions was conductivity water which had been redistilled with a silica condenser, and should have had a κ of less than 0.5×10^{-6}. The conductance of 10^{-6} *M* $BaCl_2$ should have added about 0.28×10^{-6} to this value of κ for the water, giving a total κ of less than 0.8×10^{-6}. However, it will be noted that the measured resistance of the capillary containing this solution was about 14,000 megohms, which gives a κ approximately three times larger than 0.8×10^{-6}. This could be explained in several ways: (1) the solution had become contaminated, (2) the extra conductance was the result of surface conductance, and (3) some path existed for the current other than through the solution. If (1) was the true reason, then the results are in error, but if either (2) or (3) was responsible for the high κ, then the value for the zeta-potential is correct, because the quantity required for the calculation of the zeta-potential is in reality the resistance between the ends of the capillary, which is the quantity measured.[1] The accepted value of the zeta-potential for this concentration is -115 millivolt, but it must be considered less certain than the values for the other solutions.

In order to show the relative constancy and concordance of the measurements, the zeta-potentials are plotted in Fig. 1 as functions of time, except for the 2.5×10^{-3} *M* solution which would have been so intermingled with the 10^{-3} *M* solution data as to be confusing. The data for the seventh day from Table X for the 2.5

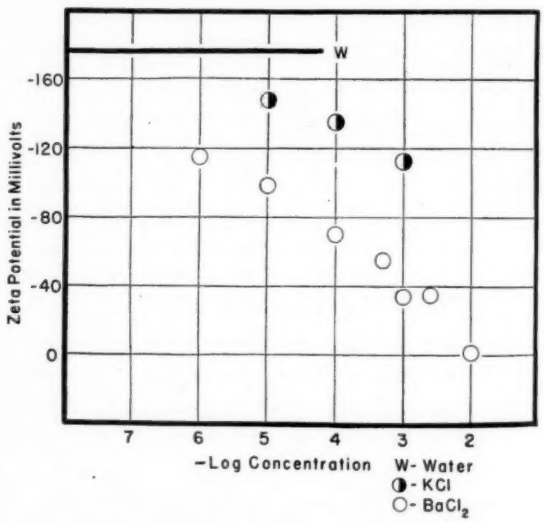

FIG. 2. Variation of the final zeta-potentials with concentration. Barium chloride: ○; potassium chloride: ◑. The line *W* is the zeta-potential of silica in contact with pure water, which the curves described by the points should approach with dilution.

$\times 10^{-3}$ M solution are shown immediately below the letter E, however. The radius of each circle is 2.5 millivolts, and it is evident that in general the agreement between the values for the two capillaries was better than this.

DISCUSSION

In Fig. 2 are plotted the accepted values for the zeta-potential with each of the barium chloride solutions, together with the zeta-potentials observed earlier[2] with three solutions of potassium chloride. The abscissa represents the logarithm of the molar concentration of salt. The solid line W is the zeta-potential of silica in contact with pure water, known to be about -177 millivolt;[8] both curves should approach this line as the concentration approaches zero and $\log c$ approaches $-\infty$. Attention is directed to the fact that neither with potassium chloride nor with barium chloride does there appear to be any maximum zeta-potential, and it cannot be considered probable that additional data would reveal a maximum. This substantiates the observations of Rutgers, Verlende, and Moorkens,[9] who reached the same conclusion about the zeta-potential of glass in contact with these solutions.

Instead of going through a maximum, the zeta-potential for these two salts has been observed to decrease with increasing concentration in a more or less regular fashion. It has been noted above, however, that the 5×10^{-4}, 10^{-3}, 2.5×10^{-3} M points are not entirely consistent, because it is evident either that the zeta-potentials for 5×10^{-4} M and particularly for 2.5×10^{-3} M $BaCl_2$ are too high, or that the potential for 10^{-3} M (and possibly 10^{-2} M) are too low. It will be recalled that the order in which the solutions were measured was 10^{-3}, 10^{-4}, 10^{-5}, 5×10^{-4}, and 2.5×10^{-3} M, so that a considerable period of time intervened between the inconsistent measurements. These observations suggest that the effect may be the result of hysteresis, but it seems improbable that any such hysteresis effect could have survived the treatment with nitric acid and steam which was given the capillaries when the concentration was changed. It seems more reasonable to conclude that this is the result of the inability to control completely for a long time the condition of the surface of the capillary. The fact that the values for the 2.5×10^{-3} M solution were 6 mv apart also indicates that the same equilibrium conditions did not prevail on each capillary surface with this solution. If the values for the 5×10^{-4} and 2.5×10^{-3} M solutions had been 5 millivolts lower, and the value for the 10^{-3} M solution had been 5 millivolts higher than they were, then the points would have described a smooth curve. Therefore, it seems evident that the discrepancy can be attributed entirely to the inability to reproduce the surface, after a long time has elapsed, so that the zeta-potential is reproduced to better than 5 millivolts of its true value. However, in spite of these minor inconsistencies, the measurements represent a substantial improvement in the state of present knowledge of zeta-potentials.

[9] A. J. Rutgers, Trans. Faraday Soc. **36**, 69 (1940); Rutgers, Verlende, and Moorkens, Proc. Ned. Akad. Wet. Amst. **41**, 763 (1938).

A Test of Langmuir's Interpretation of the Jones-Ray Effect

LLOYD A. WOOD AND LAWRENCE B. ROBINSON
Department of Chemistry, Harvard University, Cambridge, Massachusetts

(Received February 18, 1946)

Jones and Ray observed a minimum in the surface tension-concentration curve of electrolyte solutions at about 0.001*N*. Langmuir interpreted this as an instrumental effect rather than a real minimum, and advanced a quantitative theory by which the surface tension data could be corrected. To compute the Langmuir correction factor the zeta-potentials of vitreous silica in contact with the solutions measured by Jones and Ray in their capillarimeter are required. Since the zeta-potentials with barium chloride solutions have now been measured, the Langmuir theory has been tested to see whether it eliminated the minimum observed with this solute, and this paper presents the results of this test. It was found that Langmuir's interpretation was strikingly substantiated.

JONES and Ray[1] measured the capillary rise of water and of barium chloride solutions in their silica capillarimeter, and found, as with other electrolytes, that the first trace of added salt brought about an apparent decrease in the surface tension. The barium chloride surface tension-concentration curve appeared to have a minimum at about 0.0005 *M*, at which the surface tension was 99.982 percent of that of pure water. Langmuir[2] suggested that this minimum was not real but was the result of variation in the thickness of the wetting film on the capillary wall, and he advanced a quantitative theory by which the thickness could be calculated provided that the zeta-potential of the silica in contact with the various solutions was known. Jones and Frizzell[3] have discussed the application of this theory to 1–1 electrolytes, and Jones and Wood[4] made the first test of it with data on potassium chloride, in which it was found that application of the Langmuir correction eliminated the minimum. Another test[5] was made with data on the same potassium chloride solutions but with 10^{-6} *M* thorium chloride added, but application of the correction only served to deepen the minimum. With the zeta-potential of silica in contact with various barium chloride solutions reported in the preceding paper, it is possible to make another test of the Langmuir theory, and that is the purpose of this paper.

[1] Grinnell Jones and W. A. Ray, J. Am. Chem. Soc. **63**, 288 (1941).
[2] I. Langmuir, Science **88**, 430 (1938); J. Chem. Phys. **6**, 894 (1938).
[3] Grinnell Jones and L. D. Frizzell, J. Chem. Phys. **8**, 986 (1940).
[4] Grinnell Jones and L. A. Wood, J. Chem. Phys. **13**, 106 (1945).
[5] L. A. Wood, J. Chem. Phys. **13**, 429 (1945).

LANGMUIR'S METHOD FOR CALCULATING THE THICKNESS OF THE WETTING FILM APPLIED TO BARIUM CHLORIDE SOLUTIONS

The method by which Langmuir proposed that the wetting film thickness be calculated has been previously developed and applied[2,3,5] to solutions of 1–1 electrolytes, but this treatment is not applicable directly to the barium chloride solutions. Therefore, the adaptation to this class of electrolytes is given below.

The Poisson-Boltzmann equation for the electrical potential in an electrolyte solution in the region of a uniformly charged plane is

$$\frac{d^2\psi}{dx^2}=-\frac{4\pi}{D}\sum_{i=1}^{s} n_i z_i \epsilon \exp\left(\frac{-z_i\epsilon\psi}{kT}\right), \qquad (1)$$

wherein ψ is the electrical potential, D is the dielectric constant of the solution, n_i is the number of ions per cc of species i, z_i is the charge on an ion of species i, and ϵ is the magnitude of the electronic charge. Integration of this equation yields

$$p^2=[2A\sum_i n_i \exp(-z_i\eta)]+C, \qquad (2)$$

wherein

$$\eta\equiv\epsilon\psi/kT, \quad 1/A\equiv\sum_i n_i z_i^2, \quad p\equiv d\eta/d\theta, \quad \theta\equiv\kappa x. \qquad (3)$$

κ is the well-known Debye-Hückel parameter, and C is the constant of integration. The constant C is evaluated through use of the boundary condition that at the air surface, where $\theta=0$,

the potential is assumed to have its minimum magnitude ψ_m so that $\eta=m$ and $p=0$. Thus

$$d\theta=d\eta/[2A\sum_i n_i\{\exp(-z_i\eta)-\exp(-z_i m)\}]^{\frac{1}{2}}. \quad (4)$$

Let

Ba^{++} be species 1; $z_1=+2$,
H^+ be species 2; $z_2=+1$,
Cl^- and OH^- be species 3; $z_3=-1$.

Then substituting $K=\exp(m)$ and $y=\exp(\eta)$,

$$d\theta=\frac{dy}{y[2A(n_1y^{-2}+n_2y^{-1}+n_3y-n_1K^{-2}-n_2K^{-1}-n_3K)]^{\frac{1}{2}}}. \quad (5)$$

Since $n_i=c_iN\times10^{-3}$, where c_i is the molar concentration of species i and N is Avogadro's number, Eq. (5) becomes

$$d\theta=\frac{(3c_1+c_2)^{\frac{1}{2}}dy}{[a_1y^3+a_2y^2+a^3y+a_4]^{\frac{1}{2}}}, \quad (6)$$

wherein

$$a_1\equiv c_3=2c_1+c_2;$$
$$a_2\equiv-[c_1K^{-2}+c_2K^{-1}+(c_2+2c_1)K]; \quad (7)$$
$$a_3\equiv c_2;\quad a_4\equiv c_1.$$

The constant m introduced into Eq. (4) must be evaluated, so that K and a_2 may be known. According to Langmuir, if the film is thick enough so that van der Waals and other short range forces may be neglected, there are then the following three forces in equilibrium at the air surface of the film: (1) the pressure $-(d-\beta)hg$, owing to the pull of gravity, which tends to make the film thinner (d is the density of the solution; β, the density of air; h, the height above the surface of the main body of the liquid; and g, the acceleration of gravity); (2) the pressure $(d-\beta)hg/2$, resulting from the surface tension of the cylindrical surface which tends to make the film thicker; and (3) the difference between the osmotic pressure in the bulk solution and in the air interface of the wetting film. From van't Hoff's simple law and the Maxwell-Boltzmann equation, this difference in osmotic pressure is

$$\sum_i n_ikT(K^{-z_i}-1)$$

tending to make the film thicker. At equilibrium, the sum of these pressures is zero, and therefore:

$$\sum_i n_ikT(K^{-z_i}-1)-(d-\beta)hg/2=0. \quad (8)$$

Substituting $n_i=c_iN\times10^{-3}$:

$$c_1K^{-2}+c_2K^{-1}+(c_2+2c_1)K=\frac{500(d-\beta)hg}{NkT}+3c_1+2c_2=-a_2. \quad (9)$$

This equation may be solved for K to give the value of ψ_m. Because the potentials to be considered are negative and m is therefore negative, and since $K=e^m$, the root of Eq. (9) between 0 and +1 is the only possible value of K.

The thickness of the wetting film, Δr, is given by

$$\kappa\cdot\Delta r=\int_{y_0}^{y_1}d\theta=(3c_1+c_2)^{\frac{1}{2}}\int_{y_0}^{y_1}\frac{dy}{Q^{\frac{1}{2}}}, \quad (10)$$

wherein $Q=a_1y^3+a_2y^2+a_3y+a_4$, $y_0=K$, and y_1 is the value of y at the solid surface where $\psi=\zeta$. For numerical evaluation of Δr, Eq. (10) must be transformed into the Legendrian form of an elliptic integral. Let Q be factored such that $e_1>e_2>e_3$:[6]

$$Q=a_1(y-e_1)(y-e_2)(y-e_3). \quad (11)$$

Substituting

$$y=(p+qt)/(1+t),$$

wherein

$$p=e_1+((e_1-e_2)(e_1-e_3))^{\frac{1}{2}},$$
$$q=e_1-((e_1-e_2)(e_1-e_3))^{\frac{1}{2}};$$

then

$$\Delta r=-M\int_{t_0}^{t_1}\frac{dt}{[(t^2-1)(t^2-b^2)]^{\frac{1}{2}}}, \quad (12)$$

wherein

$$b^2\equiv-\frac{(p-e_2)(p-e_3)}{(q-e_2)(q-e_3)},$$
$$M\equiv\frac{(p-q)}{\kappa}\left[\frac{3c_1+c_2}{a_1(q-e_1)(q-e_2)(q-e_3)}\right]^{\frac{1}{2}}.$$

Substituting $\sin\phi=b/t$, $\sin\alpha=1/b$,

$$\Delta r=(M/b)\int_{\phi_0}^{\phi_1}\frac{d\phi}{[1-\sin^2\alpha\sin^2\phi]^{\frac{1}{2}}}$$
$$=-(M/b)[F(\alpha,\phi_0)-F(\alpha,\phi_1)], \quad (13)$$

wherein $F(\alpha,\phi)$ denotes an elliptic integral of the first kind. Although it is not immediately apparent, it is true that $\phi_0=\pi/2$. Thus

$$\Delta r=-(M/b)[F(\alpha,\pi/2)-F(\alpha,\phi_1)], \quad (14)$$

[6] e_1, e_2, e_3 are numerically equal to the roots of Eq. (9), and $e_2=K$ for the systems to be considered.

TABLE I. Calculation of wetting film thicknesses.

c	0.0025	0.001	0.0005	0.0001
e_1	1.1895	1.3200	1.4880	2.4840
$e_2(=K)$	0.84865	0.77546	0.70345	0.49077
e_3	−0.49522	−0.48824	−0.47721	−0.40810
m	−0.16411	−0.25430	−0.35175	−0.71177
b	2.6349	3.4321	4.4322	10.7772
α	22.304°	16.939°	13.039°	5.324°
ψ_m(mv),	−4.21	−6.53	−9.03	−18.28
ζ(mv) (experimental)	−35	−34	−55	−70
y_1	0.25596	0.26612	0.11749	0.065517
i_1	−9.6622	−33.226	−20.277	−275.05
$\sin\phi_1$	−0.27384	−0.10330	−0.21859	−0.039182
ϕ_1	−15.893°	−5.929°	−12.626°	−2.242°
$F(\alpha, \pi/2)-F(\alpha, \phi_1)$	1.9103	1.7093	1.8118	1.6129
$1/\kappa(\times 10^8)$	35.13	55.54	78.54	175.4
M(A)	120.5	224.2	372.7	1487
Δr(A)	87	112	152	223

and the integral is now in a form suitable for computation. In some instances the angle ϕ_1 is negative, and it should be noted that

$$F(\alpha, -\phi_1) = -F(\alpha, \phi_1).$$

The negative sign of Δr is a result of the fact that the potential is negative. This means that although $|\zeta| > |\psi_m|$, $\zeta < \psi_m$, so that the integration must be regarded as performed in the negative direction.

COMPUTATION OF Δr

The surface tensions of the 2.5×10^{-3}, 1×10^{-3}, 5×10^{-4}, and 1×10^{-4} M $BaCl_2$ solutions were measured by Jones and Ray,[1] and with the reliable values of the zeta-potentials reported in the preceding paper, their surface tension data can be corrected in accordance with Langmuir's suggestion. The Langmuir correction requires the thickness of the wetting film at the meniscus in the capillary of the surface tension capillarimeter. The capillary radius was 0.0136 cm, and the meniscus was 10.862 cm above the surface of the main body of the liquid. In Table I is given an outline with numerical values of the computation of Δr. With each solution it was assumed, although the effect was negligible, that the concentration of the ions from the water was 1×10^{-6} M. The values for the fundamental physical constants are those of Birge;[7] the other required data are found in the paper of Jones and Ray.[1] The experimental values of the zeta-potential were used, rather than those given by a smoothed curve. The ψ_m values are given to show that the condition is fulfilled that these are the minimum values, being in each instance less than the zeta-potential (in absolute value). In Fig. 1 is shown the variation of Δr with different values of the zeta-potential. It is evident that had smoothed values for the zeta-potentials been used, the Δr's then obtained would have differed at most by 5 angstroms from the values in Table I.

THE REFERENCE LIQUID

The differential method of Jones and Ray yields the surface tension values which are relative to the surface tension of the reference liquid, water, and this observed surface tension is called the "apparent relative surface tension." The "corrected relative surface tension" is obtained by multiplying the apparent relative surface tension by the Langmuir correction factor, $(r-\Delta r_c)/(r-\Delta r_0)$, wherein Δr_c is the wetting film thickness of a solution at the meniscus in the capillary, and Δr_0 is the wetting film thickness with the reference water. According to Langmuir, because the value of Δr_0 depends on the concentration of ions in the reference water, it seems probable that the wetting film thickness with water should have varied somewhat with the purity of the water. However, Jones and Frizzell found that there was no variation in capillary rise with various samples of water with specific conductivities from 0.37×10^{-6} to 1.67×10^{-6}. If the equivalent conductances of the ions in the water (presumably H^+, HCO_3^-, OH^-) are assumed to total about 400, this range corresponds

[7] R. T. Birge, Rev. Mod. Phys. **13**, 233 (1941); Am. J. Phys. **13**, 63 (1945).

to a variation in concentration of 0.9×10^{-6} to 4.2×10^{-6} M. Actually Jones and Frizzell[8] gave a value for the capillary rise of the 0.9×10^{-6} M water which was 0.003 percent lower than that of the less pure samples, but they apparently did not consider this a significant difference, the probable error having been about the same magnitude. Since the work of Jones and Frizzell, it has been learned that the zeta-potential of vitreous silica in contact with water of $\kappa=0.2\times10^{-6}$ to 0.4×10^{-6} is about -177 millivolt.[9] With this knowledge it is possible to reexamine the question of whether the Langmuir theory would predict a variation for these samples of water. Although it is improbable that the zeta-potential is -177 millivolt over the entire range, it is not likely that the variation is large, since it has been shown that the addition of 10^{-5} M KCl lowers it only to -148 millivolt. It seems justifiable to assume a value of -177 millivolt over this range as an approximation.

On this basis the wetting film corrections for the surface tension data of Jones and Frizzell have been calculated as a function of the ion concentration of the water. In Table II are given the wetting film corrections for four different samples of water, including three samples measured by Jones and Frizzell, and a fourth of lower ion concentration than those. The Langmuir correction is given with reference to the 2×10^{-6} M water. It is evident that the 0.003 percent difference given by Jones and Frizzell is in the direction predicted by the Langmuir theory, whether or not any significance may be attached to it. From the column of "corrected relative surface tensions" it may be concluded that no significant variation should have been observed by Jones and Frizzell with the various water samples measured. It is also evident that had they measured water of the lowest ion concentration given, they would have detected a significant variation as a result of the wetting film, according to the Langmuir theory, because the correction factor is large enough to indicate that there should have been an observable difference, 0.011 percent, easily detectable within the precision of their method, in the apparent relative surface tensions. These arguments are of course all based upon the predicate that the true surface tension of the various samples of water is the same. It may be pointed out that if the zeta-potential decreases somewhat with increasing concentration, as it probably does, the evidence becomes still more favorable to the Langmuir theory, because the Δr's would then be somewhat smaller for the 2×10^{-6} and 4.2×10^{-6} M samples. It is apparent from these considerations that the observations of Jones and Frizzell with the various water samples do not offer any contradiction to the Langmuir theory. It is also apparent that the choice of the reference water with which to compare the $BaCl_2$ surface tensions does not matter greatly, provided it is chosen from the range measured by Jones and Frizzell.

TABLE II. Wetting film thicknesses and surface tensions for various water samples.

c	Δr(A)	Langmuir correction	Apparent relative s.t.	Corrected relative s.t.
0.54×10^{-6}	366	1.000,11	[a]	
0.95×10^{-6}	442	1.000,05	0.999,97[c]	1.000,02
2×10^{-6}	508	(1.000,000[b])	(1.000,000)	(1.000,000)
4.2×10^{-6}	543	0.999,97	1.000,00	0.999,97

[a] Surface tension not available for this sample.
[b] This sample is considered the reference liquid for the purposes of these calculations. Had any other sample been chosen as reference, the same relative values would have been held by all the numbers.
[c] It has been considered preferable to take this value literally from Table VI of Jones and Frizzell (reference 5) and to reserve considerations of significance for the "corrected relative surface tensions."

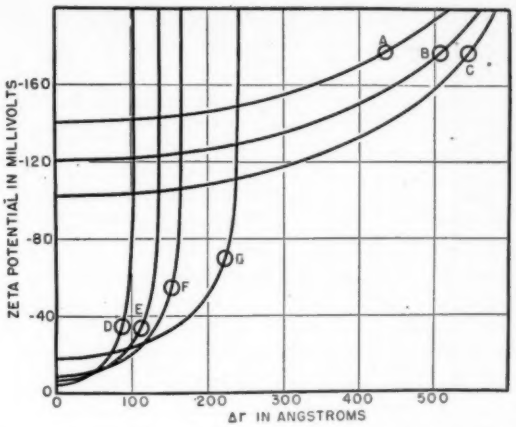

FIG. 1. Variation of the wetting film thickness in the Jones-Ray capillarimeter as a function of the zeta-potentials.

Water: A: $c=0.95\times10^{-6}$; B: $c=2\times10^{-6}$; C: $c=4.2\times10^{-6}$.
Barium chloride solutions: D: $c=0.0025$; E: $c=0.001$;
F: $c=0.0005$; G: $c=0.0001$.

[8] See Table VI, p. 996 in reference 3.
[9] L. A. Wood, J. Am. Chem. Soc. 68, 437 (1946).

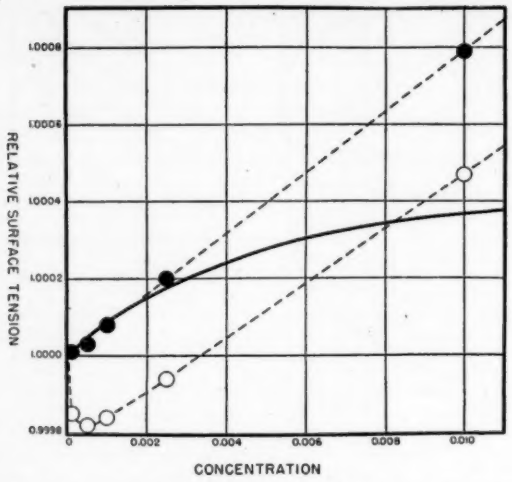

FIG. 2. Apparent and corrected relative surface tensions. Open circles are the measurements of Jones and Ray. Solid circles are the same measurements after application of the Langmuir correction. Solid line is given by the limiting law of Onsager and Samaras.

APPLICATION OF THE LANGMUIR CORRECTION TO THE $BaCl_2$ SURFACE TENSIONS

Whether or not it is proper to place much weight on the above considerations as a test of the Langmuir theory, a far more impressive substantiation can be observed with the barium chloride data. In Table III are given the corrected relative surface tensions of the barium chloride solutions with reference to the three samples of water. Since the Langmuir correction factor depends on the wetting film thickness for the reference water, the magnitudes of the factors are slightly different, depending on which Δr_0 is used. It is assumed in accord with the observations of Jones and Frizzell that the values for the observed apparent relative surface tensions are independent of the reference water, provided it is within the range discussed. It is clear from Table III that application of the Langmuir correction serves to eliminate the minimum from the surface tension curve no matter which reference Δr_0 is used. The effect of the Langmuir correction is shown graphically in Fig. 2, wherein the dashed curve with open circles represents the observed apparent relative surface tensions, and the dashed line with solid circles represents the corrected relative surface tensions with reference to the 0.95×10^{-6} M water. The radius of each circle is 0.001 percent, and it is seen that the corrected surface tensions fall almost exactly on a straight line. Had the corrected surface tensions with reference to the other water samples been plotted, the corresponding points for each concentration would have been 0.000,05 and 0.000,08 units above the given ones, for the 2×10^{-6} and 4.2×10^{-6} M samples, respectively. For the general interest, the relative surface tensions of these solutions have been computed according to the limiting law of Onsager and Samaras[10] and are given by the solid line. In these computations, the distance of approach of the ions was neglected, but the Y_c and Y_f series of Onsager and Samaras were evaluated to enough terms so that no approximation was introduced from that source. It may be observed that the limiting law curve appears to approach tangentially the line described by the corrected surface tensions. It is thus apparent that the Langmuir correction not only eliminates the minimum in the surface tension curve, but yields surface tensions which approach infinite dilution with a slope in agreement with the limiting law of Onsager and Samaras.

TABLE III. Corrected surface tensions for $BaCl_2$ solutions.

Conc.	Δr (angstroms)	Correction factor	Apparent relative s.t.	Corrected relative s.t.
		Reference water: 4.2×10^{-6} M		
Water	548	(1.000,00)	(1.000,00)	(1.000,00)
0.0001	223	1.000,24	0.999,85	1.000,09
0.0005	152	1.000,29	0.999,82	1.000,11
0.0010	112	1.000,32	0.999,84	1.000,16
0.0025	87	1.000,34	0.999,94	1.000,28
0.0100	0	1.000,40	1.000,47	1.000,87
		Reference water: 2.0×10^{-6} M		
Water	508	(1.000,00)	(1.000,00)	(1.000,00)
0.0001	223	1.000,21	0.999,85	1.000,06
0.0005	152	1.000,26	0.999,82	1.000,08
0.0010	112	1.000,29	0.999,84	1.000,13
0.0025	87	1.000,31	0.999,94	1.000,25
0.0100	0	1.000,37	1.000,47	1.000,84
		Reference water: 0.95×10^{-6} M		
Water	442	(1.000,00)	(1.000,00)	(1.000,00)
0.0001	223	1.000,16	0.999,85	1.000,01
0.0005	152	1.000,21	0.999,82	1.000,03
0.0010	112	1.000,24	0.999,84	1.000,08
0.0025	87	1.000,26	0.999,94	1.000,20
0.0100	0	1.000,32	1.000,47	1.000,79

[10] L. Onsager and N. N. T. Samaras, J. Chem. Phys. 2, 528 (1934).

THE JOURNAL OF CHEMICAL PHYSICS VOLUME 14, NUMBER 4 APRIL, 1946

Statistical Mechanics of Multimolecular Adsorption. I

TERRELL L. HILL
Department of Chemistry, University of Rochester, Rochester, New York
(Received December 26, 1945)

Cassie's statistical treatment of multimolecular adsorption on a free surface, leading to the BET equation, is criticized and corrected. The method is generalized to include adsorption when the maximum number of layers of adsorbate is restricted. The isotherm equation obtained is the same as that found by Brunauer, Emmett, and Teller for this case, rather than the equation proposed by Pickett. The BET equation, though not completely satisfactory, is apparently the correct equation for the particular model used. Real improvements in the theory should follow from refinements in the model rather than from modifications in the treatment of the BET model. A more refined model is proposed and the general method of using it is discussed. The BET model is shown to be a crude special case of the model suggested here, but it has the advantage of presenting no mathematical difficulties. Preliminary results, based on improved models, indicate that a somewhat refined multimolecular adsorption theory is capable of predicting capillary condensation for suitable values of parameters, thus suggesting that the ideas of multimolecular adsorption and capillary condensation are not really in conflict, as is generally assumed. Further discussion is deferred to a subsequent paper.

SEVERAL papers have appeared recently which direct attention to the foundations of the Brunauer-Emmett-Teller[1] theory of multimolecular adsorption. Cassie[2] has derived the BET equation for adsorption on a free surface (Eq. (15)) using a statistical argument. Pickett[3] has proposed a modification of the BET equation for adsorption when the number of layers of adsorbate is restricted (Eq. (27)). Actually, it appears to the present writer that Cassie has obtained the correct result by an incorrect argument and that Pickett's modification lacks theoretical justification,[4] though it seems to extend the range of agreement with experiment in some cases. The work of Cassie and of Pickett will be discussed further below in the light of results obtained here. We consider only localized adsorption in this paper.

MULTIMOLECULAR ADSORPTION ON A FREE SURFACE

We adopt the notation of Cassie as far as convenient and the BET model. That is, we suppose that there are B localized sites per unit surface area of adsorbent, that X of these sites are occupied by adsorbed molecules (first layer of adsorbate), and that $A-X$ molecules have been adsorbed on top of the X molecules in the first layer (thus forming second and higher layers). Also, molecules in the first adsorbed layer are characterized by a potential energy $-\epsilon_1$ and those in the second and higher layers by $-\epsilon_L$ (assumed the same as in the liquid state), both referred to infinite separation as energy zero. The partition function for a molecule in the first layer is then $j_S \exp(\epsilon_1/kT)$ and that for a molecule in higher layers is $j_L \exp(\epsilon_L/kT)$. One can approximate j_S and j_L by harmonic oscillator models:[5]

$$j_S=(kT/h\nu_S)^3 j, \tag{1}$$

$$j_L=(kT/h\nu_L)^3 je, \tag{2}$$

where j is the partition function for all internal degrees of freedom. This approximation is not essential to the argument.

The separate partition functions for the X molecules in the first layer and the $A-X$ in higher layers are then

$$Q_S=\frac{B!}{(B-X)!X!}[j_S \exp(\epsilon_1/kT)]^X, \tag{3}$$

$$Q_L=\frac{(A-1)!}{(A-X)!(X-1)!}[j_L \exp(\epsilon_L/kT)]^{A-X}. \tag{4}$$

The factor $B!/(B-X)!X!$ is the number of distinguishable ways X identical molecules may be distributed among B sites. The factor

[1] S. Brunauer, P. H. Emmett, and E. Teller, J. Am. Chem. Soc. 60, 309 (1938).
[2] A. B. D. Cassie, Trans. Faraday Soc. 41, 450 (1945).
[3] G. Pickett, J. Am. Chem. Soc. 67, 1958 (1945).
[4] T. L. Hill, J. Am. Chem. Soc. (March, 1946).
[5] See Eqs. (802,7) and (803,4) of Fowler and Guggenheim, *Statistical Thermodynamics* (Cambridge University Press, London, 1939).

$(A-1)!/(A-X)!(X-1)!$ is the number of distinguishable ways $A-X$ identical molecules may be distributed on top of the X molecules of the first layer (that is, the number of ways $A-X$ objects may be placed in X boxes, there being no restriction on the number per box).

The complete partition function of the system is then

$$Q=\sum_{X=1}^{k} Q_S Q_L$$

$$=\sum_{X=1}^{k}\left\{\frac{A!B!}{(A-X)!(B-X)!(X!)^2}\times[j_S \exp(\epsilon_1/kT)]^X[j_L \exp(\epsilon_L/kT)]^{A-X}\right\} \quad (5)$$

$$k=A \quad (A<B)$$
$$k=B \quad (A>B)$$

in which we have neglected unity as compared to A and X. The difference between the present treatment and that of Cassie should now be evident. Essentially, he omitted[6] the factorial expression in Eq. (4) and then incorrectly[7] introduced a factor $A!/X!(A-X)!$ on combining Q_S and Q_L. The two errors happened to cancel each other because unity may be neglected compared to A and X in Eq. (4).

We make the usual excellent approximation of setting $\log Q$ equal to the logarithm of the largest term in the sum. The value of X which gives this term is found from

$$\frac{\partial \log Q_S Q_L}{\partial X}=0. \quad (6)$$

On taking the logarithm and differentiating as indicated, there results

$$(A-X)(B-X)=\beta X^2, \quad (7)$$

with

$$\beta=\frac{j_L}{j_S}\exp[(\epsilon_L-\epsilon_1)/kT]. \quad (8)$$

The chemical potential of the adsorbed molecules is

$$\frac{\mu_A}{kT}=-\frac{\partial \log Q_S Q_L}{\partial A} \quad (9)$$

$$=\log\frac{A-X}{A}-\frac{\epsilon_L}{kT}-\log j_L, \quad (10)$$

where X is to be obtained from Eq. (7). For the gas phase, we write

$$\frac{\mu_G}{kT}=\frac{\alpha}{kT}+\log p, \quad (11)$$

where α is a constant which need not be further specified for our purposes. Equating μ_A and μ_G:

$$\log\frac{A-X}{A}-\frac{\epsilon_L}{kT}-\log j_L=\frac{\alpha}{kT}+\log p. \quad (12)$$

For the pure liquid:

$$-\frac{\epsilon_L}{kT}-\log j_L=\frac{\alpha}{kT}+\log p_0. \quad (13)$$

Hence, we have

$$x=p/p_0=(A-X)/A. \quad (14)$$

Combining Eqs. (7) and (14) gives the BET equation

$$A/B=cx/(1-x)(1-x+cx) \quad (15)$$

with

$$c=1/\beta. \quad (16)$$

MULTIMOLECULAR ADSORPTION WITH A LIMITED NUMBER OF LAYERS

In this section we shall extend the above treatment to the case of n (the maximum number of layers) finite.

If A molecules are adsorbed, suppose X_1 are in the first layer, X_2 in the second, $\cdots$, and X_n in the nth layer. Then

$$X_1+X_2+\cdots+X_n=A. \quad (17)$$

For given values of $X_1, X_2, \cdots, X_n$, the number of distinguishable arrangements for the second and higher layers is found by taking the product of (1) the number of ways X_2 objects may be distributed among X_1 sites, (2) the number of ways X_3 objects may be distributed among X_2 sites,

[6] This resulted from his treatment of second and higher layers as being structureless—the BET model was not introduced.

[7] There is no entropy of mixing when identical molecules are exchanged between two energy levels. The argument in the introduction of Cassie's paper should refer to the corresponding factor in Eq. (4).

etc. That is,

$$\frac{X_1!}{X_2!(X_1-X_2)!}\cdot\frac{X_2!}{X_3!(X_2-X_3)!}\cdots\frac{X_{n-1}!}{X_n!(X_{n-1}-X_n)!}=\frac{X_1!}{(X_1-X_2)!(X_2-X_3)!\cdots(X_{n-1}-X_n)!X_n!}. \tag{18}$$

Then

$$Q_S=\frac{B!}{(B-X_1)!X_1!}[j_S\exp(\epsilon_1/kT)]^{X_1}, \tag{19}$$

$$Q_L=\frac{X_1![j_L\exp(\epsilon_L/kT)]^{A-X_1}}{(X_1-X_2)!(X_2-X_3)!\cdots(X_{n-1}-X_n)!X_n!}; \tag{20}$$

and

$$Q=\sum_{X_1}\cdots\sum_{X_{n-1}}Q_SQ_L, \tag{21}$$

where the limits of summation in Eq. (21) are complicated, but are not needed here.

We again set $\log Q$ equal to the logarithm of the largest term in the sum. The values of X_1, X_2, $\cdots$, X_{n-1} which give this term are found from

$$\partial\log Q_SQ_L/\partial X_i=0,\quad i=1,2,\cdots,n-1, \tag{22}$$

using Eq. (17) for X_n. One finds, in the same way as Eq. (7) is obtained,

$$\begin{cases}(B-X_1)X_n=\beta(X_1-X_2)(X_{n-1}-X_n),\\ (X_1-X_2)X_n=(X_2-X_3)(X_{n-1}-X_n),\\ \quad\vdots\\ (X_{n-3}-X_{n-2})X_n=(X_{n-2}-X_{n-1})(X_{n-1}-X_n),\\ (X_{n-2}-X_{n-1})X_n=(X_{n-1}-X_n)^2.\end{cases} \tag{23}$$

Also, from Eqs. (9), (11), (13), and (17) (the steps are the same as for Eq. (14)),

$$X_n=x(X_{n-1}-X_n). \tag{24}$$

Combining Eqs. (23) and (24),

$$\begin{aligned}X_1-X_2&=\frac{(B-X_1)x}{\beta},\\ X_i-X_{i+1}&=(X_{i-1}-X_i)x=(X_1-X_2)x^{i-1}\\ &=\frac{(B-X_1)x^i}{\beta}\quad(i=2,3,\cdots,n-1),\\ X_n&=\frac{(B-X_1)x^n}{\beta}.\end{aligned} \tag{25}$$

Finally, by Eqs. (17) and (25),

$$\frac{A}{B}=\frac{(X_1-X_2)+2(X_2-X_3)+\cdots+(n-1)(X_{n-1}-X_n)+nX_n}{(B-X_1)+(X_1-X_2)+\cdots+(X_{n-1}-X_n)+X_n} \tag{26}$$

$$=\frac{\dfrac{B-X_1}{\beta}(x+2x^2+\cdots+nx^n)}{(B-X_1)+\dfrac{(B-X_1)}{\beta}(x+x^2+\cdots+x^n)},$$

$$=\frac{cx[1-(n+1)x^n+nx^{n+1}]}{(1-x)(1-x+cx-cx^{n+1})}, \tag{27}$$

which is the BET result.

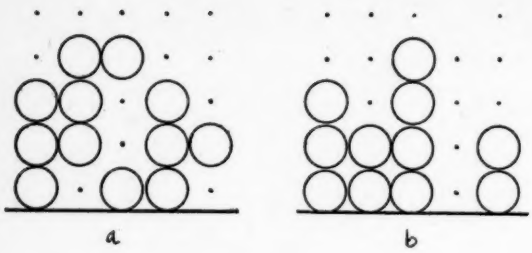

FIG. 1.

Pickett gives an alternative equation. However, the fact that Eq. (27) can be obtained from statistical mechanics (considering only possible states of the system, without recourse to a mechanism), as well as from the kinetic argument of the BET theory, indicates that it is certainly the correct equation for this model. The obvious implication is that real improvements in the theory must come from refining the model itself rather than from modifications of the type introduced by Pickett. We begin the discussion of other models in the next section.

INTRODUCTION TO A REFINED TREATMENT

In this section we shall indicate how the BET model may be considerably refined, at least in principle.[8] A more detailed treatment of the subject will be presented in a later paper of this series. We shall also treat, in future papers, multimolecular adsorption on a mobile first layer, the transition from a localized to a mobile first layer, and the relations between the adsorption isotherm and the two-dimensional equation of state (in mobile monomolecular adsorption).

The most general model to be considered here is the following. Molecules are adsorbed onto vacant sites of a lattice, with the restriction that a particular vacant lattice site cannot be occupied by a molecule unless at least one nearest neighbor site is already occupied or unless the site is in the first layer of the lattice (i.e., in the layer next to the surface of the adsorbent). The lattice is built up on the surface of the solid and sites correspond to possible equilibrium positions of molecules in the liquid state. Ordinarily the packing is assumed to be face-centered cubic, with 12 nearest neighbors ($z=12$). As before, the potential energy of interaction between the adsorbent and adsorbed molecules in the first layer is $-\epsilon_1$ and the average potential energy of a molecule in the liquid state is $-\epsilon_L$. Hence, the potential energy associated with each pair of nearest neighbors is $-2\epsilon_L/z$. The total potential energy of the system is

$$U=-\epsilon_1 X-2\epsilon_L N/z, \tag{28}$$

where X is the number of adsorbed molecules in the first layer and N is the number of pairs of nearest neighbors in the particular configuration being considered, *including* pairs involving molecules in the first layer.

As an example, in the two-dimensional simple cubic configuration of Fig. 1a, $z=4$, $X=3$, and $N=11$. This may be contrasted with a two-dimensional BET configuration, illustrated in Fig. 1b. The BET model allows (the same is true in three dimensions) only vertical additions to the lattice and also only takes into account vertical nearest neighbors. Thus, $z=2$, $N=A-X$, and, from Eq. (28),

$$U=-\epsilon_1 X-\epsilon_L(A-X). \tag{29}$$

In Fig. 1b, $X=4$ and $N=A-X=7$.

We return now to the general problem. For given values of X, A, and B, there are $p(X, A, B)$ distinguishable configurations such that each molecule has either at least one nearest neighbor or is in the first layer, or both. We group these configurations according to the value of N: there are $g(N, X, A, B)$ configurations with exactly N pairs of nearest neighbors. Hence,

$$\sum_N g(N, X, A, B)=p(X, A, B). \tag{30}$$

We have implicitly been considering the case of adsorption on a free surface ($n=\infty$). If n is finite, there is a new obvious restriction on acceptable configurations. In this case we may write

$$\begin{gathered}\sum_N G(N, X, A, B, n)=P(X, A, B, n),\\ G(N, X, A, B, \infty)=g(N, X, A, B),\\ P(X, A, B, \infty)=p(X, A, B).\end{gathered} \tag{31}$$

The partition function for the system ($n=\infty$) is

$$Q=\sum_{X=1}^{k}\{[j_S \exp(\epsilon_1/kT)]^X j_L{}^{A-X} \times\sum_N g(N, X, A, B)\exp(2\epsilon_L N/zkT)\}. \tag{32}$$

$$k=A \quad (A<B), \quad k=B \quad (A>B).$$

[8] See Chapter X of Fowler and Guggenheim (reference 5) for an analogous discussion of monolayers.

For n finite replace g by G. The general procedure is the same as in the previous sections, with Eq. (13) still applying.

The above formal treatment can easily be modified so as to apply to capillaries with two parallel walls, and with the same lattice sites available to molecules building up on either wall. This is a more satisfactory but more difficult approach than the above (n finite), where, essentially, an artificial ceiling is introduced half way between the walls.

The BET model is a very crude special case of the present one. Eqs. (5) and (21) follow from Eq. (32) if only vertical configurations are allowed and only vertical nearest neighbors counted ($z=2$). Then all configurations (for given values of A and X) have the same value of N: $N=A-X$. Also,

$$p(X, A, B)=g(A-X, X, A, B)=\frac{A!B!}{(A-X)!(B-X)!(X!)^2}, \tag{33}$$

$$P(X, A, B, n)=G(A-X, X, A, B, n)$$

$$=\sum_{X_2}\cdots\sum_{X_{n-1}}\frac{B!}{(B-X)!(X-X_2)!(X_2-X_3)!\cdots(X_{n-1}-X_n)!X_n!}. \tag{34}$$

Obvious successive improvements in the BET model would follow from (1) taking into account non-vertical configurations, (2) taking into account non-vertical nearest neighbors, and (3) using a lattice more suitable than simple cubic. To what extent the mathematics can actually be carried out in these cases is, of course, another question.

Although the subject will be discussed in more detail in a later paper, certain preliminary results for capillaries (n small), obtained by the use of improved models, may be mentioned briefly.

If one takes into account, even though crudely, interactions between horizontal as well as vertical nearest neighbors, the resulting somewhat refined theory of multimolecular adsorption predicts capillary condensation quite naturally for suitable values of the parameters. One obtains regions of instability, corresponding to a sudden jump in A/B from a small value to a large value. The phenomenon is analogous to the instabilities in monolayers discussed by Fowler and Guggenheim.[8] The multimolecular adsorption and the capillary condensation points of view are therefore really not in conflict, as is generally assumed, except that Kelvin's equation should not be considered valid on this microscopic scale.

The author is indebted to Professor W. A. Noyes, Jr. for helpful discussions.

Theory of Multimolecular Adsorption from a Mixture of Gases

TERRELL L. HILL
Department of Chemistry, University of Rochester, Rochester, New York
(Received December 26, 1945)

By making use of the evaporation-condensation properties of liquid mixtures, the Brunauer-Emmett-Teller theory of multimolecular adsorption is extended to mixtures of gases. No satisfactory experimental data are available at the present time with which to test the theory.

INTRODUCTION

PERHAPS the most important postulate in the Brunauer-Emmett-Teller[1] (BET) theory of multimolecular adsorption is that molecules of the second and higher adsorbed layers have the evaporation-condensation properties of the liquid state. If this postulate has really general validity (as a good approximation), one should be able to treat adsorption from a mixture of gases by assuming that molecules of the second and higher adsorbed layers in this more complicated case have the evaporation-condensation properties of a liquid mixture at the same temperature and composition. Hence, a comparison between experiment and a theory based on this assumption would provide a further test of the fundamental ideas underlying the BET treatment. Such a theory is developed in this paper[2a] but, unfortunately, satisfactory experimental data for comparison are apparently not yet available.

ADSORPTION FROM A MIXTURE OF TWO GASES

We shall be interested in the adsorption of two gases A and B at relative pressures $x_A=p_A/p_A^0$ and $x_B=p_B/p_B^0$, and at a temperature T below both critical temperatures. Let q_A, q_B, q_{AA}, q_{BB}, q_{AB}, q_{BA}, q_{AN_A}, and q_{BN_A} be, respectively, the heats of adsorption per mole of A on the bare surface of the solid, B on the bare surface, A on a layer of pure A, B on a layer of pure B, A on a layer of pure B, B on a layer of pure A, A on a layer of composition N_A (mole fraction of A), and B on a layer of composition N_A.

We consider various evaporation-condensation equilibria. First, if we have pure liquid A (or B) of surface area s in equilibrium with its vapor, then

$$\begin{cases} a_A s p_A^0 = b_A s \exp(-q_{AA}/RT), \\ a_B s p_B^0 = b_B s \exp(-q_{BB}/RT), \end{cases} \tag{1}$$

or

$$\begin{aligned} \frac{b_A}{a_A} &= p_A^0 \exp(q_{AA}/RT), \\ \frac{b_B}{a_B} &= p_B^0 \exp(q_{BB}/RT). \end{aligned} \tag{2}$$

Next, if a binary liquid mixture of composition N_A is in equilibrium with its vapor, we have

$$\begin{cases} a_A s p_A = b_A s N_A \exp(-q_{AN_A}/RT), \\ a_B s p_B = b_B s (1-N_A) \exp(-q_{BN_A}/RT). \end{cases} \tag{3}$$

On substituting Eqs. (2) into (3), one obtains

$$\begin{cases} p_A/p_A^0 = x_A = N_A \exp[(q_{AA}-q_{AN_A})/RT], \\ p_B/p_B^0 = x_B = (1-N_A) \\ \qquad \times \exp[(q_{BB}-q_{BN_A})/RT]. \end{cases} \tag{4}$$

In studying below the equilibria involved in adsorption, it will be necessary to have $(q_{AA}-q_{AN_A})$ and $(q_{BB}-q_{BN_A})$ as functions of N_A. The nature of the dependence of these quantities on N_A may be found from the experimental vapor pressure curves, which can be expressed in the form

$$\begin{cases} x_A = N_A/f_A(N_A), & f_A(N_A) = N_A/x_A, \\ x_B = (1-N_A)/f_B(N_A), & f_B(N_A) = (1-N_A)/x_B. \end{cases} \tag{5}$$

That is, the functions $f_A(N_A)$ and $f_B(N_A)$ may be tabulated from the experimental values of x_A, x_B, and N_A. Comparing Eqs. (4) and (5):

$$\begin{cases} \exp[(q_{AN_A}-q_{AA})/RT] = f_A(N_A), \\ \exp[(q_{BN_A}-q_{BB})/RT] = f_B(N_A). \end{cases} \tag{6}$$

We turn now to adsorption equilibria. In addition to the postulates of the BET theory,

[1] S. Brunauer, P. H. Emmett, and E. Teller, J. Am. Chem. Soc., 60, 309 (1938).
[2a] See also T. L. Hill, J. Chem. Phys., 14, 46 (1946).

we make a further assumption:[2b] the average energy of attachment of a molecule on top of the $(i-1)$th layer (to become a member of the ith layer) depends on the composition of the $(i-1)$th layer only. Let s_i represent the surface area covered by exactly i layers of adsorbed molecules and let N_{A_i} be the composition of the ith layer. Then, when equilibrium is established between all of the layers, we will have

$$\begin{cases} a_A s_0 p_A = b_A s_1 N_{A_1} \exp(-q_A/RT), \\ a_B s_0 p_B = b_B s_1 (1-N_{A_1}) \exp(-q_B/RT), \end{cases} \tag{7}$$

$$i=2, 3, \cdots \begin{cases} a_A s_{i-1} p_A = b_A s_i N_{A_i} \\ \qquad \times \exp(-q_A N_{A(i-1)}/RT), \\ a_B s_{i-1} p_B = b_B s_i (1-N_{A_i}) \\ \qquad \times \exp(-q_B N_{A(i-1)}/RT). \end{cases}$$

If we use Eqs. (2) and (6) in Eqs. (7), we can write

$$\begin{cases} s_1 N_{A_1} = s_0 x_A Q_A, \\ s_1 (1-N_{A_1}) = s_0 x_B Q_B, \end{cases} \tag{8}$$

$$i=2, 3, \cdots \begin{cases} s_i N_{A_i} = s_{i-1} x_A f_A(N_{A_{i-1}}), \\ s_i (1-N_{A_i}) = s_{i-1} x_B f_B(N_{A_{i-1}}), \end{cases}$$

where

$$\begin{aligned} Q_A &= \exp[(q_A - q_{AA})/RT], \\ Q_B &= \exp[(q_B - q_{BB})/RT]. \end{aligned} \tag{9}$$

By combining Eqs. (8) in an appropriate manner, there results

$$s_i = s_{i-1} E_{i-1} = s_0 E_0 E_1 E_2 \cdots E_{i-1}, \qquad i=1, 2, \cdots \tag{10}$$

$$\begin{cases} E_0 = x_A Q_A + x_B Q_B, \\ E_i = x_A f_A(N_{A_i}) + x_B f_B(N_{A_i}), \end{cases} \qquad i=1, 2, \cdots \tag{11}$$

$$\begin{cases} N_{A_1} = x_A Q_A / E_0, \\ N_{A_i} = x_A f_A(N_{A_{i-1}})/E_{i-1}, \quad i=2, 3, \cdots. \end{cases} \tag{12}$$

Let v_A and v_m^A be the volume of A adsorbed and the volume of A necessary to give a complete unimolecular layer, respectively. Then, as in the BET theory, we can relate v_A/v_m^A to the areas $s_0, s_1, s_2, \cdots$. If γ_{A_i} is the fraction of the area of the ith layer $(s_i+s_{i+1}+\cdots)$ which is made up of A molecules, we have

$$\frac{v_A}{v_m^A} = \frac{(s_1+s_2+\cdots+s_n)\gamma_{A_1} + (s_2+\cdots+s_n)\gamma_{A_2} + \cdots + s_n\gamma_{A_n}}{s_0+s_1+\cdots+s_n}. \tag{13}$$

In writing Eq. (13), the number of layers is restricted to n. The case of most interest is $n=\infty$. Substituting Eq. (10) into Eq. (13) gives

$$\frac{v_A}{v_m^A} = \frac{E_0[(1+E_1+E_1E_2+\cdots+E_1E_2\cdots E_{n-1})\gamma_{A_1} + (E_1+\cdots+E_1E_2\cdots E_{n-1})\gamma_{A_2} + \cdots + E_1\cdots E_{n-1}\gamma_{A_n}]}{1+E_0(1+E_1+E_1E_2+\cdots+E_1E_2\cdots E_{n-1})}. \tag{14}$$

We assume that the area fraction γ_A is related to the mole fraction N_A, to a sufficient approximation, by

$$\gamma_A = \frac{N_A}{N_A + (1-N_A)(v_B^0/v_A^0)^{\frac{1}{3}}}, \tag{15}$$

where v_A^0 and v_B^0 are molar volumes. In ordinary cases, the error made by replacing the γ_{A_i} in Eq. (14) by the N_{A_i} is not serious. For example, if v_A^0 and v_B^0 differ by 20 percent, γ_A and N_A differ on the average (from $N_A=0$ to $N_A=1$) by about 5 percent. In a more exact treatment of any given case, a curve of γ_A against N_A should be plotted for the appropriate v_B^0/v_A^0. Then, in using Eq. (14), γ_{A_i} may be read from the curve, for each N_{A_i} obtained from Eq. (12).

The quantity v_B/v_m^B may be obtained from Eq. (14) by replacing the γ_{A_i} by $1-\gamma_{A_i}$.

If $E_\infty \geqslant 1$, Eq. (14) does not converge for $n=\infty$: v_A/v_m^A and v_B/v_m^B become infinite. This corresponds physically to condensation on the surface of the adsorbent. The value of E_∞ may be obtained easily from

$$N_{A_\infty} = \frac{x_A f_A(N_{A_\infty})}{x_A f_A(N_{A_\infty}) + x_B f_B(N_{A_\infty})}, \tag{16}$$

$$E_\infty = x_A f_A(N_{A_\infty}) + x_B f_B(N_{A_\infty}). \tag{17}$$

[2b] It will be seen from the statistical mechanical discussion of the BET theory in the accompanying paper that this assumption is the most natural one to make for this model. In fact, from the point of view of this statistical treatment (where only vertical interactions are taken into account), no new postulate is really necessary. That is, the assumption under discussion follows from the BET model.

It will be noted that $N_{A\infty}$ and E_∞ are independent of the nature (Q_A and Q_B) of the surface of the adsorbent. The influence of the surface dies out as the number of layers increases. As one should expect, if we put $E=1$ (condensation) in Eqs. (16) and (17), we obtain the vapor pressure equations, Eqs. (5).

There is no difficulty in applying these equations when liquid A and B are immiscible over part or all of the range in N_A. The experimental vapor pressure curves are used as in other cases.

If $x_B=0$ (or $x_A=0$), Eq. (14) reduces to the usual BET equation with $\gamma_{Ai}=N_{Ai}=1$, $E_i=x_A=x$, and $E_0=x_AQ_A=xc$. A similar result is obtained in the very special case: $E_1=E_2=E_3=\cdots=E$ and $N_{A1}=N_{A2}=N_{A3}=\cdots=N_A$. In this event,

$$\frac{v_A}{v_m{}^A}=\frac{E_0N_A}{(1-E)(1-E+E_0)}. \tag{17a}$$

ADSORPTION FROM A MIXTURE OF MORE THAN TWO GASES

Suppose we have a mixture of gases A, B, C, $\cdots$. We retain the same symbols as above except that we use q_{AN}, $f_A(N)$, etc., in which N represents the composition (N_A, N_B, N_C, $\cdots$). The extension of Eqs. (3) to (17) to this more general case is obvious. In particular, Eqs. (10), (13), and (14) are unchanged and Eqs. (11), (12), and (15) become, respectively,

$$\begin{cases} E_0=x_AQ_A+x_BQ_B+x_CQ_C+\cdots, \\ E_i=x_Af_A(N_i)+x_Bf_B(N_i) \\ \qquad +x_Cf_C(N_i)+\cdots, \quad i=1, 2, \cdots \end{cases} \tag{18}$$

$$\begin{cases} N_{A1}=x_AQ_A/E_0, \\ N_{Ai}=x_Af_A(N_{i-1})/E_{i-1}, \quad i=2, 3, \cdots \end{cases} \tag{19}$$

$$\gamma_A=\frac{N_A}{N_A+N_B(v_B{}^0/v_A{}^0)^{\frac{1}{3}}+N_C(v_C{}^0/v_A{}^0)^{\frac{1}{3}}+\cdots}. \tag{20}$$

In order to use Eq. (20) in Eq. (14), it is clear that the N_{Bi}, N_{Ci}, etc., must also be computed as in Eq. (19). However, $\gamma_{Ai}=N_{Ai}$ will still be a fairly good approximation in most cases.

APPROXIMATIONS

Vapor Pressure Curves

If the vapor pressure curves of A and B show the usual Henry's law and Raoult's law characteristics at small and large mole fractions, respectively, it may prove convenient to represent the experimental vapor pressure curves by simple analytical expressions and use these in place of $f_A(N_A)$ and $f_B(N_A)$. Suitable equations for this purpose are[3]

$$\begin{aligned} &x_A=N_A/Q_{AB}{}^\beta, \qquad \beta=(1-N_A)^2 \\ &x_B=(1-N_A)/Q_{BA}{}^\alpha, \quad \alpha=N_A{}^2 \end{aligned} \tag{21}$$

with

$$\begin{aligned} Q_{AB}&=\exp\left[(q_{AB}-q_{AA})/RT\right], \\ Q_{BA}&=\exp\left[(q_{BA}-q_{BB})/RT\right]. \end{aligned} \tag{22}$$

The connection between w_{AB} of Fowler and Guggenheim[3] and our symbols is

$$\exp\left(-2w_{AB}/kT\right)=Q_{AB}Q_{BA}=Q^2. \tag{23}$$

If $Q=1$, the solution is ideal and Raoult's law is obeyed over the whole range of composition. If $Q>1$, A and B attract each other more than do like molecules, hence x_A and x_B are less than N_A and $1-N_A$, respectively. If $Q<1$, the situation is reversed. If $Q\leqslant 1/e^2=0.135$, two phases exist over part of the range in composition and Eqs. (21) can no longer be used as satisfactory approximations to the true state of affairs.

In this approximation

$$f_A(N_A)=Q_{AB}{}^\beta, \quad f_B(N_A)=Q_{BA}{}^\alpha. \tag{24}$$

Hence, from Eqs. (11) and (12),

$$E_i=x_AQ_{AB}{}^{\beta(i)}+x_BQ_{BA}{}^{\alpha(i)}, \quad i=1, 2, \cdots \tag{25}$$

$$N_{Ai}=x_AQ_{AB}{}^{\beta(i-1)}/E_{i-1}, \quad i=2, 3, \cdots. \tag{26}$$

For more than two gases,

$$\begin{aligned} E_i=x_AQ_{AB}{}^{\varphi(B)}Q_{AC}{}^{\varphi(C)}\cdots \\ +x_BQ_{BA}{}^{\varphi(A)}Q_{BC}{}^{\varphi(C)}\cdots+\cdots, \end{aligned} \tag{27}$$

etc., with

$$\varphi(A)=N_{Ai}{}^2, \quad \varphi(B)=N_{Bi}{}^2, \quad \text{etc.}$$

[3] See, for example, R. H. Fowler and E. A. Guggenheim, *Statistical Thermodynamics* (Cambridge University Press, London, 1939), p. 357. By not necessarily requiring, in Eqs. (21), that $Q_{AB}=Q_{BA}$, it is possible in some cases to fit the experimental data better (if $Q_{AB}=Q_{BA}$, the curves for x_A and x_B are required to be identical except for inversion). This practical advantage is at the expense of thermodynamics, however, since Eqs. (21) satisfy

$$N_A\frac{\partial\log x_A}{\partial N_A}=N_B\frac{\partial\log x_B}{\partial N_B}$$

only if $Q_{AB}=Q_{BA}$. This suggests the policy of using Eqs. (21) only when a satisfactory fit may be obtained with $Q_{AB}=Q_{BA}$, and employing the experimental vapor pressure curves otherwise. If this policy is adopted, read $Q_{AB}=Q_{BA}$ throughout the paper.

Approximations of Eq. (14)

In addition to approximating the experimental vapor pressure curves, it is highly desirable to have approximate forms of Eq. (14). It should be emphasized that the approximate equations given below are in the nature of suggestions only, based, however, on the calculation of a number of widely different cases (using Eq. (24)). It is possible that a more complete study would lead to significant improvements.

The sequences N_{A_1}, N_{A_2}, N_{A_3}, $\cdots$ and E_1, E_2, E_3, $\cdots$ approach limits N_{A_∞} and E_∞, respectively, given by Eqs. (16) and (17). In most cases studied, successive values of N_{A_i} oscillate above and below N_{A_∞}, with steadily decreasing amplitude, while the E_i do not show such oscillations.[4] In all cases studied, the E_i converge much more rapidly than the N_{A_i}.

The method of approximation used is to break off the sums in Eq. (14) at a certain value of i, and use mean values to obtain closed expressions representing the rest of the sum. For example,

$$\begin{aligned}1+E_1+E_1E_2+E_1E_2E_3+\cdots &\\ \doteqdot 1+E_1+E_1E_2(1+E+E^2+\cdots) &\\ \doteqdot 1+E_1+E_1E_2/(1-E), &\end{aligned} \tag{28}$$

where E is some mean value, say, $(E_3E_\infty)^{\frac{1}{2}}$.

On the basis of an incomplete study, the following scheme is suggested (for $n=\infty$) in order to obtain approximate values which differ from those given by Eq. (14) by less than about 3 percent:

I. If E_1 differs from E_2 by less than 4 percent:

$$X=\left(\gamma_{A_1}+\frac{E\gamma_A}{1-E}\right)\frac{1}{1-E}, \tag{29}$$

$$Y=1/(1-E) \tag{30}$$

with

$$E=E_\infty \quad \text{and} \quad \gamma_A=\gamma_{A_\infty}. \tag{31}$$

II. If E_1 differs from E_2 by from 4 percent to about 50 percent:

$$X=\gamma_{A_1}+\left(\gamma_{A_1}+\gamma_{A_2}+\frac{E\gamma_A}{1-E}\right)\frac{E_1}{1-E}, \tag{32}$$

$$Y=1+E_1/(1-E), \tag{33}$$

with $E=(E_2E_\infty)^{\frac{1}{2}}$ and

$$\begin{aligned}\gamma_A&=\gamma_{A_\infty}(\text{osc.})\\ &=(\gamma_{A_3}\gamma_{A_\infty})^{\frac{1}{2}}(\text{non-osc.}).\end{aligned} \tag{34}$$

III. If E_1 differs from E_2 by more than about 50 percent:

$$\begin{aligned}X=\gamma_{A_1}+(\gamma_{A_1}+\gamma_{A_2})E_1&\\ +\left(\gamma_{A_1}+\gamma_{A_2}+\gamma_{A_3}+\frac{E\gamma_A}{1-E}\right)\frac{E_1E_2}{1-E},&\end{aligned} \tag{35}$$

$$Y=1+E_1+E_1E_2/(1-E) \tag{36}$$

with $E=(E_3E_\infty)^{\frac{1}{2}}$ and

$$\begin{aligned}\gamma_A&=\gamma_{A_\infty}(\text{osc.})\\ &=(\gamma_{A_4}\gamma_{A_\infty})^{\frac{1}{2}}(\text{non-osc.}).\end{aligned} \tag{37}$$

In the above equations, $n=\infty$, and

$$\frac{v_A}{v_m{}^A}=\frac{E_0X}{1+E_0Y}. \tag{38}$$

The mean values suggested are, of course, rather arbitrary, but have some justification. Values of γ_A are obtained from the corresponding values of N_A, using Eq. (15). In Eqs. (34) and (37), where two values of γ_A are given, the first is to be used if the N_{A_i} exhibit oscillations of the type discussed above. Otherwise, the second value is to be used.

For finite values of n, Eq. (14) itself is only a rough approximation since capillary condensation is neglected. Also, approximate equations of the type given above become rather complicated. Hence, it is probably not worth while to use approximate equations for finite values of n except, perhaps, in case I above. The complete Eq. (14) is almost as easy to use in cases II and III. For case I, one finds

$$\frac{v_A}{v_m{}^A}=\frac{E_0\{\gamma_{A_1}(E^{n+1}-E^n-E+1)+\gamma_A[(n-1)E^{n+1}-nE^n+E]\}}{(1-E)[1-E-E_0(E^n-1)]}, \tag{39}$$

with

$$E=E_\infty \quad \text{and} \quad \gamma_A=\gamma_{A_\infty}.$$

[4] Oscillations of this type in E, are, in fact, not possible. For it is not difficult to show, using the thermodynamic equation in footnote 3, that $E(N_A)$ has a maximum ($Q<1$) or a minimum ($Q>1$) at that value of N_A which satisfies Eq. (16). That is, E_∞ is the largest or smallest possible value of E and N_{A_∞} is the associated value of N_A.

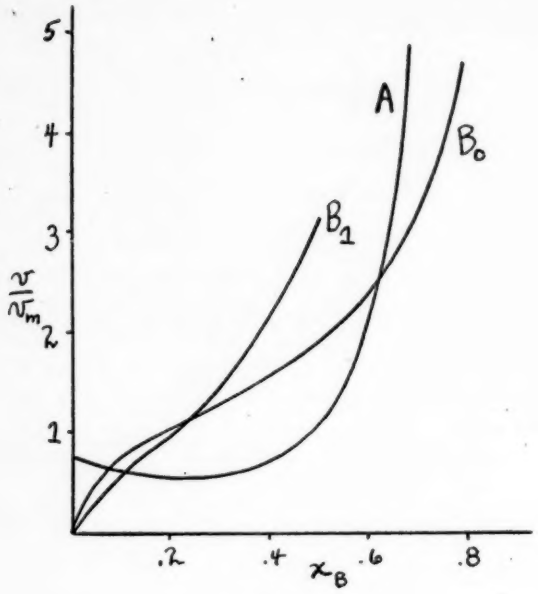

FIG. 1.

Since Eq. (14) holds regardless of the number of gases in the mixture, the above approximations to this equation should have essentially the same validity in the general problem of any number of gases as they have in the special case of a mixture of two gases.

EXAMPLE

As far as the author is aware, no experimental data are available at the present time which can be used to test the theory properly. The following experimental results are desirable: (1) vapor pressure curves for A and B as functions of N_A; (2) adsorption isotherms (at the same temperature as in the vapor pressure experiments) for pure A and pure B, preferably on a non-porous adsorbent (to reduce complications); (3) adsorption isotherms (at the same temperature and on the same adsorbent) of A and B from mixtures of gases. Curves of $v_A/v_m{}^A$ and $v_B/v_m{}^B$ should be obtained as functions of, say, x_A for a series of values of x_B. The vapor pressure curves give $f_A(N_A)$ and $f_B(N_A)$ (or Q) while the adsorption isotherms for pure A and pure B can be used to obtain Q_A, Q_B, $v_m{}^A$, and $v_m{}^B$. Then the theoretical isotherms for mixtures of A and B may be calculated and compared with experiment. For more than two gases, the vapor pressures can be studied in pairs, as implied in Eq. (27).

In order to illustrate certain features predicted by theory, we have plotted in Fig. 1 isotherms for a hypothetical case (using Eq. (24), $v_A{}^0=v_B{}^0$ and $n=\infty$). We have chosen a fairly typical case: $Q=4$, $Q_A=Q_B=Q'=20$. In this figure, curve B_0 gives $v_B/v_m{}^B$ as a function of x_B for $x_A=0$. Curve B_1 shows the effect of a constant pressure of A: $v_B/v_m{}^B$ is plotted against x_B for $x_A=.1$. At the lower pressures of B, the presence of A inhibits the adsorption of B, but this effect is reversed at higher pressures. Curve A of Fig. 1 represents the adsorption of A as a function of x_B for constant $x_A=.1$. The adsorption of A at constant pressures of A is reduced by the presence of small amounts of B but greatly increased for sufficiently large pressures of B. These effects are due to Q' being considerably larger than Q. A and B compete for positions in the first layer and the molecules of the first layer do not attract additional molecules to the extent that the bare surface does. Hence, at low pressures, the competition reduces adsorption of both A and B.

CAPILLARY CONDENSATION

It has been recognized that capillary condensation cannot be treated satisfactorily by merely assigning an appropriate finite value to n in the original[1] BET theory. In a later paper,[5] Brunauer, Deming, Deming, and Teller improved the theory by taking into account the additional energy of adsorption in the last adsorbed layer. More recently, Pickett[6] has introduced a modification of the BET theory which appears to be an empirical improvement (for n finite) but which lacks theoretical justification (in the opinion of the present writer[7]).

Before considering mixtures, several corrections to the capillary condensation equations[5] of the BET theory will be suggested. For simplicity we shall not consider the most general of these equa-

[5] S. Brunauer, L. S. Deming, W. E. Deming, and E. Teller, J. Am. Chem. Soc. 62, 1723 (1940).
[6] G. Pickett, J. Am. Chem. Soc. 67, 1958 (1945).
[7] T. L. Hill, J. Am. Chem. Soc. 68, 535 (1946).

tions (Eq. (E)) but the same argument holds. Eq. (D) is derived from

$$\frac{v}{v_m}=\frac{2[s_1+2s_2+\cdots+(n-1)s_{n-1}]+ns_n}{2(s_0+s_1+\cdots+s_{n-1})+s_n} \tag{40}$$

for the case of $2n-1$ layers fitting into a capillary. It appears to the writer that the contribution of s_n to both numerator and denominator has been handled incorrectly and Eq. (40) should read

$$\frac{v}{v_m}=\frac{2[s_1+2s_2+\cdots+(n-1)s_{n-1}]+(2n-1)s_n}{2(s_0+s_1+\cdots+s_n)}. \tag{41}$$

This gives

$$\frac{v}{v_m}=\frac{cx\left[1+\left(\frac{2n-1}{2}g-n\right)x^{n-1}-(2ng-g-n+1)x^n+\frac{2n-1}{2}gx^{n+1}\right]}{(1-x)[1+(c-1)x+(cg-c)x^n-cgx^{n+1}]} \tag{42}$$

instead of Eq. (D). For the case of $2n$ layers fitting into a capillary, similar reasoning leads to

$$\frac{v}{v_m}=\frac{2(s_1+2s_2+\cdots+ns_n)}{2(s_0+s_1+\cdots+s_n)} \tag{43}$$

$$=\frac{cx[1+(ng-n)x^{n-1}-(2ng-n+1)x^n+ngx^{n+1}]}{(1-x)[1+(c-1)x+(cg-c)x^n-cgx^{n+1}]}. \tag{44}$$

Using the principle of Pickett's modification, one finds, instead of Eqs. (42) and (44),

$$\frac{v}{v_m}=\frac{cx\left[1+\left(\frac{2n-1}{2}g-n\right)x^{n-1}+\left(n-1-\frac{2n-1}{2}g\right)x^n\right]}{(1-x)\{1-x+c[x^n(g-1)+x]\}}, \tag{45}$$

and

$$\frac{v}{v_m}=\frac{cx[1+(ng-n)x^{n-1}+(n-1-ng)x^n]}{(1-x)\{1-x+c[x^n(g-1)+x]\}}. \tag{46}$$

Eq. (46) is thus a correction to Pickett's Eq. (8).

In dealing with a mixture of gases (say, two, for example), Eqs. (8) remain unchanged except for $i=n$:

$$\begin{cases} s_nN_{A_n}=s_{n-1}x_Af_A(N_{A_{n-1}})g_A, \\ s_n(1-N_{A_n})=s_{n-1}x_Bf_B(N_{A_{n-1}})g_B, \end{cases} \tag{47}$$

where $g=\exp(\epsilon/RT)$ as in reference 5 (ϵ replacing Q). The quantities ϵ_A and ϵ_B will depend here on the composition of the $(n-1)$th layer. The E_i and N_{A_i} are unchanged except for $i=n-1$ and $i=n$, respectively. In these cases we write

$$\mathcal{E}_{n-1}=x_Ag_Af_A(N_{A_{n-1}})+x_Bg_Bf_B(N_{A_{n-1}}), \tag{48}$$

and

$$\mathfrak{N}_{A_n}=x_Ag_Af_A(N_{A_{n-1}})/\mathcal{E}_{n-1}. \tag{49}$$

Eq. (10) holds except for $i=n$:

$$s_n=s_{n-1}\mathcal{E}_{n-1}. \tag{50}$$

Then, for $2n-1$ layers fitting into a capillary,

$$\frac{v_A}{v_m{}^A}=\frac{2[(s_1+s_2+\cdots+s_n)\gamma_{A1}+(s_2+\cdots+s_n)\gamma_{A2}+\cdots+(s_{n-1}+s_n)\gamma_{A_{n-1}}]+s_n\gamma_{A_n}}{2(s_0+s_1+\cdots+s_n)}, \tag{51}$$

where s_n is obtained from Eq. (50) and γ_{A_n} is given by Eq. (15) using $\mathfrak{N}_{A_n}$. For $2n$ layers fitting into a capillary, the two factors of 2 in Eq. (51) should be omitted.

Using Pickett's modification,

$$\mathcal{E}_{n-1}=\frac{x_A g_A f_A(N_{A_{n-1}})}{1-x_A}+\frac{x_B g_B f_B(N_{A_{n-1}})}{1-x_B} \tag{52}$$

and

$$\mathfrak{N}_{A_n}=\frac{x_A g_A f_A(N_{A_{n-1}})}{(1-x_A)\mathcal{E}_{n-1}}. \tag{53}$$

The next problem is the evaluation of the g's. We can write[5]

$$\epsilon_A=2k_A S_A \sigma_{N_{A(n-1)}}, \quad \epsilon_B=2k_B S_B \sigma_{N_{A(n-1)}}, \tag{54}$$

where $\sigma_{N_{A(n-1)}}$ is the surface tension of a solution of A and B of composition $N_{A_{n-1}}$, and S_A and S_B are the surface areas covered by one mole of A and B, respectively, spread out into a unimolecular layer. As an approximation, the constants k_A and k_B may be taken as equal to each other. Then,

$$\frac{\epsilon_A}{\epsilon_B}=\frac{S_A}{S_B}=\frac{V_A^{\frac{2}{3}}}{V_B^{\frac{2}{3}}}, \tag{55}$$

where V_A and V_B are molar volumes. This equation can be used to reduce the number of parameters by one, since it gives a relation between g_A and g_B. A further approximation is to assume $k_A=k_B=1$ and a particular type of packing. If the surface tensions of A and B are known, and a linear relationship[8] between surface tension and composition assumed (or the actual relationship measured), then g_A and g_B may be calculated using Eqs. (54).

The author is indebted to Dr. P. H. Emmett for his helpful comments.

APPENDIX

In this section two miscellaneous points which may be of interest will be mentioned briefly.

1. The logic used by Brunauer, Emmett, and Teller[1] in deriving the equation

$$\frac{v}{v_m}=\frac{cx}{(1-x)(1-x+cx)} \tag{56}$$

can be improved a little. After obtaining the equation

$$\frac{v}{v_m}=c\sum_{i=1}^{\infty} ix^i \Big/ 1+c\sum_{i=1}^{\infty} x^i, \tag{57}$$

it is really not legitimate to rewrite the sums in closed form (as is done in reference 1) without first making clear that values of x greater than unity have no physical significance (at this point in the derivation we know only that x is proportional to p). After writing Eq. (57), the next step should be either: (1) use the equations (in the BET notation)

$$x=(a/b)p \exp(E_L/RT), \tag{58}$$

and

$$asp^0=bs \exp(-E_L/RT), \tag{59}$$

to obtain

$$x=p/p^0, \tag{60}$$

where Eq. (59) is the same as Eq. (1); or (2) point out that in Eq. (57) v is finite for $x<1$ and infinite for $x\geq 1$ and furthermore that we desire v to be finite for $p<p^0$ and to be infinite for $p\geq p^0$, hence $x=1$ should be identified with $p=p^0$. One may then proceed from Eq. (57) to Eq. (56).

2. In the usual BET theory with $n=\infty$, it is instructive to have some idea of the extent to which

[8] N. A. Yajnik, R. K. Sharma, and M. C. Bharadway, J. Indian Chem. Soc. **3**, 63 (1926).

the surface of the adsorbent is covered as a function of v/v_m and c. If we use

$$1-\frac{s_0}{A}=\frac{cx}{1-x+cx}=\frac{v}{v_m}(1-x), \tag{61}$$

and Eq. (56) (to give x as a function of v/v_m), we find

$$1-\frac{s_0}{A}=\frac{c\left(\frac{v}{v_m}+1\right)-\left[\left(1-\frac{v}{v_m}\right)^2c^2+4\frac{v}{v_m}c\right]^{\frac{1}{2}}}{2(c-1)} \tag{62}$$

as the desired expression relating the fraction of the surface covered to c and v/v_m. For $v/v_m=1$,

$$1-\frac{s_0}{A}=\frac{c-(c)^{\frac{1}{2}}}{c-1}, \tag{63}$$

and for $v/v_m=2$,

$$1-\frac{s_0}{A}=\frac{3c-(c^2+8c)^{\frac{1}{2}}}{2(c-1)}. \tag{64}$$

Some values of $1-(s_0/A)$ are given in Table I for these two cases. It is fairly customary to view the process of adsorption, as the pressure is gradually increased from $p=0$, as taking place essentially in the following manner: first, the first layer is laid down and then, at about $v=v_m$, the second layer begins to fill in, etc. It should be clear from Table I that, according to the BET theory, this picture of the process is satisfactory for large values of c, but not otherwise. For very small values of c, most of the adsorption when $v/v_m=1$ takes place primarily by attaching to molecules already adsorbed rather than by attaching to the bare surface. For example, for $c=.01$, when sufficient molecules have been adsorbed to cover the entire surface with a unimolecular layer ($v=v_m$), actually only about one-tenth of the surface is covered. Hence, that part of the surface which is covered has, on the average, adsorbed molecules about ten layers thick.

TABLE I.

c	$1-(s_0/A)$	
	$v/v_m=1$	$v/v_m=2$
.001	.031	.043
.01	.091	.128
.1	.240	.333
1.	.500	.667
10.	.760	.921
100.	.909	.990
1000.	.969	.999

THE JOURNAL OF CHEMICAL PHYSICS VOLUME 14, NUMBER 4 APRIL, 1946

On Phase Changes of Bose-Einstein Fluid Models

LOUIS GOLDSTEIN*
35 Hamilton Place, New York 31, New York
(Received January 16, 1946)

It is shown that all Bose-Einstein (B.E.) fluid models investigated thus far undergo first-order transformations in phase space. The ideal fluid condenses smoothly, e.g., without any possibility of supersaturation, insofar as its thermodynamic characteristic functions and their first derivatives, with respect to the independent variables, are continuous along the transition or saturation curve. The non-ideal B.E. fluids considered, in which attractive interatomic forces averaged over the volume of the fluid are assumed to operate, undergo sudden condensation strictly similar to that exhibited by ordinary fluids in coordinate space. This process is accompanied by the occurrence of discontinuities of the first derivatives of the characteristic functions. By introducing a suitable repulsive interatomic force, smeared over the volume of the fluid, the smooth condensation of the ideal fluid is changed to a phase transformation of the third order. Here the second derivatives of the characteristic functions exhibit discontinuities along the transformation curve. The same interatomic force lifts the order of the sudden first-order transformation by changing it to a second-order one. This is accompanied by the appearance of the lambda-point type discontinuity of the constant pressure heat capacity along the transition or lambda line. The interplay of forces of parallel and opposing tendencies in modifying the nature of a phase transformation without changing its order and in lifting or lowering their order is thus brought out in these studies over B.E. fluid models. The bearing of these results on the problems connected with the thermal properties of liquid helium is touched upon briefly.

INTRODUCTION

THE possible intervention of the Bose-Einstein (B.E.) condensation phenomenon in the peculiar transition liquid He I→liquid He II, as first suggested by London[1] has led us to investigate different B.E. fluid models. The ideal fluid undergoes what may be called a smooth condensation process in phase space. In this smooth transformation, beside the thermodynamic characteristic functions, their first derivatives with respect to the chosen independent variables remain also continuous at the transition. For instance, the heat capacity at constant volume remains continuous at the transition line but has a break, i.e., its temperature derivative is discontinuous. In the modified B.E. fluid models,[2,3] the phase changes exhibited were strictly of the ordinary first-order type. The condensation process shown by these fluids resembled strictly that undergone by ordinary fluids in coordiate space. Since the transformation undergone by liquid He is of the second order, these models are even formally unsatisfactory for its description. It is intended here to investigate further the B.E. fluid models exhibiting first-order phase changes and to clarify and point out some of their properties which were not considered before. A modification of the assumed properties of these models will then be described. This modification has the effect of lifting the order of the phase change from the first to the second or third order. Apart from the theoretical interest of the B.E. fluid models which allow a complete and rigorous analysis of their phase transformations, the study of lifting or lowering the order of phase changes may also shed some light on some of the more elementary aspects of other cooperative phenomena.

I. THE SMOOTH CONDENSATION PROCESS OF THE IDEAL B.E. FLUID

The proof that the ideal B.E. fluid undergoes a smooth condensation process is already apparent on the thermodynamic diagram of this fluid in the pressure-volume plane.[1,4] For volumes less than the saturation volume, at a given temperature, the pressure becomes independent of the volume, e.g., the isothermals coincide with the isobars in the mixed two-phase or condensation region. The smoothness of the condensation of the ideal B.E. fluid is also apparent on the shape of its isothermals. These reach the saturation or

* Now with the Federal Telecommunication Laboratories, Inc., New York, New York.
[1] F. London, Nature **141**, 643 (1938); Phys. Rev. **54**, 947 (1938).
[2] F. London, J. Phys. Chem. **43**, 49 (1939).
[3] L. Goldstein, J. Chem. Phys. **9**, 472 (1941).
[4] B. Kahn, Dissertation, Utrecht (1938).

transition line with a horizontal slope. The isothermal compressibility of the ideal fluid tends in a continuous way toward infinity as the fluid approaches saturation and remains infinite in the condensation region. It is equally worth noting in this connection that the zero slope of the isothermals of the non-condensed saturated ideal fluid is associated with a maximum of these curves. One has indeed for the isothermal curves of the fluid of spinless atoms:

$$\begin{aligned} p_+ &= NkTG(\alpha)/VF(\alpha), \quad V \geqslant V_0 \\ p_- &= \frac{NkT}{V}\left(\frac{T}{T_0}\right)^{\frac{3}{2}} G(0)/F(0), \quad V \leqslant V_0. \end{aligned} \tag{1}$$

Here V_0 is the condensation volume at temperature T, T_0 is the condensation temperature at volume V defined, respectively, by

$$\begin{aligned} V_0 &= Nh^3/F(0)(2\pi mkT)^{\frac{3}{2}}; \\ T_0 &= \frac{h^2}{2\pi mk}\left(\frac{N}{VF(0)}\right)^{\frac{2}{3}}. \end{aligned} \tag{2}$$

In (1) and (2), α is the negative Gibbs potential per atom of mass m, divided by kT, N is the total number of atoms forming the fluid, and the functions $G(x)$, $F(x)$ are generalized ζ-functions;

$$\begin{aligned} &G(x) = \sum_{n=1}^{\infty} e^{-nx}/n^{5/2}; && F(x) = -dG/dx; \\ &E(x) = -dF/dx; && D(x) = -dE/dx, \text{ etc.} \\ &G(0) = \zeta(5/2) = 1.341; && F(0) = \zeta(3/2) = 2.612; \\ &E(x) \underset{x \ll 1}{=} \pi^{\frac{1}{2}}/x^{\frac{1}{2}}; && D(x) \underset{x \ll 1}{=} \pi^{\frac{1}{2}}/2x^{\frac{3}{2}}. \end{aligned} \tag{3}$$

One finds then easily

$$\begin{aligned} &\lim_{V \to V_0} (\partial p_+/\partial V)_T = 0; \\ &(\partial p_-/\partial V)_{T \leq T_0} = 0; \\ &\lim_{V \to V_0} (\partial^2 p_+/\partial V^2)_T = \lim_{\alpha \to 0} \left(-\frac{NkT}{V_0^3}\right)\frac{(F(\alpha))^2 D(\alpha)}{(E(\alpha))^3} \\ &\qquad = -1.09NkT/V_0^3, \end{aligned} \tag{4}$$

which shows that the isothermal curves $p_+(V)_T$ have a maximum at the saturation line. In other words, an extrapolation of the isothermal $p_+(V)_T$ of the non-condensed fluid into the condensation region leads to a physically inadmissible portion of the curve along which the pressure decreases with decreasing volume. A physical interpretation of the vanishing slope of the isothermals $p_+(V)_T$ at the saturation line and the impossibility of their continuation into the two-phase region corresponds to the absence of supersaturation in phase space where the condensation of the ideal fluid takes place. In regard to this, the condensation of the ideal B.E. fluid might be compared to what seems to happen with ordinary fluids between the temperatures T_m of disappearance of the meniscus and the critical temperature T_c.[5] The experimental evidence for the existence of a temperature T_m less than T_c is rather scarce.[5] The experimental results favor in the range (T_m, T_c) the same trend of the isothermal curves of ordinary fluids as that shown by the ideal B.E. fluid. The interpretation of the condensation of ordinary fluids in the temperature interval (T_m, T_c) corresponds to the absence of surface tension. Now, in an ideal B.E. fluid where there are no forces acting in coordinate space one would naturally expect that surface forces be absent and that the condensation in phase space should proceed without the intervention of surface tension. It may be recalled in this connection that clusters of 3, 4 or more atoms play but a negligible role in the condensation of the ideal B.E. fluid.[6] It seems, therefore, that there is here an interesting argument favoring the interpretation given by Mayer[5] to the condensation of ordinary fluids in the temperature interval (T_m, T_c) provided that further experimental evidence be accumulated assuring the existence of a temperature T_m less than T_c.

This condensation accompanied by the above-mentioned behavior of the isothermals may be considered as a continuous or smooth first-order phase change, in which only the second derivatives of the characteristic functions of the fluid are discontinuous. One has indeed

$$\Delta(\partial p/\partial V)_{T, V=V_0} = (\partial p_+/dV)_{T, V=V_0} - (\partial p_-/\partial V)_{T, V=V_0} = 0. \tag{5}$$

Similarly, one finds that, C_v denoting the constant volume heat capacity,

$$\Delta C_v = C_{v+}(V_0) - C_{v-}(V_0) = 0. \tag{6}$$

[5] J. E. Mayer and M. G. Mayer, *Statistical Mechanics* (John Wiley and Sons, Inc., New York, 1940), pp. 295–317.
[6] L. Goldstein, J. Chem. Phys. **10**, 295 (1942).

But

$$\Delta(\partial^2 p/\partial V^2)_T = \lim_{\alpha\to 0}\left(-\frac{NkT}{V_0^3}\right)\frac{(F(\alpha))^2 D(\alpha)}{(E(\alpha))^3} = -1.09NkT/V_0^3. \quad (7)$$

We recall here that, E being the total energy of the fluid,

$$C_{v+}/Nk = \frac{1}{Nk}\frac{dE_+}{dT} = \frac{15}{4}G(\alpha)/F(\alpha) - \frac{9}{4}F(\alpha)/E(\alpha),$$
$$C_{v-}/Nk = \frac{1}{Nk}\frac{dE_-}{dT} = \frac{15}{4}\left(\frac{T}{T_0}\right)^{\frac{1}{2}} G(0)/F(0), \quad (8)$$

and, consequently,

$$\Delta\left(\frac{dC_v}{dT}\right) = \Delta\left(\frac{d^2E}{dT^2}\right) = -\frac{27}{8}\frac{Nk}{T}\lim_{\alpha\to 0}\left(\frac{(F(\alpha))^2 D(\alpha)}{(E(\alpha))^3}\right) = -3.66Nk/T, \quad (9)$$

using the asymptotic values of $D(x)$ and $E(x)$ as given by (3).

Finally the trend of variation of the constant pressure heat capacity is worth noting. One finds

$$\frac{C_{p+}}{Nk} = \frac{5}{4}\frac{G(\alpha)}{F(\alpha)}5\left[\frac{G(\alpha)E(\alpha)}{(F(\alpha))^2} - 3\right], \quad (10)$$

showing that as the fluid approaches saturation, e.g., as $\alpha\to 0$, $C_{p+}\to\infty$ as $1/\alpha^{\frac{1}{2}}$ according to the asymptotic value of $E(\alpha)$ for $\alpha \ll 1$. Clearly, in the condensation region C_{p-} remains infinite.

2. THE ORDINARY CONDENSATION PROCESS IN PHASE SPACE OF SOME B.E. FLUID MODELS

In contrast with the preceding behavior of an ideal B.E. fluid, the modified fluid models considered thus far undergo condensation in phase space as do ordinary fluids in coordinate space. They exhibit supersaturation in phase space and their heat capacity at constant volume has a lambda point along the saturation or transition curve as is the case with ordinary fluids along their vapor saturation curve, at volumes larger than their critical volume. Of these modified B.E. fluid models the one studied before[3] seems to have the simplest formalism generalizing that of the ideal fluid. It is assumed that the influence of the $(N-1)$ atoms of the system acting on the particular atom in question can be described by a potential energy well independent of the volume and temperature. Any given atom can have one or several discrete levels in this well. The generality of the model is not reduced, however, by assuming that there is but one level $-E_0$ extending the individual free particle level spectrum of the ideal fluid. The correspondingly increased cohesion in coordinate space, as expected, hastens the condensation process in phase space. One finds thus that, at a given volume, the modified fluid starts condensing at a higher temperature, while at a given temperature it starts condensing at a larger volume than the ideal fluid.

The formulas giving the pressure of this fluid above and below the transition temperature, denoted here by T_f, are the following:

$$p_+ = \frac{NkT}{V}\frac{G\left(\alpha'+\frac{E_0}{kT}\right)}{F\left(\alpha'+\frac{E_0}{kT}\right)}, \quad T\geqslant T_f$$
$$p_- = \frac{NkT}{V}\left(\frac{T}{T_f}\right)^{\frac{1}{2}}\frac{G(E_0/kT)}{F(E_0/kT_f)}, \quad T\leqslant T_f \quad (11)$$

since now the statistical parameter α has to satisfy the inequality

$$\alpha\geqslant E_0/kT \quad \text{or} \quad \alpha' = \alpha - \frac{E_0}{kT}\geqslant 0.$$

For $T\geqslant T_f\geqslant T_0$ the family of isothermals of the ideal and modified fluids are identical.

The saturation curve whose equation is

$$p_+(V)_{T_f} = p_-(V)_{T_f} = \frac{NkT}{V}G(E_0/kT_f)/F(E_0/kT_f), \quad (12)$$

is now displaced to larger volumes. The combined thermodynamic diagrams of the ideal and modified B.E. fluid models, in the $p-v$ representation, are given in Fig. 1. The energy of the system is given by

$$E_+ = \frac{3}{2}\frac{V}{h^3}(2\pi mkT)^{\frac{3}{2}}kTG\left(\alpha'+\frac{E_0}{kT}\right), \quad T\geqslant T_f$$
$$E_- = -N_0E_0 + \frac{3}{2}\frac{V}{h^3}(2\pi mkT)^{\frac{3}{2}}kTG(E_0/kT), \quad T\leqslant T_f \quad (13)$$

where N_0 is the number of condensed particles, or

$$N_0=1/(e^{\alpha'}-1)$$
$$=N\left[1-\left(\frac{T}{T_f}\right)^{\frac{3}{2}}\frac{F(E_0/kT)}{F(E_0/kT_f)}\right], \qquad (14)$$

and $\alpha'\sim 0$ for $T\leqslant T_f$.*

The constant volume heat capacities are, as a simple calculation shows,

$$\frac{C_{v+}}{Nk}=\frac{15}{4}\frac{G\left(\alpha'+\frac{E_0}{kT}\right)}{F\left(\alpha'+\frac{E_0}{kT}\right)}-\frac{9}{4}\frac{F\left(\alpha'+\frac{E_0}{kT}\right)}{E\left(\alpha'+\frac{E_0}{kT}\right)}, \qquad (15)$$

$$\frac{C_{v-}}{Nk}=\frac{15}{4}\frac{G(E_0/kT)}{F(E_0/kT_f)}+3\left(\frac{E_0}{kT}\right)\left(\frac{T}{T_f}\right)^{\frac{3}{2}}\frac{F(E_0/kT)}{F(E_0/kT_f)}$$
$$+\left(\frac{E_0}{kT}\right)^2\left(\frac{T}{T_f}\right)^{\frac{3}{2}}\frac{E(E_0/kT)}{F(E_0/kT_f)}.$$

Therefore,

$$\frac{\Delta C_v}{Nk}=\frac{(C_{v+}-C_{v-})_{T_f}}{Nk}$$
$$=-\frac{9}{4}\frac{F(E_0/kT_f)}{E(E_0/kT_f)}-3\left(\frac{E_0}{kT_f}\right)$$
$$-\left(\frac{E_0}{kT_f}\right)^2\frac{E(E_0/kT_f)}{F(E_0/kT_f)}, \qquad (16)$$

which is negative and indicates that the constant volume heat capacity has a lambda point along the transition line.

The constant pressure heat capacity is also discontinuous but its discontinuity is negatively infinite. One finds, indeed, that

$$\frac{C_{p+}}{Nk}=\frac{C_{v+}}{Nk}+\frac{25}{4}\frac{(G(x))^2E(x)}{(F(x))^3}-\frac{15}{2}\frac{G(x)}{F(x)}+\frac{9}{4}\frac{F(x)}{E(x)};$$
$$x=\alpha'+\frac{E_0}{kT}. \qquad (17)$$

C_{p+} is thus finite at the saturation line, for $T=T_f$, but jumps to infinity in the condensation region.

* In reference 3, the energy E_+ included also the energy of the very few atoms which were in the discrete level $-E_0$. However, in order to obtain heat capacities with the discontinuities predicted by thermodynamics it is necessary to omit this energy term in (13). The ΔC_v given in reference 3 is thus incomplete.

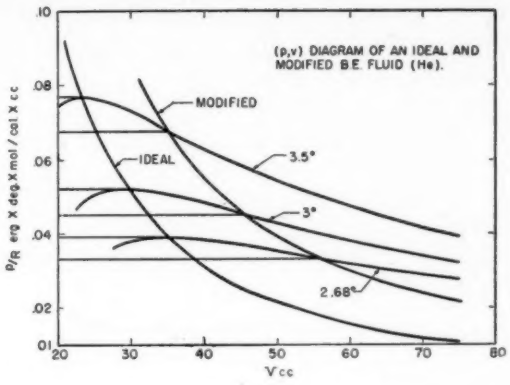

FIG. 1.

This behavior is characteristic to ordinary fluids undergoing condensation or, in general, a regular first-order phase change. One finds, indeed, that in this case and along the transition line

$$\Delta C_v=-T\frac{dV}{dT}\Delta\left(\frac{\partial p}{\partial T}\right)_V, \qquad (18)$$

in which C_{v-} is the constant volume heat capacity of the mixed phase, dV/dT is a derivative taken along the transition line, and $(\partial p/\partial T)_V$ is to be obtained from the equation of state of the fluid. This general thermodynamic relationship, of the Ehrenfest type, is indeed satisfied when ordinary condensation takes place. Using numerical data available for water[7] we have computed and constructed c_v curves around the vapor saturation curve, i.e., for volumes larger than the critical volume. Figure 2 gives typical Δc_v discontinuities for water. It is seen that Δc_v decreases with increasing temperature.

It is worth noting here that the modified B.E. fluids are the only fluids whose formalism allows a rigorous computation of the ΔC_v discontinuity and provides thus the only known case where a direct statistical checking of the thermodynamic formula (18) is at hand.

It will be shown in the next section that by introducing interatomic forces of the repulsive type, it is possible to lift the order of the phase change of such B.E. fluid models.

[7] Cf. N. E. Dorsey, *Properties of Ordinary Water Substance* (Reinhold Publishing Corporation, New York, 1940).

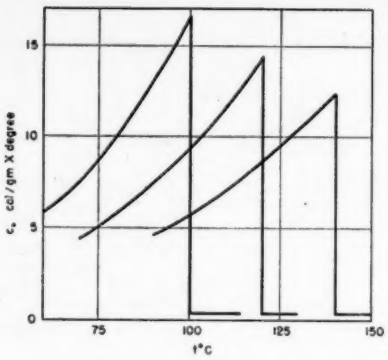

FIG. 2.

3. SECOND- AND THIRD-ORDER TRANSFORMATIONS IN PHASE SPACE

Consider a B.E. fluid model in which the total potential energy due to repulsion in coordinate space can be represented by a term of the type*

$$U(V)=a/V,$$

V being the total volume at the disposal of the fluid. The constant a will be considered independent of the temperature in a first approximation. In this model, the number of individual energy levels of spinless atoms associated with the momentum range $(p, p+dp)$ is, at temperature T,

$$dn(p)=\frac{4\pi V}{h^3}\frac{p^2dp}{\exp\left[\alpha+\left(U+\frac{p^2}{2m}\right)\Big/kT\right]-1}. \tag{19}$$

With

$$\alpha'=\alpha+\frac{U}{kT},$$

one finds again that at volume V the fluid begins to undergo a phase change at temperature T_0 given by Eq. (2). Similarly, at any given temperature T, the fluid undergoes a phase change at a volume V_0 given also by (2). It can also be shown without difficulty that

$$\begin{aligned} p_+&=p_{id+}-N\frac{\partial U}{\partial V},\\ p_-&=p_{id-}-N\frac{\partial U}{\partial V}, \end{aligned} \tag{20}$$

where p_{id} is the pressure of the ideal fluid. Since $U(V)$ is assumed to be independent of the temperature, the constant volume heat capacity of this non-ideal B.E. fluid is the same as that of the ideal fluid. The pressure, however, is still increasing with decreasing volume at temperatures and volumes less than their transition values, in the transition region. The introduction of a volume dependent repulsive force field of the atoms changes completely the nature of the phase transition of the originally ideal fluid. The modified fluid does not undergo a first-order phase change. This is already visible on the trend of variation of the isothermal curves in the transition region. In order to establish the nature of the phase change it is convenient to study the constant pressure heat capacity of the model.

One obtains after a simple calculation, $C_{v,id}$ denoting the constant volume heat capacity of the ideal fluid,

$$\begin{aligned} \frac{C_{p+}}{Nk}&=\frac{C_{v,id}}{Nk}+\frac{1}{4}\frac{\left[5\frac{G(\alpha')}{F(\alpha')}-3\frac{F(\alpha')}{E(\alpha')}\right]^2}{\frac{F(\alpha')}{E(\alpha')}+\frac{2a}{kTV}}, \quad T\geqslant T_0\\ \frac{C_{p-}}{Nk}&=\frac{C_{v,id-}}{Nk}+\frac{25}{8}\left(\frac{T}{T_0}\right)^3\frac{(G(0)/F(0))^2}{a/kTV}. \quad T\leqslant T_0 \end{aligned} \tag{21}$$

It is seen now that, in the first place, the constant pressure heat capacity is always finite and continuous along the transition line, with a break, since $(dC_p/dT)_{T_0}$ is discontinuous. One has, indeed,

$$\begin{aligned} \left(\frac{C_{p+}}{Nk}\right)_{T_0}&=\left(\frac{C_{v,id+}}{Nk}\right)_{T_0}+\frac{25}{8}\frac{(G(0)/F(0))^2}{a/kT_0V},\\ \left(\frac{C_{p-}}{Nk}\right)_{T_0}&=\left(\frac{C_{v,id-}}{Nk}\right)_{T_0}+\frac{25}{8}\frac{(G(0)/F(0))^2}{a/kT_0V}, \end{aligned}$$

and

$$\begin{aligned} \Delta C_p&=(C_{p+}-C_{p-})_{T_0}\\ &=(C_{v,id+}-C_{v,id-})_{T_0}=0. \end{aligned} \tag{22}$$

In this model, therefore, both the constant volume and constant pressure heat capacities are continuous with a break, e.g., their temperature derivatives are discontinuous along the transition line. The smooth condensation process undergone by the ideal B.E. fluid is changed by the re-

* It can be seen without difficulty that the results of this section are quite general insofar as the potential energy function $U(V)$ may contain both attractive and repulsive temperature independent terms. The choice of $U(V)$ is restricted by the trivial condition that the model so constructed behave in a physically admissible way, i.e., its compressibility has to be normal.

pulsive interatomic potential energy smeared over the whole volume of the fluid. The transition, in phase space, of the modified fluid is of the third order.

The question arises now under what conditions will a second-order phase change occur, e.g., a transition which is accompanied by a lambda-point type discontinuity of the constant pressure heat capacity of the fluid along the transition line. The answer to this question can be given at once using fluid models in which the forces between atoms are represented by the potential energy terms involved in the above discussed models. Suppose, indeed, that in a B.E. fluid model there is an attractive force field represented by the individual negative energy level $-E_0$ and a repulsive force field represented by a term a/V considered above. One then finds that such a B.E. fluid model has a constant volume heat capacity given by Eq. (15), as if the repulsive force field were absent. However, the work function of the fluid is now increased by the total potential energy term Na/V and the pressure is

$$\begin{aligned} p_+ &= p_{no+} + Na/V^2, \\ p_- &= p_{no-} + Na/V^2, \end{aligned} \tag{23}$$

where p_{no+} and p_{no-} are the pressures above and below the transition temperature of that fluid in which there are no repulsive forces. The pressures p_{no+} and p_{no-} are given by Eq. (11). It is clear from Eq. (23) that this fluid model has no coincident isobars and isothermals in the transition region. The repulsive forces giving rise to the pressure Na/V^2 have prevented the fluid from undergoing a first-order condensation as was the case above.

A long but straightforward calculation leads to the following expressions of the constant pressure heat capacity of this model:

$$\begin{aligned} \frac{C_{p+}}{Nk} &= \frac{C_{v+}}{Nk} + \Phi(x) \Big/ \left[\frac{F(x)}{E(x)} + \frac{2a}{kTV}\right]; \\ & \qquad x = \alpha' + \frac{E_0}{kT}; \quad T \geqslant T_f \\ \frac{C_{p-}}{Nk} &= \frac{C_{v-}}{Nk} + \left(\frac{T}{T_f}\right)^3 \Psi\left(\frac{E_0}{kT}, \frac{E_0}{kT_f}\right) \Big/ \frac{2a}{kTV}. \quad T \leqslant T_f \end{aligned} \tag{24}$$

The functions Φ and Ψ are given by the following expressions:

$$\begin{aligned} \Phi(x) &= \frac{25}{4}\left(\frac{G(x)}{F(x)}\right)^2 + \frac{9}{4}\left(\frac{F(x)}{E(x)}\right)^2 - \frac{15}{2}\frac{G(x)}{E(x)}; \\ & \qquad x = \alpha' + \frac{E_0}{kT}, \\ \Psi(y, z) &= \frac{25}{4}\left(\frac{G(y)}{F(z)}\right)^2 + 2y\frac{G(y)}{F(z)} + y^2\left(\frac{F(y)}{F(z)}\right)^2; \\ & \qquad y = \frac{E_0}{kT}; \quad z = \frac{E_0}{kT_f}. \end{aligned} \tag{25}$$

The constant volume heat capacity C_{v+} and C_{v-} are given by Eqs. (15).

A study of the functions Φ and Ψ shows that

$$\begin{aligned} & (C_{p-})_{T_f} > (C_{p+})_{T_f} \\ \text{or} \quad & \Delta C_p = (C_{p+} - C_{p-})_{T_0} < 0, \end{aligned} \tag{26}$$

ΔC_p is always finite but negative.

One has thus the following result. Consider any B.E. fluid composed of atoms whose interaction in coordinate space can be represented by an average constant attractive potential energy term $-E_0$ and an average repulsive potential energy term a/V, smeared over the whole volume V of the fluid, and independent of the temperature. Such fluid models exhibit a second-order phase change in which the constant pressure heat capacity has a lambda-point discontinuity along the transition line of the fluid. The repulsive force field, averaged over the whole volume of the fluid, has lifted the order of the phase change. If in the absence of this repulsive field the B.E. fluid is ideal and exhibits a smooth first-order condensation in phase space, the switching on of the repulsive forces causes the fluid to undergo instead a third-order transition in phase space. This means continuity of the energy, entropy, or any other characteristic function, with their first derivatives along the transition line. The introduction of the repulsive force field in a B.E. fluid model undergoing in its absence a sudden first-order transformation in phase space, similar to that exhibited by ordinary fluids in coordinate space, leads to a second-order transformation in phase space. This is characterized by the continuity of the characteristic functions, which have discontinuous first derivatives along the transition line.

The only actual liquid exhibiting a peculiar second-order phase change is liquid helium. And a possible explanation of the thermal properties of this liquid assimilating it to a kind of B.E. fluid has been repeatedly suggested by London.[1,2] The formalism necessary to describe the thermal properties of a B.E. fluid undergoing a second-order phase change in phase space would have to be somewhat similar to the formalism of the just discussed B.E. fluid model. However, as pointed out already,[3] the preceding models behave rather in a normal way below their transition line. Their expansion and pressure coefficients, $(\partial V/\partial T)_p$ and $(\partial p/\partial T)_V$, are positive in contrast with those of liquid He II. It is interesting to recall in this connection that in a recent investigation London[8] was lead to a qualitative argument accounting for this anomalous behavior of liquid He II on the very basis of a B.E. fluid model.

[8] F. London, J. Chem. Phys. 11, 203 (1943).

The difficulties inherent in the theoretical treatment of liquids are still further increased for a quantum liquid like He II. Here, the wave-length associated with the average thermal motion of the atoms may become of the same order of magnitude as the macroscopic dimensions of the vessel containing the liquid. This led Landau[9] to build up a continuum type or hydrodynamic model for this liquid. It is as yet not clear whether the anomalous thermal properties of liquid He II in bulk are correctly accounted for by this hydrodynamic model.

We should like finally to add here that a closer analysis of phase changes of higher order observed in cooperative phenomena might disclose also the interplay of forces of opposing tendencies as those existing in the B.E. fluid models studied here. In particular, the raising or lowering of the order of a phase change might be attributed to the intervention of forces of opposing nature.

[9] L. Landau, J. Phys. USSR 5, 71 (1941).

THE JOURNAL OF CHEMICAL PHYSICS VOLUME 14, NUMBER 4 APRIL, 1946

The Non-Planar Vibrations of Benzene

FOIL A. MILLER* AND BRYCE L. CRAWFORD, JR.
School of Chemistry, University of Minnesota, Minneapolis, Minnesota

(Received January 7, 1946)

A thorough normal coordinate treatment has been carried out for the non-planar vibrations of benzene and its deuterium derivatives. The analysis has led to a critical survey of the assignments, and has furnished strong independent support for those advanced by Pitzer and Scott. It has also furnished values for all eight force constants of the complete harmonic potential function. For four of the constants two sets of values were obtained, both of which are physically reasonable and which reproduce the frequencies equally well. It was not possible to decide between them. The force constants were then used to calculate frequencies for the various deuterobenzenes. Nearly sixty such frequencies were evaluated, of which about forty could be checked against experiment. With four exceptions the errors are less than 1.5 percent. Lastly, certain valence-force constants pertaining to hydrogen vibrations have been determined.

INTRODUCTION

BENZENE has been the subject of several normal coordinate treatments.[1–9] The first was carried out by Wilson,[1] who suggested a simplified potential function with six force con-

* National Research Fellow, 1942–1944. Now at the University of Illinois, Urbana, Illinois.

[1] E. B. Wilson, Jr., Phys. Rev. 45, 706 (1934).

[2] R. C. Lord, Jr. and D. H. Andrews, J. Phys. Chem. 41, 149 (1937).

Note added in proof: R. P. Bell [Trans. Far. Soc. 41, 293 (1945)] has recently shown how to improve Lord and Andrew's results for the non-planar vibrations of benzene while still using a simple valence force system with no cross terms and with only two force constants.

[3] M. van den Bossche and C. Manneback, Ann. Soc. Sci. Bruxelles 54-B, 230 (1934).

[4] C. Manneback, Ann. Soc. Sci. Bruxelles 55-B, 129 (1935).

[5] C. Manneback, Ann. Soc. Sci. Bruxelles 55-B, 237 (1935).

[6] J. Duchesne and W. G. Penney, Bull. Soc. Roy. Sci. Liege 8, 514 (1939).

[7] E. Bernard, C. Manneback, and A. Verleysen, Ann. Soc. Sci. Bruxelles [1] 59, 376 (1939).

[8] E. Bernard, C. Manneback, and A. Verleysen, Ann. Soc. Sci. Bruxelles 60, 45 (1940).

[9] K. S. Pitzer and D. W. Scott, J. Am. Chem. Soc. 65, 803 (1943).

stants. This function was applied to the vibrations of benzene and benzene-d_6 by Lord and Andrews,[2] but both the function and the data with which it was used are now known to be inadequate. Meanwhile Manneback[4] has obtained the most general potential function compatible with the simple harmonic approximation and with the D_{6h} symmetry of benzene. His equations contain twenty-six force constants for the planar vibrations and eight for the non-planar ones. The problem then became one of evaluating these various force constants by using this potential function with the correct set of vibrational assignments. In a second paper Manneback[5] attempted this with the data then available, but because the assignments were incomplete, and in some cases incorrect, the results have little present value. Duchesne and Penney[6] attempted a similar treatment after the assignments of Ingold and his collaborators[10] had been advanced. It too must be regarded as unsatisfactory inasmuch as several force constants had to be dropped from the potential function because of insufficient data. For example only three of the eight constants for the non-planar vibrations could be evaluated. At about this same time Bernard, Manneback, and Verleysen[7] modified Manneback's original equations to apply to the *planar* vibrations of *p*-benzene-d_2, *sym*-benzene-d_3, and *p*-benzene-d_4 as well as to benzene and benzene-d_6. They were then used with Langseth and Lord's[11] assignments for the planar vibrations of all five substances.[8] More recently Pitzer and Scott[9] appear to have carried out some calculations with Manneback's equations, but no details are given.

In summary it can be said that Manneback's equations provide the complete harmonic potential function for benzene, but that the application of these equations to actual data has not been thoroughly satisfactory. In the case of the planar vibrations the assignments of at least two frequencies (numbers 14 and 15 in Wilson's terminology[1]) are at best very dubious. There is also room for doubt concerning one or two other assignments. Any treatment is necessarily incomplete until these values have been established. No attempt to use the complete potential function on the non-planar vibrations has been described.

It, therefore, seemed worth while to attack the problem again. A successful treatment should provide two useful results. It should furnish a set of force constants which are characteristic of the benzene ring. One may very possibly be to carry these force constants over to various derivatives of benzene in much the same manner that one already transfers force constants from one aliphatic compound to another.[12] Secondly, the analysis will serve as a severe test for the validity of the assignments in benzene and its several deuterium derivatives. If one uses observed frequencies in, say, benzene and benzene-d_6 to calculate a set of force constants, these force constants must give back correct frequencies for all the various intermediate deuterium compounds. If they do not do so, the original assignments are in error.

The obvious starting place is the non-planar vibrations, for several reasons. First, the treatment of the planar vibrations by Manneback and his co-workers[7, 8] is quite satisfactory except for those cases where the assignments are dubious. The need here is for more experimental data. On the other hand there has been no thoroughgoing treatment of the non-planar vibrations. Second, the non-planar vibrations make the most important contributions to the various thermodynamic functions because the corresponding frequencies are relatively low. Hence it will be especially useful to have a set of force constants for these vibrations. Third, the non-planar vibrations split into relatively small

TABLE I. Symmetry properties of the non-planar vibrations of benzene (D_{6h} symmetry).

Class	C_2^z	C_2^x	C_2^y	i	No.	Notation Ring	Notation Hyd.	Sel. rules Ram	Sel. rules IR
A_{2u}^-	+	+	−	−	1		ν_{11}	−	+
B_{2g}	+	−	−	+	2	ν_4	ν_5	−	−
E_{ua}^+	e	+	+	−	2	ν_{16a}	ν_{17a}	−	−
E_{ub}^+	e	+	−	−	2	ν_{16b}	ν_{17b}	−	−
E_{ga}^-	e	−	+	+	1		ν_{10a}	+	−
E_{gb}^-	e	−	−	+	1		ν_{10b}	+	−

[10] C. K. Ingold, *et al.*, J. Chem. Soc. 912–987 (1936).
[11] A. Langseth and R. C. Lord, Jr., Kgl. Danske Vid. Sels. Math. Fys. Medd **16**, 6 (1938).
[12] B. L. Crawford, Jr. and S. R. Brinkley, Jr., J. Chem. Phys. **9**, 69 (1941).

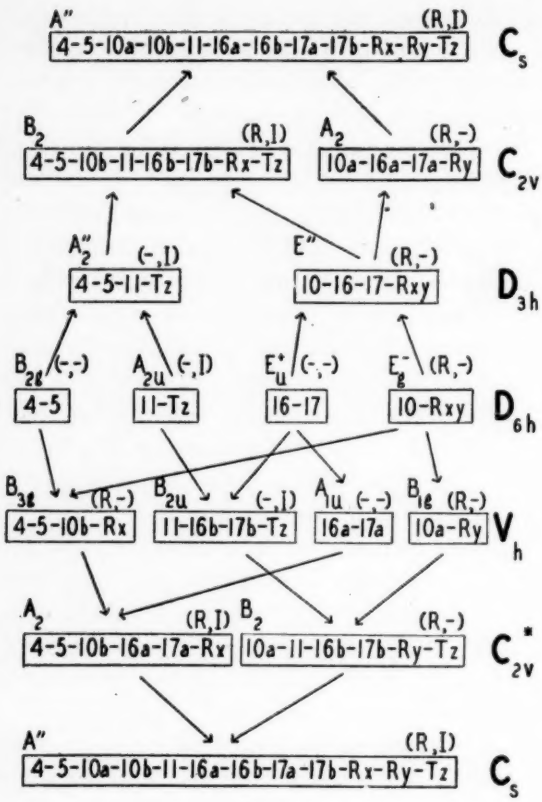

FIG. 1.

symmetry blocks, making the equations easier to handle.

We have carried out a complete normal coordinate treatment of the non-planar vibrations, evaluating all the force constants of the harmonic potential function. These constants have been used in turn to calculate a large number of frequencies for the various deuterobenzenes. The analysis has furnished valuable support for the latest assignments, those of Pitzer and Scott.

MATHEMATICAL METHODS

There are nine non-planar vibrations in benzene, of which three pairs are doubly degenerate. Their symmetry properties are shown in Table I for D_{6h} symmetry. We have followed Wilson[1] and Langseth and Lord[11] in numbering the vibrations and in defining the coordinate axes. The z axis is perpendicular to the plane of the molecule; the y axis is in the plane of the molecule and passes through atoms one and four.

The thirteen possible deuterobenzenes possess in all six different symmetries. Each of the symmetry classes of the various lower symmetries is formed by a combination of the classes of D_{6h}. Fig. 1, which is taken from the paper by Langseth and Lord, shows these combinations for the non-planar vibrations.[13] The selection rules are also indicated, R meaning Raman-active and I infra-red-active. In C_{2v} symmetry the twofold axis passes through carbon atoms, as in m-benzene-d_2. In C_{2v}* symmetry the twofold axis bisects carbon-carbon bonds, as in o-benzene-d_2.

To obtain the secular equation the technique of Wilson[14] was used. A valence-force potential function which included all the possible second-degree interactions was first set up. Two types of non-planar valence-force coordinates (VFC) were employed. (1) The perpendicular displacement of the ith hydrogen atom out of the plane defined by the two adjacent carbon-carbon bonds was termed $r_0\gamma_i$, where r_0 is the equilibrium

Class	VFSC	VFC											
		$r_0\gamma_1$	$r_0\gamma_2$	$r_0\gamma_3$	$r_0\gamma_4$	$r_0\gamma_5$	$r_0\gamma_6$	$R_0\delta_1$	$R_0\delta_2$	$R_0\delta_3$	$R_0\delta_4$	$R_0\delta_5$	$R_0\delta_6$
A_{2u}	S_{11}	$6^{-\frac{1}{2}}$	$6^{-\frac{1}{2}}$	$6^{-\frac{1}{2}}$	$6^{-\frac{1}{2}}$	$6^{-\frac{1}{2}}$	$6^{-\frac{1}{2}}$						
B_{2g}	S_4							$6^{-\frac{1}{2}}$	$-6^{-\frac{1}{2}}$	$6^{-\frac{1}{2}}$	$-6^{-\frac{1}{2}}$	$6^{-\frac{1}{2}}$	$-6^{-\frac{1}{2}}$
	S_5	$6^{-\frac{1}{2}}$	$-6^{-\frac{1}{2}}$	$6^{-\frac{1}{2}}$	$-6^{-\frac{1}{2}}$	$6^{-\frac{1}{2}}$	$-6^{-\frac{1}{2}}$						
$E_{ua}{}^{+}$	S_{16a}							$-12^{-\frac{1}{2}}$	$3^{-\frac{1}{2}}$	$-12^{-\frac{1}{2}}$	$-12^{-\frac{1}{2}}$	$3^{-\frac{1}{2}}$	$-12^{-\frac{1}{2}}$
	S_{17a}	0	$-\frac{1}{2}$	$\frac{1}{2}$	0	$-\frac{1}{2}$	$\frac{1}{2}$						
$E_{ub}{}^{+}$	S_{16b}							$\frac{1}{2}$	0	$-\frac{1}{2}$	$\frac{1}{2}$	0	$-\frac{1}{2}$
	S_{17b}	$-3^{-\frac{1}{2}}$	$12^{-\frac{1}{2}}$	$12^{-\frac{1}{2}}$	$-3^{-\frac{1}{2}}$	$12^{-\frac{1}{2}}$	$12^{-\frac{1}{2}}$						
$E_{ga}{}^{-}$	S_{10a}	0	$\frac{1}{2}$	$\frac{1}{2}$	0	$-\frac{1}{2}$	$-\frac{1}{2}$						
$E_{gb}{}^{-}$	S_{10b}	$-3^{-\frac{1}{2}}$	$-12^{-\frac{1}{2}}$	$12^{-\frac{1}{2}}$	$3^{-\frac{1}{2}}$	$12^{-\frac{1}{2}}$	$-12^{-\frac{1}{2}}$						

FIG. 2. **U** matrix for transforming *VFC* to *VFSC*. **VFSC** = **U** × **VFC**.

[13] Langseth and Lord seem to have reversed the "a" and "b" designations in their Figure 2b, p. 15, for they are not consistent with the usage in the rest of the paper. We have taken the liberty of altering them in our reproduction.

[14] E. B. Wilson, Jr., J. Chem. Phys. **7**, 1047 (1939); **9**, 76 (1941).

Class	VFSC	S_{11}	S_4	S_5	S_{16a}	S_{17a}	S_{16b}	S_{17b}	S_{10a}	S_{10b}
A_{2u}	S_{11}	$\frac{1}{M}+\frac{P}{6}$		$\frac{Q}{6}$		$\frac{T}{6\sqrt{2}}$		$\frac{Y}{2\sqrt{6}}$	$\frac{U}{6\sqrt{2}}$	$\frac{Z}{2\sqrt{6}}$
B_{2g}	S_4		$\frac{48}{M}$	$\frac{-3\sqrt{4}(1+4\rho)}{M}$						
	S_5		$\frac{-3\sqrt{4}(1+4\rho)}{M}$	$\frac{(1+4\rho)^2}{M}+\frac{P}{6}$		$\frac{U}{6\sqrt{2}}$		$\frac{Z}{2\sqrt{6}}$	$\frac{T}{6\sqrt{2}}$	$\frac{Y}{2\sqrt{6}}$
E_{ua}^+	S_{16a}				$\frac{16}{M}$	$\frac{4(1+3\rho)}{M}$				
	S_{17a}				$\frac{4(1+3\rho)}{M}$	$\frac{(1+3\rho)^2}{M}+\frac{S}{4}$		$\frac{T}{3\sqrt{4}}$	$\frac{V}{4}$	$\frac{U}{3\sqrt{4}}$
E_{ub}^+	S_{16b}						$\frac{16}{M}$	$\frac{4(1+3\rho)}{M}$		
	S_{17b}		(Symmetric)				$\frac{4(1+3\rho)}{M}$	$\frac{(1+3\rho)^2}{M}+\frac{W}{12}$	$\frac{U}{3\sqrt{4}}$	$\frac{X}{12}$
E_{ga}^-	S_{10a}								$\frac{(1+\rho)^2}{M}+\frac{S}{4}$	$\frac{T}{3\sqrt{4}}$
E_{gb}^-	S_{10b}									$\frac{(1+\rho)^2}{M}+\frac{W}{12}$

FIG. 3. **G** matrix for non-planar vibrations of the deuterobenzenes.

M = mass of carbon,
$\rho = r_0/R_0$ = C−H equilibrium distance/C−C equilibrium distance.
$P = 1/m_1+1/m_2+1/m_3+1/m_4+1/m_5+1/m_6$,
$Q = 1/m_1-1/m_2+1/m_3-1/m_4+1/m_5-1/m_6$,
$S = 1/m_2+1/m_3+1/m_5+1/m_6$,
$T = -1/m_2+1/m_3-1/m_5+1/m_6$,
$U = 1/m_2+1/m_3-1/m_5-1/m_6$,
m = mass of hydrogen (or deuterium),
$V = -1/m_2+1/m_3+1/m_5-1/m_6$,
$W = 4/m_1+1/m_2+1/m_3+4/m_4+1/m_5+1/m_6$,
$X = 4/m_1-1/m_2+1/m_3-4/m_4+1/m_5-1/m_6$,
$Y = -2/m_1+1/m_2+1/m_3-2/m_4+1/m_5+1/m_6$,
$Z = -2/m_1-1/m_2+1/m_3+2/m_4+1/m_5-1/m_6$.

carbon-hydrogen distance and γ_i is an angle thus defined. (2) The out-of-plane ring bending vibrations were regarded as torsions around carbon-carbon bonds. Carbon atoms 1, 2, and 3 define a plane; carbon atoms 2, 3, and 4 define another. These planes intersect along the C_2-C_3 bond. The angle between the planes is designated δ_2, and the corresponding VFC is $R_0\delta_2$, where R_0 is the equilibrium carbon-carbon distance. The corresponding coordinate for the C_1-C_2 bond is designated $R_0\delta_1$, that for the C_2-C_3 bond $R_0\delta_2$, and so on around the ring. Thus it is evident that motions of the hydrogen atoms do not affect the $R_0\delta_i$. It is important to note also that the $R_0\delta_i$ have a different symmetry with respect to our y and z axes than do the $r_0\gamma_i$. None of the former lie on the y axis, while two of the latter do. In other words the $R_0\delta_i$ have the symmetry of the carbon-carbon bonds, while the $r_0\gamma_i$ have the symmetry of the atoms.

Symmetry factoring was obtained by using valence-force symmetry coordinates (VFSC), which are orthogonal combinations of the VFC. The matrix **U** for the transformation **VFSC** = **U** × **VFC** is given in Fig. 2. For brevity the various VFSC are designated as S_{11}, S_4, S_5, ··· corresponding to frequencies ν_{11}, ν_4, ν_5, ···.

The **G** matrix for the VFSC is given in Fig. 3. It contains the atomic masses and internuclear distances. The outlined blocks indicate the way the matrix factors for D_{6h} symmetry. All the terms outside these blocks are interaction terms which depend only on the masses of the hydrogen (or deuterium) atoms. In evaluating them for the various deuterobenzenes it is important that the deuterium substituents be properly located

TABLE II. Comparison of Manneback's notation with that of this paper.

Manneback[a]	This paper
m	m
M	M
c	r_0
a	R_0
k	ρ
Ω^2	λ
B^+	α
B_S	φ or σ[b]
B^-	ϵ
L	48β
I	$3^{\frac{1}{2}}4\eta$
B_A	σ or φ[b]
N	16θ
J	4ω

[a] Reference 4.
[b] Reference 15.

with respect to the coordinate axes. The atoms in the benzene hexagon have been numbered one to six around the ring, with atoms one and four lying on the y axis. Then m_1 is the mass of the hydrogen (or deuterium) atom in position one (in atomic weight units), and so on. All these interaction terms go to zero for the two molecules of D_{6h} symmetry so that in this case the matrix factors as indicated. For lower symmetries this is no longer true. Some of these quantities will differ from zero, and the corresponding symmetry blocks of D_{6h} will be connected by these interaction terms. Thus for example class A_2'' of D_{3h} symmetry is formed by combining classes A_{2u} and B_{2g} of D_{6h} symmetry (cf. Fig. 1). The corresponding interaction term, $Q/6$, will be found unequal to zero for the deutero-benzene having D_{3h} symmetry, i.e., *sym*-benzene-d_3. Similarly the interaction term between E_{ua}^+ and E_{ga}^- (or between E_{ub}^+ and E_{gb}^-) will also be unequal to zero for *sym*-benzene-d_3. All other interactions will be zero.

There are many possible combinations of this type between the classes of D_{6h} to give the classes of lower symmetries (cf. Fig. 1). It therefore seemed preferable to leave the results in the form of the **F** and **G** matrices instead of reducing them to the relatively large number of formal equations. One must refer to Wilson's first paper on the subject[14] for the method of reducing the matrices to the secular equations. Wilson's method can be applied quite simply to cases where a single interaction term occurs, using an observation given in the Appendix.

The **F** matrix for the VFSC is given in Fig. 4. It contains force constants only.

A discussion of the force constants for VFC is now in order. The diagonal force constants for $r_0\gamma_i$ is termed A, while the interaction constants between the various $r_0\gamma_i$ are designated a_o, a_m, or a_p. The subscripts o, m, and p refer to the ortho-, meta-, and parapositions. Thus a_m is the constant for interaction between the out-of-plane motions of two hydrogen atoms *meta* to each other. Similarly B is the diagonal force constant for $R_0\delta_i$, and b_o, b_m, and b_p are the interaction constants between the various $R_0\delta_i$'s. The c's are constants for interactions between the $r_0\gamma_i$'s and the $R_0\delta_i$'s. The force constants and equilibrium distances for C−H and C−D are assumed to be identical.

When the VFC have been transformed to the VFSC, the force constants become:

$$\left.\begin{aligned}\alpha&=A+2a_o+2a_m+a_p\\ \epsilon&=A-2a_o+2a_m-a_p\\ \sigma&=A-a_o-a_m+a_p\\ \varphi&=A+a_o-a_m-a_p\end{aligned}\right\}\text{Hydrogen,}^{15}$$

$$\left.\begin{aligned}\beta&=B-2b_o+2b_m-b_p\\ \theta&=B-b_o-b_m+b_p\end{aligned}\right\}\text{Ring,}$$

$$\left.\begin{aligned}\eta&=2[-c_o+c_m-c_p]\\ \omega&=3^{\frac{1}{2}}[c_o-c_p].\end{aligned}\right\}\text{Hydrogen-ring interaction}^{16}\text{ (see Table II).}$$

TABLE III. Frequencies used to evaluate the force constants (cm^{-1}).

No.	Benzene	sym-Benzene-d_3	Benzene-d_6
4		691	
5		914	
10	850	712	664
11	671	533	503
16	404±3	373	
17			

[15] This does not completely agree with Manneback's results (reference 4). He would interchange our σ and φ, putting σ in class E_g^- of D_{6h} whereas we have it in E_u^+, and *vice versa*. Inasmuch as our results were checked by two independent workers, it seems probable that Manneback's B_A and B_S are reversed in his Eqs. (44) and (44′). This will cause no error whatever unless one wishes to evaluate the valence-force constants from the Greek constants. There is one other error in the second of his Eqs. (44′). The first minus sign should be replaced by a multiplication sign.

[16] It may be wondered why Manneback's notation has not been used in this paper. There are two reasons. First, four of his force constants differ from ours by a numerical factor. Our **F** or our **G** matrix would therefore have to be altered to compensate for this. Second, there is the difficulty of Manneback's force constants B_S and B_A (footnote 15). It has therefore seemed advisable to use a new terminology. Table II compares Manneback's notation with that of this paper.

It is interesting to note that the complete potential function requires only eight (Greek) force constants, but that these are expressed in terms of eleven valence-force constants. The Greek constants are the ones which are evaluated from the experimental data. Consequently we shall not always be able to calculate the valence-force constants from the Greek constants. One can do so for the hydrogen vibrations because there are four of each type. For the ring constants and the hydrogen-ring interactions it cannot be done. One must regard β, say, as being characteristic of a certain type of motion *of the benzene ring as a whole.* It will be impossible to say just how much B, b_o, b_m, or b_p contributes to the value of β. We shall therefore have no way of determining the relative magnitude of the ortho-, meta-, and paravalence-force interactions in this case.

The problem, then, is to evaluate the eight (Greek) force constants from the assigned vibrational frequencies. Table III lists the assignments which were used for this purpose. They are taken from the paper of Langseth and Lord,[11] and appear to be reasonably correct. Eight additional frequencies for the para-deutero compounds were also used,[11] but they have not been included in the table because they are not essential to our results.

The calculated value of any given force constant will vary slightly from one deuterobenzene to another. There are at least two reasons for this. First, the vibrations are not purely harmonic as assumed. The anharmonicity decreases as more deuterium atoms are introduced into the molecule because the average amplitude of vibration becomes smaller. Consequently, diagonal force constants will increase with increasing deuterium substitution. Whenever possible we have used values midway between those for the two extremes of light and heavy benzene. A second reason for inconstancy is the fact that some of the experimental frequencies were measured on the liquid and some on the vapor. It is well known that a vibrational frequency is usually somewhat higher in the gaseous than in the liquid state. Neither effect is very marked, however.

The following numerical values were employed in the calculations:

m = mass of hydrogen (or deuterium) = 1.008 (or 2.016) atomic weight units.
M = mass of carbon = 12.01 atomic weight units.
r_0 = C–H and C–D equilibrium distance = 1.08A.
R_0 = C–C equilibrium distance = 1.39A.
$\rho = r_0/R_0 = 0.777$.
ν = frequency in wave numbers = const. $\times \lambda^{\frac{1}{2}}$, where λ is a root of the secular equation. When masses are in atomic weight units, and force constants are 10^{-5} times their value in dynes/cm, the constant is 1302.9.

EVALUATION OF FORCE CONSTANTS

α and ϕ

The evaluation of α and φ scarcely needs comment. Frequency 11, which goes with α, is the only member of class A_{2u} in D_{6h} symmetry. Taking the frequency to be 671 cm^{-1} in benzene and 503 cm^{-1} in benzene-d_6, one calculates values of 0.2467 and 0.2573, respectively. These values differ by 4 percent, which is probably somewhat too much to attribute to change in anharmonicity alone and may indicate some slight experimental error. The average value of α is 0.252.

Four values of φ may be obtained with equal ease from ν_{10} in benzene and benzene-d_6 and from ν_{10a} in p-benzene-d_2 and p-benzene-d_4. The following results are obtained:

benzene	$\nu_{10} = 849.7$	$\varphi = 0.3389$
p-benzene-d_2	$\nu_{10a} = 850.0$	$\varphi = 0.3391$
p-benzene-d_4	$\nu_{10a} = 662.3$	$\varphi = 0.3405$
benzene-d_6	$\nu_{10} = 663.5$	$\varphi = 0.3417$
		φ(average) = 0.340

It is to be remembered that the force constants must be multiplied by 10^5 to convert to dynes/centimeter.

β, η, and ϵ

Now that α and φ are known, the evaluation of β, η, and ϵ can be readily carried out in either of two ways. One method is to use the equations for class A_2'' or D_{3h}. This class contains frequencies 4, 5, and 11 and force constants α, β, η, and ϵ. (Figs. 1 and 4.) The value of α is now known, so that the three frequencies will suffice to determine the three unknown force constants. The assignment of 691, 914, and 533 cm^{-1} to the three vibrations is reasonably certain. On carrying out the calculation one finds an interesting result; *two* sets of values are obtained for the

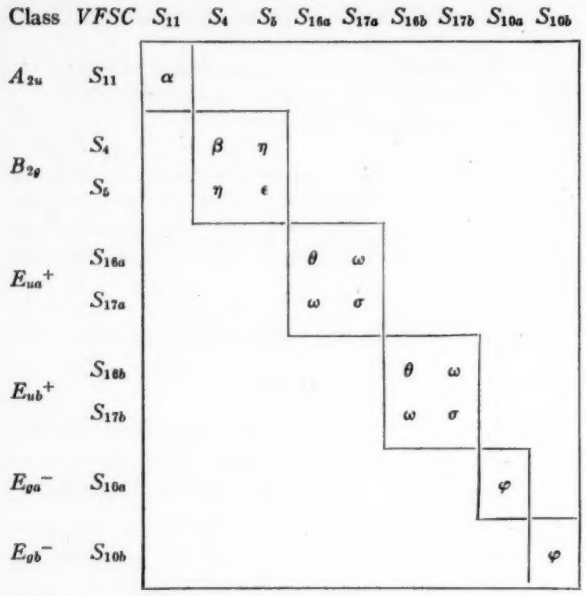
Class VFSC S_{11} S_4 S_5 S_{16a} S_{17a} S_{16b} S_{17b} S_{10a} S_{10b}
A_{2u} S_{11} α
B_{2g} S_4 β η
S_5 η ϵ
E_{ua}^+ S_{16a} θ ω
S_{17a} ω σ
E_{ub}^+ S_{16b} θ ω
S_{17b} ω σ
E_{ga}^- S_{10a} φ
E_{gb}^- S_{10b} φ

FIG. 4. **F** matrix for non-planar vibrations of the deuterobenzenes.

force constants (Table IV). The value for ϵ, which is the constant for the hydrogen vibration, is unique, but there is no obvious means of choosing between the two sets of values for β and η. The difficulty arises because β (or η) is obtained from a quadratic equation, and both roots of the quadratic are physically reasonable.

One can also evaluate β, η, and ϵ from class B_{3g} of V_h symmetry, which contains frequencies 4, 5, and 10*b* and force constants φ, β, η, and ϵ. Using Langseth and Lord's assignments of 634, 966, and 738 cm^{-1} for *p*-benzene-d_2 and of 605, 927, and 765.3 for *p*-benzene-d_4, and using the known value of φ, one gets again two sets of solutions as indicated in Table IV.

It is apparent that sets 1 and 3 are comparable, and sets 2 and 4. The differences between comparable values are large, and may be due to any of the following reasons: (*a*) an error in φ or, more probably, in α (incidentally the average values of these constants were used); (*b*) a small error in the assignments for the three compounds; (*c*) the fact that the frequencies for *sym*-benzene-d_3 are vapor-phase frequencies, while those for the *para* derivatives are liquid-phase frequencies. (This, however, probably should make the diagonal force constants ϵ and β higher for the former than for the latter, since frequencies are usually higher in the vapor state. The converse is found.) It should be mentioned that sets 1 and 2 give identical results when used to calculate frequencies, and so do sets 3 and 4. One must then decide which particular set to use, or whether to take the average of, say, sets 1 and 3. We arbitrarily chose to use set 1 in later calculations, as it seemed to give somewhat better agreement with observed results than did either set 3 or the average of sets 1 and 3.

One is now in a position to calculate ν_4 and ν_5 in benzene. These frequencies have never been assigned with certainty. Pitzer and Scott selected the weak Raman line at 685 cm^{-1} for ν_4, and then used the product rule to calculate ν_5 as 1016 cm^{-1}. We have calculated ν_4 and ν_5 from our values for ϵ, β, and η, using both sets 1 and 3. The results are:

	Set 1	Set 3
ν_4	693	669
ν_5	993	1041

It will be observed that the calculated values for ν_4 bracket the weak line at 685 cm^{-1}. This offers strong support for the choice of Pitzer and Scott, and makes an otherwise weak assignment very probable. We then follow these authors in taking ν_5 to be about 1015 cm^{-1}.

θ, σ, and ω

The obvious place from which to calculate these force constants is class E'' of D_{3h} symmetry, which contains frequencies 10, 16, and 17 and force constants φ, θ, σ, and ω. The value of φ has already been found, so that one has three frequencies with which to evaluate three unknown force constants. Langseth and Lord assigned the values 711.7, 373, and 815 cm^{-1} to ν_{10}, ν_{16}, and ν_{17}, respectively, in *sym*-benzene-d_3. Unfortunately these authors are uncertain about the assignment for ν_{17}, and we shall see later that it must be revised upward by about 100 cm^{-1}. But using their values for the moment, one can

TABLE IV. Values for ϵ, β, and η.

	From D_{3h}		From V_h	
	1	2	3	4
ϵ	0.532	0.532	0.585	0.585
β	0.203	0.339	0.205	0.367
η	0.258	0.373	0.279	0.415

TABLE V. Location of ν_{17}.

Trial	Freq. No.	Bz(calc.)	*s*-Bz-d_3(assumed)	Bz-d_6(calc.)
	10	—	711.7	—
1	16	398	373	350
	17	1002	950	805
	10	—	711.7	—
2	16	403	373	346
	17	958	920	789
	10	—	711.7	—
3	16	409	373	342
	17	912	890	772

calculate some tentative force constants. Once again two sets of results are obtained. Both sets reproduce Langseth and Lord's assignments in *m*-benzene-d_2, *sym*-benzene-d_3, *vic*-benzene-d_3, and *m*-benzene-d_4, but they do *not* give back the observed frequencies of benzene and benzene-d_1 nor of benzene-d_5 and benzene-d_6. Thus for example instead of getting 404 cm^{-1} for ν_{16} in benzene, one calculates 433 cm^{-1}. It must be concluded that Langseth and Lord's assignments are not internally consistent through this series of isotopic molecules.

Zeigler and Andrews[17] were led by a study of the heat capacity of solid benzene-d_6 to suggest that Langseth and Lord's value for ν_{17} was too low. Pitzer and Scott[9] have discussed the assignment at some length. They say that 815 cm^{-1} for ν_{17} in *sym*-benzene-d_3 leads to an unreasonable potential function, and also that it leads to a calculated heat capacity for benzene which is too high. By a consideration of weak bands they assign 985 cm^{-1} in benzene and 790 cm^{-1} in benzene-d_6. From these values they find ν_{17} to be 950 cm^{-1} in *sym*-benzene-d_3.

We arrive at essentially the same results, but by a different procedure. There are three relevant cases where one can be fairly certain that ν_{10} and ν_{16} are correctly assigned, namely 712 and 373 cm^{-1} in *sym*-benzene-d_3 and 404 cm^{-1} in benzene. The correct set of force constants *must* reproduce these three values. Only two of these frequencies belong to *sym*-benzene-d_3, however. Our procedure was to estimate a value for the third frequency in *sym*-benzene-d_3 (ν_{17}), and then to use these three frequencies to calculate a trial set of values for θ, σ, and ω. These in turn were then used to calculate ν_{16} and ν_{17} in benzene, with the hope that they would give 404 cm^{-1} for ν_{16}. It soon became apparent that in order to obtain 404 cm^{-1}, one has to choose ν_{17} for *sym*-benzene-d_3 within the range 890–950 cm^{-1}. The results for three such trials are indicated in Table V. Obviously ν_{17} is confined within the following ranges: (*a*) 890–950 cm^{-1} in *sym*-benzene-d_3; (*b*) 910–1000 cm^{-1} in benzene; (*c*) 770–805 cm^{-1} in benzene-d_6. One cannot locate ν_{17} more precisely in this way because the calculated value of ν_{16} in benzene is rather insensitive to changes of ν_{17} in *sym*-benzene-d_3. Furthermore the numerical value of ν_{16} in benzene has an uncertainty of about 3 cm^{-1}.[18]

The next step is to look in these regions of the spectra for weak bands that may be attributed to ν_{17}. It may be noted that ν_{10a}, ν_{16a}, and ν_{17a} will have the same numerical values in the following groups of compounds because the corresponding portions of the **G** matrices are identical: (*a*) benzene, benzene-d_1, and *p*-benzene-d_2; (*b*) *m*-benzene-d_2, *sym*-benzene-d_3, *vic*-benzene-d_3, *m*-benzene-d_4; (*c*) *p*-benzene-d_4, benzene-d_5, benzene-d_6. Thus the search may be extended to the spectra of these additional compounds.

Starting with benzene, one finds a very weak infra-red band in the vapor at 962 cm^{-1}, and in the liquid at 985 cm^{-1}. Inasmuch as ν_{17} is forbidden to appear in benzene, and as selection rules are rigorous in the vapor phase, the first of these cannot be accepted. The second would be a possibility if it really belonged to a vibration different from the 962 cm^{-1} one, and if liquid forces were breaking down the selection rules. This 985 cm^{-1} band appears as a shoulder on the strong 1033-cm^{-1} absorption, so that it is difficult to estimate the frequency and intensity accurately. One concludes that the spectrum of benzene offers little help. In benzene-d_6 a very weak line is observed at 790 cm^{-1} in the Raman spectrum of the liquid. If this is ν_{17}, it appears in violation of the selection rules. Pitzer and Scott were the first to assign 985 and 790 to ν_{17}. Going now to the intermediate isotopic derivatives, we find a possibility in the weak Raman

[17] W. Zeigler and D. H. Andrews, J. Am. Chem. Soc. 64, 2482 (1942).

[18] See p. 928 of reference 10.

TABLE VI. Values of the force constants ($k \times 10^{-5}$ dynes/cm).*

	1	2
α	0.252	—
φ	0.340	—
ϵ	0.532	—[a]
β	0.203	0.339[a]
η	0.258	0.373[a]
σ	0.402	—
θ	0.157	0.757
ω	−0.154	−0.515

* Set 1 was used in most of the calculations.
[a] See also Table IV.

line at 920 cm^{-1} in *vic*-benzene-d_3, observed by Langseth and Lord. They had assigned it to ν_{9b}, but questioned their choice. There are no other observed frequencies in these ranges than these three (with the exception of the very intense breathing frequency ν_1, which cannot be mistaken). We therefore take ν_{17} to be 920 cm^{-1} in *sym*-benzene-d_3, and 790 cm^{-1} in benzene-d_6. In benzene it will be somewhere near 985 cm^{-1}, the uncertainty being due to its appearance as a shoulder on another strong band.

The justification for this assignment will be found in its results. Using 711.7, 373, and 920 cm^{-1} for ν_{10}, ν_{16}, and ν_{17} in *sym*-benzene-d_3, and taking $\varphi = 0.340$, one calculates the following two sets of values for the force constants.

	1	2
σ	0.402	0.402
θ	0.157	0.757
ω	−0.154	−0.515

Again there is no obvious reason for preferring one set over the other. We arbitrarily chose set 1 for later calculations.

Using these force constants, one calculates ν_{17} to be 789 cm^{-1} in benzene-d_6, in good agreement with the observed 790 cm^{-1}. For benzene, one calculates 958 cm^{-1} in place of the (rather indefinite) 985 cm^{-1}. Pitzer and Scott have already pointed out that this assignment explains the rather strong infra-red bands in benzene at 1810 and 1965 cm^{-1}, which appear in both gas and liquid, as the allowed combination tones $\nu_{10}+\nu_{17}$ and $\nu_5+\nu_{17}$. A value of about 955 cm^{-1} is indicated for ν_{17} from these considerations.

This assignment of ν_{17} is further strengthened by some results for *p*-benzene-d_2. Frequencies 16*b* and 17*b* become infra-red active in this derivative. Their values were calculated from the force constants σ, θ, and ω to be 360 and 868 cm^{-1}, respectively. A sample of *p*-benzene-d_2 was prepared and the infra-red spectrum of the vapor obtained.[19] A strong band was observed at 872 cm^{-1}, which may very well be ν_{17}. This offers valuable support for the assignments and for the values of the force constants.

Thus we have arrived at virtually the same conclusions concerning ν_{17} as did Pitzer and Scott, but by quite a different method. Indeed, our assignments for all the out-of-plane vibrations are essentially the same as theirs.

This completes the determination of the force constants. For convenience they have been gathered together in Table VI. Where two or more sets of values were obtained, the first set was the one which was used in our calculations.

FURTHER RESULTS

Once all the force constants are at hand, one can proceed to calculate many of the non-planar frequencies for the various deuterium derivatives. This has been done for those cases where the symmetry blocks are not too large to make the labor prohibitive. Table VII gives the results. Thirty-nine of the fifty-nine calculated frequencies may be checked against experiment. The maximum error is 4.3 percent or 16 cm^{-1}. With but four exceptions, calculated and observed values agree within 1.5 percent. The results may, therefore, be considered satisfactory.

One is also now able to evaluate the valence-force constants which are associated with the hydrogen vibrations—i.e., A, a_o, a_m, and a_p. Introducing the numerical values of α, ϵ, σ, and φ, one calculates $A = 0.378$, $a_o = -0.057$, $a_m = 0.007$, and $a_p = -0.026$. It is interesting to note that the force constant connecting the out-of-plane displacements of two hydrogen atoms para to each other is about half of that for the case where they are ortho. From the signs of these force constants it is evident that the potential energy required for a "dishing" of the hydrogens (i.e., all the hydrogens above the carbon ring) is less than that for a "puckering" of the hydrogens (hydrogen atoms alternately

[19] Detailed results of this investigation will be published separately.

TABLE VII. Calculated *vs.* observed frequencies.

Freq. No.	Benzene Calc.	Obs.	Diff. (%)	Benzene-d_1 Calc.	Obs.	Diff.	*o*-benzene-d_2 Calc.	Obs.	Diff.	*m*-benzene-d_2 Calc.	Obs.	Diff.	*p*-benzene-d_2 Calc.	Obs.	Diff.	*sym*-benzene-d_3 Calc.	Obs.	Diff.
4	693	*685*[a]	+1.2										633	634	−0.2	691	(691)	—
5	993	v.											959	966	−0.7	914	(914)	—
11	678	(671)	+1.0				579	582	−0.5				600	594[a]	+1.0	533	(533)	—
10*a*				851	852	−0.1	783	782	+0.1	712	711	+0.1	851	850	+0.1			
	851	(850)	+0.1													712	(712)	—
10*b*													729	738	−1.2			
16*a*				403	403	0.0				373	374	−0.3	403	*400*[b]	+0.8			
	403	*(404)*[a]	−0.7													373	(373)	—
16*b*							391	384	+1.8				360	i.r.				
17*a*				958	—					920	—		958	v.				
	958	*~985*[a]	?													920	d.	
17*b*							945	—					868	872[c]				

Freq. No.	*vic*-benzene-d_3 Calc.	Obs.	Diff.	*o*-benzene-d_4 Calc.	Obs.	Diff.	*m*-benzene-d_4 Calc.	Obs.	Diff.	*p*-benzene-d_4 Calc.	Obs.	Diff.	Benzene-d_5 Calc.	Obs.	Diff.	Benzene-d_6 Calc.	Obs.	Diff.
4										615	605	+1.7				600	v.	
5										918	927	−1.0				812	v.[e]	
11				534	—					549	i.r.					498	(503)	−1.0
10*a*	712	712	0.0	737	739	−0.3	712	711	+0.1	662	662	0.0	662	664	−0.3			
																662	(664)	−0.3
10*b*										759	765	0.8						
16*a*	373	374	−0.3				373	375	+0.5	346	v.		346	—				
				353	369	−4.3										346	*337*[a]	+2.7
16*b*										377	i.r.							
17*a*	920	920	0.0				920			789	v.		789	—				
																789	*790*[a]	−0.1
17*b*				863	—					918	i.r.							

Observed values taken from references 10 and 11.
( )—Used to evaluate force constants.
Italic numbers indicate values which appear in violation of selection rules
v.—Forbidden in both Raman and infra-red.
i.r.—Allowed in infra-red only; hasn't been studied.

[a] Reference 10.
[b] Reference 11, p. 21, p. 67 (footnote).
[c] Footnote 19.
[d] Would be hidden by strong i.r. band at 914.
[e] Would be hidden by strong i.r. band at 811.

above and below the carbon ring). This is borne out by the frequencies of the corresponding vibrations. The "dishing" frequency (ν_{11}) is 671 cm^{-1}; the "puckering" frequency (ν_5) is about 1015 cm^{-1} (calculated).[20]

One might deduce from this that attractive forces prevail between the hydrogen atoms, making it energetically cheaper to displace two hydrogen atoms in the same direction out of the equilibrium plane than in opposite directions. And indeed this is compatible with the geometry of the molecule. The van der Waals radius of hydrogen is 1.2±0.1A,[21] while the closest hydrogen atoms in benzene are approximately 2.47A apart. Thus they may well be far enough removed so that repulsive forces no longer predominate. However, it must be admitted that according to this concept a_m cannot be more positive than *both* a_o and a_p—although actually it is. One must, therefore, conclude that this simple hypothesis is untenable. We have no adequate explanation to suggest.

In conclusion it may be pointed out that the numerical values for these force constants should be applicable to derivatives of benzene. Crawford and Brinkley[12] have already outlined methods for such a transfer of force constants between aliphatic compounds

ACKNOWLEDGMENT

One of us (FAM) wishes to express his appreciation to the National Research Council for the grant of a fellowship.

APPENDIX

In most of the isotopic molecules of lower symmetry, two blocks of the D_{6h} G matrix (Fig. 3) were connected by only one interaction term, so that the complete block of the G matrix for the isotopic case could be written

$$\left[\begin{array}{ccc|ccc} g_1^1 & \cdots & g_m^1 & 0 & \cdots & 0 \\ \cdots & \cdots & \cdots & \cdots & \cdots & \cdots \\ g_1^m & \cdots & g_m^m & d & \cdots & 0 \\ \hline 0 & \cdots & d & g_{m+1}^{m+1} & \cdots & g_{m+n}^{m+1} \\ \cdots & \cdots & \cdots & \cdots & \cdots & \cdots \\ 0 & \cdots & 0 & g_{m+1}^{m+n} & \cdots & g_{m+n}^{m+n} \end{array}\right], \quad \text{(A1)}$$

[20] The frequencies depend also on the reduced masses and on interaction with other vibrations which may be in the same symmetry class, but these effects alone could hardly produce the large difference of 340 cm^{-1} which is observed.

[21] L. Pauling, *The Nature of the Chemical Bond* (Cornell University Press, New York, 1940), second edition, p. 189.

with d representing the interaction. If we denote the secular equations for the separate blocks (setting $d=0$) by

$$0=A(\lambda)=\sum_{i=0}^{m} a_i\lambda^{m-i}, \tag{A2}$$

$$0=B(\lambda)=\sum_{i=0}^{n} b_i\lambda^{n-i}, \tag{A3}$$

and their product by

$$0=C(\lambda)=A(\lambda)\cdot B(\lambda)=\sum_{k=0}^{m+n} c_k\lambda^{m+n-k}, \tag{A4}$$

$$c_k=\sum_{i=0}^{k} a_i b_{k-i},$$

then the secular equation with $d\neq 0$ is simply obtained from $C(\lambda)$: wherever the product $g_m{}^m g_{m+1}{}^{m+1}$ appears, one has only to substitute therefor $(g_m{}^m g_{m+1}{}^{m+1}-d^2)$.

This is easily seen. For, of all possible minors of the **G** matrix (A1) containing d, those which do not obviously vanish will be of the same form as (A1)—i.e., will have d's "bridging" the principal diagonal—or will be of the form

$$\left[\begin{array}{cccc|c} g_1{}^1 & \cdots & g_k{}^1 & g_m{}^1 & \\ \cdots & \cdots & \cdots & \cdots & \\ g_1{}^k & \cdots & g_k{}^k & g_m{}^k & X \\ 0 & \cdots & 0 & d & \\ \hline \multicolumn{4}{c|}{0} & X \end{array}\right], \tag{A5}$$

or of the form

$$\left[\begin{array}{ccc|c} g_k{}^k & \cdots & g_m{}^k & \\ \cdots & \cdots & \cdots & 0 \\ g_k{}^m & \cdots & g_m{}^m & \\ \hline 0 & \cdots & d & \\ \cdots & \cdots & \cdots & X \\ 0 & \cdots & 0 & \end{array}\right]. \tag{A6}$$

The determinants of the form (A6) will clearly not contain d, while determinants of the form (A5) will correspond to vanishing minors of the **F** matrix; hence no contribution from d will arise in either of these cases. So we need consider only minors of the form (A1). Such a determinant may be expanded, by Laplace's development, in the second minors of second-order determinants based on the mth and $(m+1)$th columns. To be non-vanishing, these second minors must be obtained by striking out one of the first m rows and one of the last n; this restricts the second-order determinants which will actually contribute to those of the types

$$\begin{vmatrix} X & 0 \\ 0 & X \end{vmatrix}, \quad \begin{vmatrix} X & 0 \\ d & X \end{vmatrix}, \quad \begin{vmatrix} X & d \\ d & X \end{vmatrix}.$$

There is but one of this last type, and it will contribute the term $(g_m{}^m g_{m+1}{}^{m+1}-d^2)$—the only way in which d can appear in the final secular equation.

Similar considerations can be applied if more than one interaction couples two blocks, but the increased complexity makes it scarcely worth while.

THE JOURNAL OF CHEMICAL PHYSICS VOLUME 14, NUMBER 4 APRIL, 1946

The Infra-Red Spectra of *p*-Benzene-d_2 and *p*-Benzene-d_4

FOIL A. MILLER
Department of Chemistry, University of Illinois, Urbana, Illinois

AND BRYCE L. CRAWFORD, JR.
School of Chemistry, University of Minnesota, Minneapolis, Minnesota

March 5, 1946

INTRODUCTION

IN a paper by the authors which appears in this issue[1] reference is made to some experimental work on the infra-red spectrum of *p*-benzene-d_2. The purpose of this note is to present the data on this compound, together with that on *p*-benzene-d_4, in detail sufficient for the above-mentioned paper. The work was originally undertaken for the purpose of locating ν_{14} and ν_{15} and for completing the analysis of the vibrational spectrum of benzene. This aspect will be discussed in a later report.

PREPARATION OF SAMPLES

The deuterium compounds were prepared by the method of Langseth and Klit,[2] which involves the continuous formation of a Grignard reagent and its decomposition with deuterium chloride. The last step is the separation of the deutero-benzene from the great excess of diethyl ether solvent by distillation. In the case of the *p*-benzene-d_4 an unknown intermediate fraction boiling at 70–75° was obtained in addition to the desired *p*-benzene-d_4 fraction at 76.3–77.0°.[3] On exposure to air this intermediate fraction

[1] F. A. Miller and B. L. Crawford, Jr., J. Chem. Phys. **14**, 282 (1946).

[2] A. Langseth and A. Klit, Kgl. Danske Vid. Sels. Math. fys. Medd. **15**, No. 13 (1938).

[3] Because these temperatures are uncorrected for atmospheric pressure (745 mm) and for errors in calibration of the thermometer (at least 1.2°), they have only relative significance. The boiling point of benzene was observed to be 77.0° under the same conditions, although the correct value is 80.1°.

gradually turned pink. To eliminate any absorption bands in the spectrum of the *p*-benzene-d_4 sample which may be due to this impurity, the spectrum of the 70–75° fraction was obtained under identical conditions. It was found that all absorption bands but one in the spectrum of the 70–75° fraction were of the same order of intensity as those in the spectrum of the *p*-benzene-d_4 sample. They were therefore thought to be due to *p*-benzene-d_4, since the 70–75° fraction is certainly rich in this. The one exception (1213 cm^{-1}) was very intense in the 70–75° fraction, but was weak in the *p*-benzene-d_4 sample. Consequently it was considered to originate with the impurity and was rejected from the spectrum of the deuterobenzene. The diminution of intensity was so great that there is little likelihood of having overlooked any other such interferences.

SPECTROSCOPIC PROCEDURES

The spectrum of *p*-benzene-d_2 was obtained on two different spectrometers: (1) one constructed at the University of Minnesota, using fluorite (CaF_2), rocksalt, and KBr prisms. (2) a Perkin-Elmer instrument with rocksalt optics at the University of Illinois. Results agreed well, so only averaged or preferred values will be tabulated here.

The spectrum of *p*-benzene-d_4 was obtained in the rocksalt region with the Perkin-Elmer instrument only.

All the spectra were measured in the gas phase with a vapor pressure of 85 mm of mercury. The cell length of the Minnesota spectrometer was 20 cm; that of the Perkin-Elmer instrument 10 cm.

TABLE I.

p-benzene-d_2 cm^{-1}	Int.	*p*-benzene-d_4 cm^{-1}	Int.
594	*vs*	780	*w*
657	*w*	817	*vs*
693	*m*	832	*s*
766	*m*	865	*s*
778	*vs*	925	*vs*
792	*m*	938	*s*
815	*s*	1058	*m*
829	*m*	1122	*m*
873	*vs*	1180	*w*
924	*s*	1207	*m*
1034	*m*	1281	*w*
1097	*vw*	1301	*w*
1227	*w*	1341	*w*
1325	*vw*	1396	*vw*
1416	*s*	1447	*vs*
1473	*vs*	1563	*m*
1609	*w*	~1722	*vw*
1719	*m*	1831	*vs*
1814	*s*	2283	*vs*
1924	*s*	~2320	*m*
2101	*vw*		
2194	*w*		
2276	*vs*		
2314	*m*		
2866	*w*		
2992	*m*		
3044	*m*		
3083	*vs*		
3279	*w*		

TABLE II.

	p-benzene-d_2 Calc.	Obs.	*p*-benzene-d_4 Calc.	Obs.
ν_{11}	600	594	549	
ν_{16b}	360		377	
ν_{17b}	868	873	918	925

RESULTS AND COMMENT

The results are tabulated in Table I.

Several assignments can immediately be made to the non-planar vibrations which are infra-red-active. These are indicated in Table II.[4]

There is little doubt that the absorptions of 873 and 925 cm^{-1} originate from the same vibration, for both are very intense and the band contours are similar. Even if calculated values were not already at hand, one would probably want to assign the two bands to ν_{17b} because the frequency in *p*-benzene-d_2 is *lower* than that in *p*-benzene-d_4. It is nevertheless noteworthy that the value of ν_{17b} can be calculated so precisely. This provides convincing support for the assignment of ν_{17} advanced by the authors in the accompanying paper, and leads one to feel that force constants σ, θ, and ω cannot be far wrong.

More complete experimental details and an analysis of the remainder of the spectra will be presented in a later paper.

ACKNOWLEDGMENT

The preparation of the samples was carried out while one of the authors (F. A. M.) held a National Research Fellowship at the University of Minnesota in 1942–43.

[4] The calculated values are taken from Table VII of reference 1.

Letters to the Editor

THIS section will accept reports of new work provided these are terse and contain few figures, and especially few halftone cuts. The Editorial Board will not hold itself responsible for opinions expressed by the correspondents. Contributions to this section should not exceed 600 words in length and must reach the office of the Managing Editor not later than the 15th of the month preceding that of the issue in which the letter is to appear. No proof will be sent to the authors. The usual publication charge ($3.00 per page) will not be made and no reprints will be furnished free.

On the Force Constants of the XY_2 Molecule

DELIA M. SIMPSON
Laboratory of Physical Chemistry, Cambridge, England
February 25, 1946

IN a recent paper Glockler and Jo-Yun Tung[1] have suggested a method whereby the four force constants required to describe the behavior of the triatomic molecule XY_2 ($X=M$, $Y=m$) can be determined from its three vibrational frequencies. They employ force constants c_1, c_2, c_3, c_4 defined by the potential field:

$$2V=c_1[\Delta r_1^2+\Delta r_2^2]+c_2\cdot r_0^2[\Delta(2\alpha)]^2 +2c_3\cdot r_0\cdot\Delta(2\alpha)[\Delta r_1+\Delta r_2]+2c_4\cdot\Delta r_1\cdot\Delta r_2, \quad (1)$$

where Δr_1, Δr_2 are the changes in length of the XY bonds, equilibrium value r_0, and $\Delta(2\alpha)$ is the change in the apical angle. These authors discuss the conditions necessary for all four force constants to be real, and suggest that the real value of c_4 should be chosen which makes c_1 approximately the same as the force constant of the corresponding diatomic molecule XY. The limits of reality of c_4 are given by the relationship:

$$\partial c_4/\partial c_2=\partial c_4/\partial c_3=0, \quad (2)$$

which also defines its maximum and minimum values. Glockler and Jo-Yun Tung show that if the maximum value of c_4 is chosen, then for molecules such as H_2O and H_2S, c_1 is very similar to the force constants of the radicals OH and SH. The force constants calculated for these triatomic molecules using the three equations for the vibrational frequencies and the maximum value of c_4 are used to derive the frequencies of the isotopic molecules D_2O and D_2S, when good agreement with the observed values is obtained.

The set of force constants defined by Eq. (1) is not unique. Kohlrausch,[2] for example, uses the potential field:

$$2V=f[\Delta r_1^2+\Delta r_2^2]+f'\cdot\Delta R^2+d\cdot r_0^2[\Delta(2\alpha)]^2 +d'\cdot r_0\cdot R_0[\Delta\beta_1^2+\Delta\beta_2^2], \quad (3)$$

where ΔR is the change of the YY bond length, equilibrium value R_0, and $\Delta\beta_1$ and $\Delta\beta_2$ are the changes in the basal angles. Both c_1 and f define the behavior of the XY bond, and c_2 and d that of the YXY angle, but they are not identical for:

$$c_1=f+f'\sin^2\alpha+2d'\cos^2\alpha,$$
$$c_2=d+d'/2+f'\cos^2\alpha. \quad (4)$$

The method of Glockler and Jo-Yun Tung may be criticized on the following general grounds.

(i) In a polyatomic molecule the force constant of a particular bond will not necessarily be the same as that of the corresponding diatomic molecule, even if the number of electrons involved is identical, for the bond environment must be different in the two cases.

(ii) The force constant of a bond in a polyatomic molecule is not uniquely defined, as is shown by (4) above. There is thus no fundamental reason for preferring to make c_1 rather than f equal to the force constant of the diatomic molecule.

(iii) The relationship (2) gives other relationships if different sets of force constants are used, for example for (3):

$$\partial d'/\partial f'=\tan^2\alpha/2. \quad (5)$$

Neither (2) nor (5) seems to have any obvious physical justification.

(iv) Since c_4 is essentially an interaction constant it is surely extraordinary that it should be given its largest possible value.

(v) For the particular case $m=M$ the relationship (2) gives the remarkable condition that $f'=f$ whatever the value of 2α. This conclusion is clearly ridiculous unless 2α is approximately $\pi/3$.

Although Glockler and Jo-Yun Tung have obtained good results for a number of molecules, it would, therefore, appear that their method is not one of general applicability and that the information obtained by using it should not be considered entirely reliable.

[1] G. Glockler and Jo-Yun Tung, J. Chem. Phys. **13**, 388 (1945).
[2] K. W. F. Kohlrausch, *Der Smekal-Raman-Effekt* (Verlagsbuchhandlung, Julius Springer, Berlin-1938), p. 65.

Comment on "On the Force Constants of the XY_2 Molecule"

GEO. GLOCKLER AND JO-YUN TUNG
University of Iowa, Iowa City, Iowa
March 1, 1946

WE appreciate the fact that the Editor has permitted us to see the above note by Miss Simpson on "Force Constants of the XY_2 Molecule."

We would like to point out that the idea of the paper by Glockler and Tung was first to indicate a simple representation of all the real values of the force constants of the XY_2 molecule and secondly to make an attempt to find a simple empirical method which might be useful in determining a *unique* set of force constants from all the possible ones. So far the empirical condition studied was shown to hold with seven molecules. We ourselves pointed out that similar considerations would not apply to the COS molecule. Since we are continuing our calculations we will refrain at this time from taking valuable space and will answer the criticism of Miss Simpson at a later date.

The Photoelectric Effect in Metal-Ammonia Solutions

RICHARD A. OGG, JR.
Department of Chemistry, Stanford University, California
March 14, 1946

THE previous studies[1] of *inner* photoelectric effect (i.e., of photo-conductivity) of metal-ammonia solutions have been extended to include the *external* photoelectric effect—i.e., the emission of electrons into the vapor phase. Extremely dilute (some 10^{-5} to 10^{-4} molar) sodium solutions were employed, in a special photo-cell maintained just above the freezing point of ammonia. The light source was a tungsten filament projection lamp, in conjunction with a carefully tested set of light filters. The quantum efficiency of photoelectric emission appeared to be similar in magnitude to that previously observed[2] for relatively concentrated solutions, but the spectral dependence proved entirely different. Whereas the long wave-length threshold[2] varies from some 7700A for a saturated solution to some 8500–8700A for a 4×10^{-2} molar solution, the highly dilute systems here studied displayed their *maximum* sensitivity in the near infra-red. Exact determination of the corresponding threshold requires more precise work with an infra-red monochromator, but with the filters employed it is estimated to be in the region around 15,000A. The extremely dilute solutions in question would thus appear to possess a work function of the order of one-half of that of the concentrated solutions.

The extraordinary difference in photoelectric behavior of extremely dilute and relatively concentrated sodium-ammonia solutions is best explained by the previously proposed[1,3] equilibrium between trapped electron pairs and trapped single electrons, and by the striking difference in absorption spectrum[3] between these two components. At the very great dilutions employed in the present studies, the proportion of trapped pairs is negligible, and the estimated photo-threshold at $\lambda\sim15{,}000$A corresponds to the work function of the process

$$e(\text{trapped in } NH_3)+h\nu\rightarrow e(\text{gas}), \quad \phi\sim0.8 \text{ volt}. \qquad (1)$$

However, measurements of magnetic susceptibility[4,5] indicate that even the most dilute solution previously studied[2] is characterized by a great predominance of trapped electron pairs over trapped single electrons. Further, in the red and near infra-red regions, the absorption coefficient[3] of trapped pairs greatly exceeds that of trapped single electrons. Consequently, in such solutions the above process (1) is quantitatively negligible, and the observed photo-threshold at $\lambda<8700$A corresponds to the work function of the process

$$e_2(\text{trapped in } NH_3)+h\nu\rightarrow e(\text{trapped in } NH_3)+e(\text{gas}), \quad \phi>1.42 \text{ volts}. \qquad (2)$$

The possibility of precise experimental determination of the work function for process (1) is especially interesting as affording an *upper limit* to the "solvation energy" of single electrons in liquid ammonia solution. (The excess over the "true" energy results from application of the Franck-Condon principle to the non-adiabatic removal of the electron from the solvent cavity). This allows a strictly *experimental* approach to the long standing theoretical problem[6] of separation of *sums* of solvation energies of positive and negative ions into the respective contributions of the individual ionic species.

The difference in work functions between processes (2) and (1) provides an *upper limit* (for reasons similar to those outlined above) to the dissociation energy of the trapped electron pair into two electrons trapped in separate cavities. The *provisional* value obtained here seems not unreasonably greater than that roughly estimated from the temperature dependence of the magnetic susceptibilities,[4,5] and from current calorimetric studies which show dilute (some 10^{-2} to 10^{-1} molar) sodium-ammonia solutions to display a definitely *negative* heat of dilution—in contrast to the *positive*-effect expected for simple electrolytes, and experimentally observed with ammonia solutions of sodium bromide.[7]

[1] R. A. Ogg, Jr., J. Am. Chem. Soc. **68**, 155 (1946).
[2] J. Häsing, Ann. d. Physik [5] **37**, 509 (1940).
[3] R. A. Ogg, Jr., J. Chem. Phys. **14**, 115 (1946).
[4] E. Huster, Ann. d. Physik **33**, 477 (1938).
[5] S. Freed and N. Sugarman, J. Chem. Phys. **11**, 354 (1943).
[6] For literature references, see O. K. Rice, *Electronic Structure and Chemical Binding* (McGraw-Hill Book Company, Inc., New York, 1940).
[7] C. A. Kraus and F. C. Schmidt, J. Am. Chem. Soc. **56**, 2297 (1934).